

## Durham E-Theses

---

*An experimental study of the atmospheric electric elements at a rural site in conditions of low air pollution*

Sharpless, Graham T.

### How to cite:

---

Sharpless, Graham T. (1968) *An experimental study of the atmospheric electric elements at a rural site in conditions of low air pollution*, Durham theses, Durham University. Available at Durham E-Theses Online: <http://etheses.dur.ac.uk/8744/>

### Use policy

---

The full-text may be used and/or reproduced, and given to third parties in any format or medium, without prior permission or charge, for personal research or study, educational, or not-for-profit purposes provided that:

- a full bibliographic reference is made to the original source
- a [link](#) is made to the metadata record in Durham E-Theses
- the full-text is not changed in any way

The full-text must not be sold in any format or medium without the formal permission of the copyright holders.

Please consult the [full Durham E-Theses policy](#) for further details.

AN EXPERIMENTAL STUDY OF THE ATMOSPHERIC  
ELECTRIC ELEMENTS AT A RURAL SITE IN CONDITIONS  
OF LOW AIR POLLUTION

BY

GRAHAM T. SHARPLESS, B.Sc.

Presented in Candidature for the Degree of Doctor  
of Philosophy, in the University of Durham.

The copyright of this thesis rests with the author.  
No quotation from it should be published without  
his prior written consent and information derived  
from it should be acknowledged.

September 1968.



## Foreword

The investigation described herein was carried out entirely at the Geography Department Field Centre at Lanehead in Upper Weardale. Initially, Mr. D.M. Smith was working with the author in making the preliminary preparations at the site, but left before the end of the first year of the investigation.

In this Thesis, the SI (Systeme International d'Unites) Units have been employed throughout, except in describing apparatus where they are unnecessary and English units are more applicable. Prefixes, such as in pA ( $= 10^{-12}$  A), have been used without comment as they conform to SI.

The author wishes to express his thanks to all the people who gave assistance during the course of this investigation.

First to Dr. W.C.A. Hutchinson for his guidance and encouragement throughout the work. Secondly, to Professor G.D. Rochester for providing facilities for the research.

Thanks are especially due to Professor Fisher, and other members of the Department of Geography, for generously granting the use of their Field Centre, without which this investigation would not have been possible.

Also, thanks are due to the technical staff of the Physics Department especially Mr. Jack Moralee for his assistance with the construction of apparatus.

The author would like to express his appreciation for assistance and advice given by fellow research students,

especially Mr. I.M. Stromberg who is to be thanked also for providing transport to Lanehead for the last 18 months of the investigation. Also to Mr. D.M. Smith for the design and construction of the field mill.

The author is indebted to the Science Research Council for the maintenance grant, and grant for apparatus, held for the 3 years of the investigation.

Finally, thanks are due to Mrs. Milburn for maintaining comfortable accommodation at Lanehead, and to Mrs. S. Naylor for the efficiency with which she typed this thesis.

G.T.S.

September, 1968.

### Abstract

Continuous measurements have been made of the air-earth current density, by the direct method, potential gradient, space charge density, by filtration, and the positive conductivity at Lanehead, situated in the N. Pennines, 440m above sea level. Wind speed, wind direction and rate of rainfall were also recorded, but the measurements used only qualitatively. The problems of making continuous measurements for long periods of time and under difficult weather conditions are discussed.

The results can be divided into two types: fair weather and disturbed weather. Of the former, diurnal variations for the one-year period July 1967 to June 1968 were calculated. That of potential gradient shows a close similarity with the variation found on the Carnegie in the Pacific (TORRESON et al. 1946), contrary to expectations for a land station within the austausch region. The air-earth current, on the other hand, is found to depend on the variation in columnar resistance, and its variation is similar to that of the space charge density. The diurnal variation of columnar resistance is estimated, and the role of pollution in controlling this variation is discussed.

For disturbed weather, a high positive correlation has been found between space charge density and potential gradient at the ground during steady precipitation. Both were mostly negative during the precipitation, i.e. of opposite sign to the

precipitation current. Splashing and point discharge are ruled out as sources of the space charge, so that the results imply some charge separation process within a few tens of metres of the ground giving positive charge to the rain and negative to the air. For 42 periods of steady rain, with some of snow, relations of the form  $F = A \rho + B$  were calculated and the frequency distributions of A and B are given.

The importance of making continuous measurements of several electric parameters is stressed, together with the necessity of using statistical methods to eliminate the effects of unknown variables such as meteorological conditions. An atmospheric electric station has been set up at Lanehead, where air pollution is low, and an atmospheric electric climate for the station has been established.

## CONTENTS

CHAPTER 1	<u>Some Relevant Aspects of Atmospheric Electricity</u>	
1.1	The General Principles Involved	
1.1.1	Definitions for some frequently used terms	1
1.1.2	The electrosphere and the fine-weather potential gradient	3
1.1.3	The conduction of charge in the atmosphere	4
1.1.4	Convection currents	7
1.1.5	Space charge in the air	8
1.1.6	Displacement currents and the relaxation time of the atmosphere	9
1.1.7	The electrode effect	11
1.2	Fair-Weather Diurnal Variations	
1.2.1	World-wide thunderstorm activity	12
1.2.2	Some results of diurnal variations	13
1.3	Numerical Values of Atmospheric Electric Parameters	
1.3.1	The potential gradient	15
1.3.2	The air-earth current density	15
1.3.3	Space charge density	16
1.3.4	Summary of average values	17
1.4	Disturbed Weather Phenomena	
1.4.1	Non-precipitating conditions	18
1.4.2	Precipitation electricity	19
1.4.3	Space charge in rain	21

CHAPTER 2	<u>The Nature of the Present Investigation at Lanehead</u>	
2.1	The Scope of the Work	
2.1.1	Preliminary considerations	23
2.1.2	Continuous observations at Lanehead	25
2.1.3	Choice of the site	26
2.2	The Lanehead Field Station	
2.2.1	Introduction	27
2.2.2	General location of the site	29
2.2.3	Description of the site	30
2.3	Preliminary Work	
2.3.1	Introduction	31
2.3.2	The Field drains and cable ducts	32
2.3.3	Concrete pits and fences	33
CHAPTER 3	<u>Apparatus for Continuous Recording</u>	
3.1	Air-earth Current Collector	
3.1.1	Methods of measurement of air-earth current	35
3.1.2	Compensation for displacement currents	36
3.1.3	Construction of collector	38
3.2	The Field Mills	
3.2.1	Principle of operation	39
3.2.2	Design and construction of the field mills	41
3.2.3	The electronics	43
3.2.4	Installation and calibration	44



3.3	The Space Charge Collector	
	3.3.1 Principle of operation	46
	3.3.2 Installation	48
	3.3.3 Fan Unit	49
3.4	The Conductivity Chamber	
	3.4.1 The Gerdien chamber	50
	3.4.2 Installation	51
3.5	The Wind Vane and Anemometer	
	3.5.1 The wind vane	53
	3.5.2 The anemometer	54
	3.5.3 Installation	54
3.6	Rate of Rainfall Measurement	
	3.6.1 Existing methods of measurement	55
	3.6.2 The acoustic rate-of-rainfall recorder	55
3.7	The Recording System and Power Supplies	
	3.7.1 The pen recorders	58
	3.7.2 The power supplies	59
CHAPTER 4	<u>The Instrumental Problems of Continuous Recording</u>	
4.1	The General Problems	
	4.1.1 Maintenance and facilities	60
	4.1.2 Sensitivity of instruments	61
4.2	Accuracy of Measurements	
	4.2.1 General	62
	4.2.2 Air-earth current	63
	4.2.3 Potential gradient	64
	4.2.4 Space charge	65
	4.2.5 Conductivity	65

4.3	Reliability of Instruments	
4.3.1	The field mill	66
4.3.2	The vibrating reed electrometers (V.R.E.)	67
4.3.3	Insulation breakdown	67
4.3.4	The suction fan	68
CHAPTER 5	<u>The Analyses of the Recorded Data</u>	
5.1	Synopsis of Data	
5.1.1	Periods of recording	71
5.1.2	Meteorological observations	72
5.2	Analysis of the Data	
5.2.1	Fair-weather diurnal variations	72
5.2.2	Precipitation electricity data	74
5.3	Statistical Methods	
5.3.1	Correlation coefficients	75
5.3.2	Lines of best fit	77
5.3.3	Tests of significance	80
CHAPTER 6	<u>The Fair-Weather Diurnal Variations</u>	
6.1	General Results	
6.1.1	The average diurnal variations for the full year	82
6.1.2	The seasonal diurnal variations	83
6.1.3	The monthly diurnal variations	85
6.1.4	The annual variations	86

6.2	The Total Diurnal Variations	
6.2.1	The potential gradient	87
6.2.2	Air-earth current and space charge	89
6.2.3	The columnar resistance	90
6.3	Some Further Results	
6.3.1	The effect of wind	92
6.3.2	Diurnal variation of conductivity for July	93
<b>CHAPTER 7</b>	<b><u>Space Charge and Potential Gradient in Precipitation</u></b>	
7.1	General Observations of Precipitation Electricity	
7.1.1	Introduction	95
7.1.2	Light precipitation	96
7.2	Correlation of Space Charge and Potential Gradient	
7.2.1	The recording periods	98
7.2.2	Correlation coefficients	99
7.2.3	Mean values and standard deviations	100
7.2.4	Time lags	101
7.3	The Relation Between Space Charge and Potential Gradient	
7.3.1	The lines of best fit	102
7.3.2	Distribution of slopes of lines	103
7.3.3	Estimate of height of space charge	105
7.3.4	The constant term, B	108

CHAPTER 8	<u>Discussion of Results</u>	
8.1	The Fair-Weather Diurnal Variations	
8.1.1	Summary of results	110
8.1.2	Potential gradient and air-earth current	111
8.2	Atmospheric Pollution Effects	
8.2.1	Ions and nuclei	112
8.2.2	The diurnal variation of the columnar resistance	114
8.2.3	The effects of pollution at atmospheric electric stations	116
8.2.4	Seasonal variations	117
8.2.5	Concluding remarks	119
8.3	Space Charge in Precipitation	
8.3.1	Summary of results	119
8.3.2	The correlation of space charge and potential gradient	120
8.4	The Electrification of Precipitation	
8.4.1	Distribution of charge	122
8.4.2	Origin of charge separation	126
8.4.3	Further discussion	128
CHAPTER 9	<u>Conclusion and Suggestions for Further Work</u>	
9.1	General Conclusions	
9.1.1	The fair-weather electric climate	130
9.1.2	The Lanehead investigation	130

9.2	Improvements	
	9.2.1	The apparatus 131
	9.2.2	The recording system 132
9.3	Suggestions for Further Work	
	9.3.1	Space charge and conductivity 133
	9.3.2	A mountain-top site 134
	References	136

## CHAPTER 1

### SOME RELEVANT ASPECTS OF ATMOSPHERIC ELECTRICITY

#### 1.1 The General Principles Involved

##### 1.1.1 Definitions for some frequently used terms

The scope of this chapter is to outline the general principles of Atmospheric Electricity, in particular those aspects which are directly relevant to the present work. It is not intended that a detailed review of past work be given as this may be found elsewhere, such as in CHALMERS (1967a). It is convenient here to define some of the terms which are used later in the chapter and which are peculiar to atmospheric electricity.

In the atmosphere, charges are constantly moving and give rise to electric currents. However, if these currents are steady then there exists a condition of dynamic equilibrium known as a quasi-static state. Charges which move out of a region are constantly being replaced by others, so maintaining a constant distribution of charge. By the principle of the quasi-static state the usual laws of electrostatics can be applied. Also it follows that the vertical current density must not vary with height, otherwise the distribution of charge would vary, and Ohm's Law may be used to describe the electrical properties associated with this flow of charge. In non-steady conditions only the initial and final states, if these are steady, may be described by the principle of the quasi-static state, although ~~even here~~ care must be taken to consider



the time taken for conditions to settle down to the new quasi-static state. This time is dependent upon the relaxation time, which is discussed in 1.1.6.

An explanation for the use of the expression Potential gradient instead of field is needed here. A positive potential gradient at a point in the atmosphere is defined as that which is produced by a positive charge vertically above that point. In such a case the electric field,  $E$ , is given by

$$E = -\frac{dV}{dh}$$

where  $h$ , the height of the point, is measured positively upwards. On the other hand from the above definition it is seen that the potential gradient,  $F$ , must be given by

$$F = \frac{dV}{dh}$$

giving  $F = -E$ . Earlier workers used the word field to describe  $F$  not  $E$  so that ambiguities resulted. As a result the term potential gradient, which is non-ambiguous, is used instead.

The columnar resistance is defined as the resistance of a column of air of unit cross-section,  $1\text{m}^2$  in M.K.S., from the earth up to the electrosphere (see 1.1.2). The units are  $\Omega$ , although dimensional problems occur when applying Ohm's Law, which implies the use of  $\Omega\text{m}^2$  as the unit of columnar resistance. This can be seen to be physically unacceptable as a choice of unit.

1.1.2 The electrosphere and the fine weather potential gradient

The existence of a highly conducting layer in the upper atmosphere has been demonstrated by the reflection of radio waves. This layer, the ionosphere, is about 140km above the earth's surface, although radio waves are reflected from layers as low as 80km, and its high conductivity is due to ionization mainly by solar radiation. For the purposes of atmospheric electricity the atmosphere is sufficiently conducting down to about 50km where it is referred to as the Electrosphere. The combination of the earth and electrosphere then form a giant spherical condenser with the atmosphere as its dielectric. In fine weather there exists a positive potential gradient at the earth's surface implying a positive charge on the electrosphere. Since the air is not a perfect insulator then this charge, unless replenished, would be reduced to zero in a few minutes. The conductivity of the air is due to ionization by cosmic rays and, near the ground, by radioactivity in the air itself. The columnar resistance, that is the total resistance of a column of cross section  $1 \text{ m}^2$ , is about  $10^{17}$  ohms so that the total resistance between earth and electrosphere is about 200 ohms.

One of the main problems in atmospheric electricity has been accounting for the maintenance of the potential difference between earth and electrosphere. WILSON (1920) first showed that thunder clouds usually behaved as if they contained a dipole of positive polarity, that is with the positive charge



above the negative charge. Therefore a positive conduction current would flow upwards between the ground and the cloud and from the cloud to the electrosphere. This charge transfer would then help to maintain the fine weather conduction current which is directed downwards. Lightning discharges to the ground on balance bring negative charge, and point discharge currents, from points on the earth's surface, provide a further means of charge transfer. If the positive charge transferred to the electrosphere and negative charge to earth are both quickly distributed evenly over fine weather areas, then the potential of the electrosphere will at any one time be dependent on the simultaneous thunderstorm activity over the whole earth. The world-wide thunderstorm activity does show a definite variation with time of day and the extent to which the atmospheric electric parameters reflect this variation will be discussed in 1.2.

### 1.1.3 The conduction of charge in the atmosphere

Considering only electrical processes, and neglecting any horizontal transfer of charge, then the vertical air-earth conduction current density must be constant with height to agree with the principle of the quasi-static state. The conductivity of the air is due almost entirely to small ions of mobility approximately  $10^{-4}$   $\text{ms}^{-1}$  per  $\text{Vm}^{-1}$ . These small ions each consist of an ionized molecule, with, attached to it, a cluster of neutral molecules. The mobility of large ions, which are formed

by small particles becoming attached to small ions, is very small so these play little part in conduction unless their concentration is high enough.

Since the current remains constant with height then Ohm's Law can be used to show the relation between the potential gradient,  $F$ , and the conductivity  $\lambda$ . The conduction current density,  $I$ , is given by

$$I = \lambda F$$

where  $I$  is in  $\text{Am}^{-2}$ ,  $\lambda$  in  $\Omega^{-1} \text{m}^{-1}$  and  $F$  in  $\text{Vm}^{-1}$ .

Dimensionally, then, the equation is correct. From this it can be seen that for  $I$  to be constant then  $F \propto 1/\lambda$ .

Poisson's equation can be used to determine the density of space charge resulting from the variation of conductivity with height. Consider a horizontal layer of air at height  $Z$  and thickness  $dz$  containing a space charge density,  $\rho$ , due to the change in conductivity across this layer. Ohm's Law gives, at this level

$$I = \lambda F$$

where  $I$  is the current density vertically through this horizontal layer. Differentiating:

$$dI = \lambda dF + Fd\lambda$$

If there is a discontinuity in  $\lambda$  then only  $I$  remains constant

$$\therefore dI = 0 = \lambda dF + Fd\lambda$$

$$\therefore \frac{dF}{d\lambda} = \frac{-F}{\lambda} = \frac{-I}{\lambda^2}$$

Here, of course, all three variables  $I, F$  and  $\lambda$  are functions

of  $z$ . From Poisson's equation

$$\begin{aligned}\frac{dF}{dz} &= - \frac{\rho}{\epsilon_0} \\ \therefore \rho &= - \epsilon_0 \frac{dF}{dz} = - \epsilon_0 \frac{dF}{d\lambda} \times \frac{d\lambda}{dz} \\ &= \epsilon_0 \frac{I}{\lambda^2} \frac{d\lambda}{dz}\end{aligned}$$

This may be written more conveniently as

$$\rho = - \epsilon_0 I \frac{d}{dz} \left( \frac{1}{\lambda} \right)$$

This means that if the conductivity increases with height then the space charge will be positive. Physically this can be interpreted in terms of the number of lines of force decreasing with height, bearing in mind that the fine weather potential gradient is positive.

Ohm's Law may be written in two forms:

$$\begin{aligned}I &= \lambda F \\ \text{and } I &= \frac{V}{R_c}\end{aligned}$$

where  $V$  and  $R_c$  are the potential of the electrosphere and the columnar resistance. The difficulties, mentioned in 1.1.1, involved in the choice of units for  $R_c$  are obvious here, since in the second equation  $I$  appears to be a current and not a current density. However, in the second equation,  $I$  is seen to be dimensionally the same as in the first if one considers that  $R_c$  is the resistance of a column of unit cross-section. The potential gradient can now be written as

$$F = \frac{I}{\lambda} = \frac{V}{\lambda R_c}$$

If  $R$  remains constant then  $I$  is proportional to  $V$  whereas  $F$  is proportional to  $V/\lambda$ . In practice the conductivity is greatly affected by local pollution and so will often influence  $F$  more than  $V$  will. Since  $I$  is not dependent on  $\lambda$ , except in so far as  $\lambda$  affects  $R$ , then this should give a better indication, than  $F$ , of the variation of  $V$  in regions influenced by local pollution. This deduction is very important in the comparison of the world-wide thunderstorm activity with the fine-weather atmospheric elements.

#### 1.1.4 Convection currents

In fine weather, convection will carry any excess space charge near the ground up to the top of the austausch region. Within this region, which is the lowest part of the atmosphere, thorough mixing of the air occurs. Its upper limit depends on meteorological conditions and may be at any height up to about 3km. It may coincide with a temperature inversion level. The resulting convection currents, which will be positively upwards for an excess of positive space charge, will therefore oppose the conduction current. Since there can be little or no convection above the austausch region, then only conduction currents will be present here, while within the austausch region both components exist. The conduction current density within the austausch region will therefore be greater than that above, to prevent accumulation of space charge at the boundary.

Direct measurements of air-earth current density, by collecting charge on an isolated section of the earth's surface, should yield the value of the conduction current density above the austausch region and so give the total current density between the earth and upper atmosphere. Indirect measurements, using the expression  $I = \lambda F$ , will give only the conduction current within the austausch, so excluding the convection current component. CHALMERS (1967b) considered the effect of the positive space charge near the ground in assisting the maintenance of the earth's negative charge and came to the conclusion that the convection current component, in theory, was probably negligible. In practice, the extent to which convection influences the air-earth current is not accurately known.

#### 1.1.5 Space charge in the air

The space charge density denotes the net density of unbalanced charge in the atmosphere and may be either primary or secondary. Primary space charges, which may be produced either artificially, from industrial smoke, vehicle exhaust etc., or naturally, from precipitation, point discharge etc., are transported mostly by wind and diffusion. As well as these there are also secondary space charges, which are due, for example, to the variation of conductivity with height and also, close to the ground, as a consequence of the electrode effect (see 1.1.7). Wind motion may convert secondary space charge to primary. Packets of space

charge are responsible for the short term fluctuations in the fine weather potential gradient. These packets may be due to a sudden burst of space charge from a vehicle exhaust, or else due to convection cells carrying excess space charge from close to the ground. A packet of space charge of density  $8.85 \text{ pC m}^{-3}$  and of vertical thickness 1 m will produce a change in the potential gradient, neglecting edge effects, of  $1 \text{ Vm}^{-1}$ .

#### 1.1.6 Displacement currents and the relaxation time of the atmosphere

The total air-earth current in fine weather comprises both conduction and convection currents and may be measured by observing the rate at which an isolated section of the earth's surface accumulates charge. The surface of such a collector will contain a bound charge as a result of the fine-weather potential gradient. Any variation in this latter quantity will cause displacement currents to be observed due to similar variations in the bound charge. A potential gradient changing at  $1 \text{ Vm}^{-1} \text{ s}^{-1}$  will produce a displacement current of  $8.85 \text{ pA m}^{-2}$  compared with the normal value for conduction current of around  $2 \text{ pA m}^{-2}$ . If over a period of some minutes, during fine weather, the net potential gradient change is no more than, say,  $10 \text{ Vm}^{-1}$ , then the net change in bound charge will be within  $\pm 88.5 \text{ pC m}^{-2}$ . For a period of, say, 10 minutes the average displacement current will be only  $0.15 \text{ pA m}^{-2}$  which is less than 10% of the normal conduction current. This means that a simple means of eliminating

the displacement currents would be to use a time constant of the order of several minutes in the measuring instrument. An improvement of this method was due to KASEMIR (1955) who showed that by connecting his collector to earth via a parallel combination of resistance and capacitance, of time constant numerically equal to  $\epsilon_0 / \lambda$ , complete compensation could be achieved.

The quantity  $\epsilon_0 / \lambda$  is numerically equal to the relaxation time of the atmosphere. Considering two horizontal planes, each of area A, in the atmosphere, one d metres vertically above the other then the resistance, R, between the two planes will be

$$R = \frac{d}{A \lambda}$$

and the capacitance of this parallel plate condenser is given by

$$C = \frac{\epsilon_0 A}{d}$$

The time constant CR then is

$$CR = \frac{\epsilon_0 A}{d} \times \frac{d}{A \lambda} = \frac{\epsilon_0}{\lambda}$$

which is the relaxation time of the atmosphere, so that it can be seen that Kasemir's method of compensation amounts to matching the measuring instrument to the atmosphere. Since capacitative effects are involved in the atmosphere, Ohm's Law will hold only for changes slow compared with the relaxation time, which is typically about 15 minutes. For faster changes, the variation of air-earth current will lag behind that of the potential gradient. When applying the condition of the quasi-static state,

then only slow changes must be considered. If there is a rapid change in field due perhaps to a lightning discharge, from one steady value to a final one, then the charges in the atmosphere will be redistributed in a time dependent on the relaxation time, until a new steady state or quasi-static state has been established. Here again, then, the principle of the quasi-static state can be employed but only when describing initial and final conditions and not the changes in between.

#### 1.1.7 The electrode effect

BENT and HUTCHINSON(1966) defined the electrode effect in such a way as to be applicable to widely different conditions. Their definition states: "In atmospheric electricity the electrode effect is the modification of elements such as space charge distribution, conductivity and potential gradient near an earthed electrode, which may be a raised object or the surface of the Earth itself, because in the prevailing electric field ions of one sign are attracted towards the electrode, whilst those of the opposite sign are repelled from it." CHALMERS (1966) has thoroughly investigated the theoretical considerations to explain the non-existence of the simple electrode effect. In fine weather, with the normal positive potential gradient, the electrode effect should manifest itself by producing a large excess of space charge close to the ground. Most workers have either found very little or no evidence of the electrode effect.



Ionization by radioactivity is one possible cause for the lack of the electrode effect, which may also be inhibited by wind motion. CROZIER (1963), however, found strong evidence of the electrode effect in New Mexico during calm night-time periods, when he found a very high excess of positive space charge very close to the ground. BENT and HUTCHINSON (1965) observed unusual space charge effects which they attributed to the electrode effect near the top of a 21m mast.

## 1.2 Fair Weather Diurnal Variations

### 1.2.1 World-wide thunderstorm activity

APPLETON (1925) first suggested that the variation of fine weather potential gradient might be similar to the variation in number of thunderstorms over the whole earth. The diurnal variation of potential gradient measured by MAUCHLY (1923) during the cruise of the 'Carnegie' was found to agree well with the diurnal variation of the world-wide thunderstorm activity as given by WHIPPLE and SCRASE (1936). Both variations show a minimum at about 03 hours G.M.T. with a gradual increase to a maximum at about 19 hours with a more rapid fall-off. The thunderstorm variation also contains another maximum at 14 hours but for the potential gradient it is much less pronounced. HOGG (1950), using results from 18 stations, found a similar agreement with air-earth current, which would be expected to suffer less

from pollution. CHALMERS (1967a) provides more details of similar results which agree with the world-wide thunderstorm activity. Apart from these some workers have found diurnal variations dependent on local pollution and showing no similarity with world-wide effects.

ISRAËL and de BRUIJN(1967) endeavoured to correlate the simultaneous daily means of potential gradient for pairs of stations in N. America at large mutual distances. From the very low correlation coefficients obtained, they concluded that local disturbances were too pronounced for any world-wide effect to be discernible. They also took readings of potential gradient, air-earth current density and conductivity from two stations in the Alps at altitudes of over 3,000 m. The three correlation coefficients which they obtained were low, but the largest was for the air-earth current and the lowest for conductivity, indicating the effect pollution has on conductivity and potential gradient. From this it was suggested that more detailed observations of the world-wide thunderstorm activity were needed as well as increasing the scope of atmospheric electric measurements.

#### 1.2.2 Some results of diurnal variations

In contrast to measurements made at sea, SCRASE (1933) at Kew found diurnal variations of the air-earth current which showed different forms at different times of the year. In Winter he

found the maximum and minimum to occur at 6 hours and 21 hours respectively while in Summer these were midnight and 13 hours G.M.T. The potential gradient showed a greater variation with double maxima and minima. HATAKEYAMA and KAWANO (1953) measured the diurnal variation of potential gradient at 8 stations in the Japan archipelago. They found semi-diurnal components also, and the main maxima and minima at all stations generally coincided. In larger cities they found the diurnal variation to be controlled mostly by the conductivity while in rural conditions only the semi-diurnal component was controlled in this way. The maximum of the diurnal component occurred at about 22 hours G.M.T.

COBB and PHILLIPS (1962), from a year's continuous measurements at a station in Hawaii, produced sets of diurnal variations for a number of the fine-weather parameters. Their site, at a height of 3,394 m above sea level on the side of the mountain Mauna Loa, suffered very little from local pollution or weather effects, so that a comparison with the world-wide effects could be made. The diurnal variations of potential gradient, air-earth current and conductivity were compared with those of TORRESON et al. (1946) whose measurements were made in the Pacific Ocean during the cruise of the 'Carnegie', 1929. The variations for air-earth current agreed very well, while for potential gradient there was a time lag of about 2 hours between the two variations. The measurements of conductivity showed little resemblance as might be expected between a land station and one at sea.

### 1.3 Numerical Values of Atmospheric Electric Parameters

#### 1.3.1 The Potential Gradient

Most measurements of potential gradient have been made at or near the earth's surface by a number of different methods. Earlier workers used antennas for measuring the potential of the air at different heights, while more recently field mills have been used. In comparing measurements of potential gradient, and other parameters, at different locations it is convenient to take annual means of fair-weather values so as to eliminate seasonal or diurnal variations. SCRASE (1933) found means for Summer and Winter at Kew to be  $285 \text{ V m}^{-1}$  and  $485 \text{ V m}^{-1}$  respectively, the difference being because the greater pollution in Winter, from domestic fires for example, lowered the conductivity. In general the higher the pollution the higher is the potential gradient, so that at sea the average values are only about  $100 \text{ V m}^{-1}$ . Potential gradients measured on high mountains are usually found to be greater than at sea even after correction has been made for the exposure factor of the station. ISRAEL (1957) attributed the mean value, at the Jung fraujoeh, of  $149 \text{ V m}^{-1}$  to the high altitude causing a reduction in the columnar resistance. At Mauna Loa COBB and PHILLIPS (1962), although at a similar altitude, found the somewhat lower mean value of  $120.5 \text{ V m}^{-1}$ .

#### 1.3.2 The air-earth current density

Indirect measurements of conduction current density using

the relation  $I = \lambda F$ , give different results from direct measurements of the total fine-weather air-earth current density, due to the presence of convection currents. Average values by direct measurement usually lie between 1 and 4 pA m<sup>-2</sup> for land stations and sometimes greater for mountain stations and at sea, due to the smaller columnar resistance. At Mauna Loa, for example, a value of 5.4 pA m<sup>-2</sup> was found whilst at Kew the corresponding value was 1.1 pA m<sup>-2</sup>.

### 1.3.3 Space charge density

Values of space charge density, in fine weather, differ widely from place to place both in magnitude and sign. KÄHLER (1927) measured the space charge density by the cage method. He used a water dropper to measure the potential at a point in an earthed metal cage, containing the space charge to be measured, and found positive values between 60 and 300 pC m<sup>-3</sup> with a mean of 193 pC m<sup>-3</sup>. OBOLENSKY (1925) was the first to measure space charge by sucking air through a filter which collects the charge. His results, which gave negative values in Summer, averaged +1.2 pC m<sup>-3</sup>. An average of +28 pC m<sup>-3</sup> was found by BROWN (1930) and at Cambridge, LAW (1963) found average values of +10 pC m<sup>-3</sup> by day and -20 pC m<sup>-3</sup> at night at a height of 0.5 m above the ground. CROZIER (1963), on the New Mexico semi-desert, found high values of up to 500 pC m<sup>-3</sup>, very close to the ground in still night-time conditions. He attributed this to a manifestation of the

electrode effect. SMIDDY and CHALMERS (1960) found a mean value of  $-20 \text{ pC m}^{-3}$  from 1 to 3m, using a double field mill, while BENT and HUTCHINSON (1966), also in Durham but using filtration apparatus, found values nearly always to be within the limits  $\pm 60 \text{ pC m}^{-3}$ .

1.3.4 Summary of average values

In Table 1 are given the average values of the more important atmospheric electric parameters. It is reproduced from CHALMERS (1967a). The actual values given are from earlier measurements, and exclude more recent values. However, they do present an indication of the average values to be expected at stations in different locations.

---

TABLE 1

	<u>Units</u>	<u>Kew</u>	<u>Land Stations</u>	<u>Oceans</u>
Potential gradient	$\text{V m}^{-1}$	365	130	126
Air-earth current density	$\text{pA m}^{-2}$	1.12	2.4	3.7
Conductivity	$10^{-14} \Omega^{-1} \text{ m}^{-1}$	0.3	1.8	2.8
Space charge density	$\text{pC m}^{-3}$	10	10	-
Columnar resistance (for $1 \text{ m}^2$ cross-section)	$10^{17} \Omega$	4.0	1.9	1.2

---

## 1.4 Disturbed Weather Phenomena

### 1.4.1 Non-precipitating conditions

Even in apparently fine weather the atmospheric electric elements can be influenced by minor meteorological phenomena, as well as by man-made pollution. Convection is one example already discussed, while turbulent air motion can also play a part, especially where space charge densities are high. This means that true fine-weather periods, where there are no disturbances, may be so rare that no very useful information can be gained during these periods. It is therefore necessary to consider the importance of these other periods, which may be termed fair weather periods, as distinct from fine weather, where the disturbances are an inherent part of the atmospheric electric climate. This will be further discussed in Chap. 5 where a definition of fair weather is given as relevant to the present work.

Excluding fair-weather conditions then, disturbed weather covers mist, fog, precipitation, lightning, blowing and melting snow and associated phenomena. Even non-precipitating clouds can give rise to high potential gradients, especially thunderclouds where the potential gradient can exceed  $15,000 \text{ Vm}^{-1}$ . In mist and fog the conductivity is reduced to about one third its normal value, by the presence of small particles to which the small ions become attached. The potential gradient therefore

increases while the air-earth current density remains nearly constant. In mountain fogs, which are more localized, the current flows round the poorly conducting region so that no appreciable increase in potential gradient is found. Negative potential gradients have been observed in mist and fog on some occasions and were found by BENT and HUTCHINSON (1966) to be due to negative space charge from insulation breakdown at high tension power lines.

#### 1.4.2 Precipitation electricity

Measurements of the charge brought to earth by precipitation have been made by two distinct methods: single drop measurements and total precipitation currents. Shielded collectors have been used to measure precipitation currents, as then both conduction and displacement currents are eliminated. In windy conditions, though, the shielded collector excludes many of the smaller drops, so that the results may not represent a fair sample of rain. SCRASE (1938) found that his collector received only half the amount of rain caught by a standard rain gauge. On the other hand the exposed receiver suffers from displacement currents which, in showery and stormy conditions, can invalidate the results obtained unless adequate compensation is provided. This type of collector will also measure the conduction current but for some purposes this may be more of an advantage than a disadvantage.



Many observers have divided rain into three types: continuous rain, showery rain and stormy rain. For all but very light rain, the precipitation current has been found to be usually opposite in sign to the potential gradient and for continuous rain is mostly positive. SIMPSON (1949) derived empirically a relation between precipitation current density  $I$ , rate of rainfall  $R$ , in  $\text{mm hr}^{-1}$ , and potential gradient  $F$  as:

$$I = -1.33 \times 10^{-14} R (F-400)$$

CHALMERS (1956), without taking rate of precipitation into account, found the following two relations for the total current to earth:

$$I = -1.18 \times 10^{-14} (F - 150) \text{ for rain}$$

$$\text{and } I = -0.92 \times 10^{-14} (F-440) \text{ for snow}$$

In each case the subtractive term is stated to be the fine weather potential gradient. REITER (1965) gives similar expressions for different conditions of non-stormy precipitation with the exception of the subtractive term, which was only  $40 \text{ V m}^{-1}$  but which agreed with the measured value of the fine weather potential gradient. All the above relations show that for potential gradients greater than the fine-weather value, the precipitation current is negative. This inverse relation has been observed by most workers, sometimes together with the mirror image effect, where the precipitation current and potential gradient change sign almost simultaneously, one being the mirror image of the other in the time axis.

### 1.4.3 Space charge in rain

Very little information is available of space charge densities during precipitation. One reason for this is that the usual filtration method is difficult to use, with success, in rain, especially if this is heavy. ADKINS (1959b) made some measurements of space charge during rain and found low values, unless the rain became heavy when the sign of the space charge was found to be opposite to that of the potential gradient. By means of laboratory experiments, he showed that in low potential gradients this inverse relation was due to splashing at the ground, while for higher potential gradients point discharge produced considerable space charge. In these latter conditions, the charge released by splashing was in the form of small ions of high mobility. These may have been either singly charged clusters of water molecules or more highly charged larger droplets. ADKINS pointed out that the space charge near the ground can have a pronounced influence on the potential gradient in all weather conditions. He stressed the importance of taking great care when interpreting results of potential gradient measurements.

Contrary to the results of ADKINS, SMIDDY and CHALMERS (1960) found only negative space charges during rain, often accompanied by a negative potential gradient. In earlier times KELVIN (1860) discovered that, during steady rain, his measurements of the potential gradient at the ground sometimes gave negative values,

while at the top of a 30m tower the values were positive. CHAUVEAU (1900) found similar results for the Eiffel Tower. This suggests that near the ground there is a concentration of negative space charge which is controlling the potential gradient at the ground. If this negative space charge is related to the positive charge usually found on rain, then some process of charge separation near the ground may be occurring. SIMPSON (1915) suggested that the shattering of drops by the wind might cause separation but later (SIMPSON, 1942) abandoned the idea. SMITH (1955) suggested splashing, although the extent of this would depend on the rate of rain-fall and the surface of the ground. ADKINS (1959a) suggested melting as a means of producing the negative charge and REITER (1955) gave results agreeing with this theory.

COLLIN, RAISBECK and CHALMERS (1963) measured the potential gradient at the top and bottom of a 25m mast. After correcting for the exposure factor of the mast, the space charge between the two was calculated from the difference between the two potential gradients. They found a linear relation between the ground level potential gradient and the deduced space charge density for results on 3 different occasions. The actual relation varied from one occasion to another.

## CHAPTER 2

### THE NATURE OF THE PRESENT INVESTIGATION AT LANEHEAD

#### 2.1 The Scope of the Work

##### 2.1.1 Preliminary considerations

When making measurements of the atmospheric elements it is necessary to consider the aim of the work, before deciding on the type of observations that are to be made. This includes the decision as to whether the observations should be continuous or intermittent. In earlier work, continuous observations were made over long periods of time, often only of potential gradient. From measurements in fair weather the average diurnal and seasonal variations were calculated. Extending these measurements to several parameters, one can obtain what ISRAËL (1957) calls an "electric climatology" for that station. As mentioned in Chapter 1, the results of such measurements are very variable, as both local pollution and weather conditions can disguise any world-wide tendencies. ISRAËL and de BRUIJN (1967) have made comparisons between measurements of the fair-weather potential gradient from different stations at large mutual distances. The lack of correlation prompted them to propose that a new situation existed. "An isolation of the global effects from daily, monthly and annual means of the atmospheric electric elements at continental stations must be assumed impossible."

It must be accepted, therefore, that local weather conditions play an important part in controlling the atmospheric electric climate. At meteorological stations, usually, many parameters are continually observed. In much the same way it is necessary to make continuous observations of the important atmospheric electric elements, at sites free from unnatural pollution. COBB and PHILLIPS (1962) established what they term "an atmospheric benchmark" at Mauna Loa, Hawaii. The station, at an altitude of 3.4 km, is well above the trade inversion, and COBB (1968) considers that "the monitored electrical elements will yield data interpretable as an index of the amount of particulate matter suspended in the atmosphere." DOLEZALEK (1958) pointed out that electrical measurements might be able to help in the elucidation of meteorological problems, since meteorological effects which are similar may have different electrical characteristics.

The effect of local weather conditions can make it difficult to select non-disturbed periods for analysis. ISRAËL and LAHMEYER (1948) have pointed out the wide range of choices of periods which have been used. They proposed that every observation should be used, unless precipitation was actually falling at the time. This criterion relies on the disturbances occurring randomly, and in such a way that the results show no dependence on local effects. As already discussed, the results of diurnal and seasonal variations will depend a great deal on

local pollution, if this is present, since no amount of averaging will cancel out the disturbances which themselves have definite diurnal or seasonal variations. However, by taking an average of a large number of observations, the results probably have more general application than single measurements made under carefully specified conditions. In disturbed weather it is very difficult to specify all the conditions, so that individual observations are not of much value on their own. By taking a larger number of observations, in conditions which may be specified less precisely, an average result can be found, together with an indication of the spread of the results. Statistical methods can be used to test the reproducibility of results and provide a means of eliminating some of the unknown variables. Individual observations may differ widely from the mean, but the analysis of a large number of observations may yield better information of the processes involved than a small number of observations under closely specified conditions.

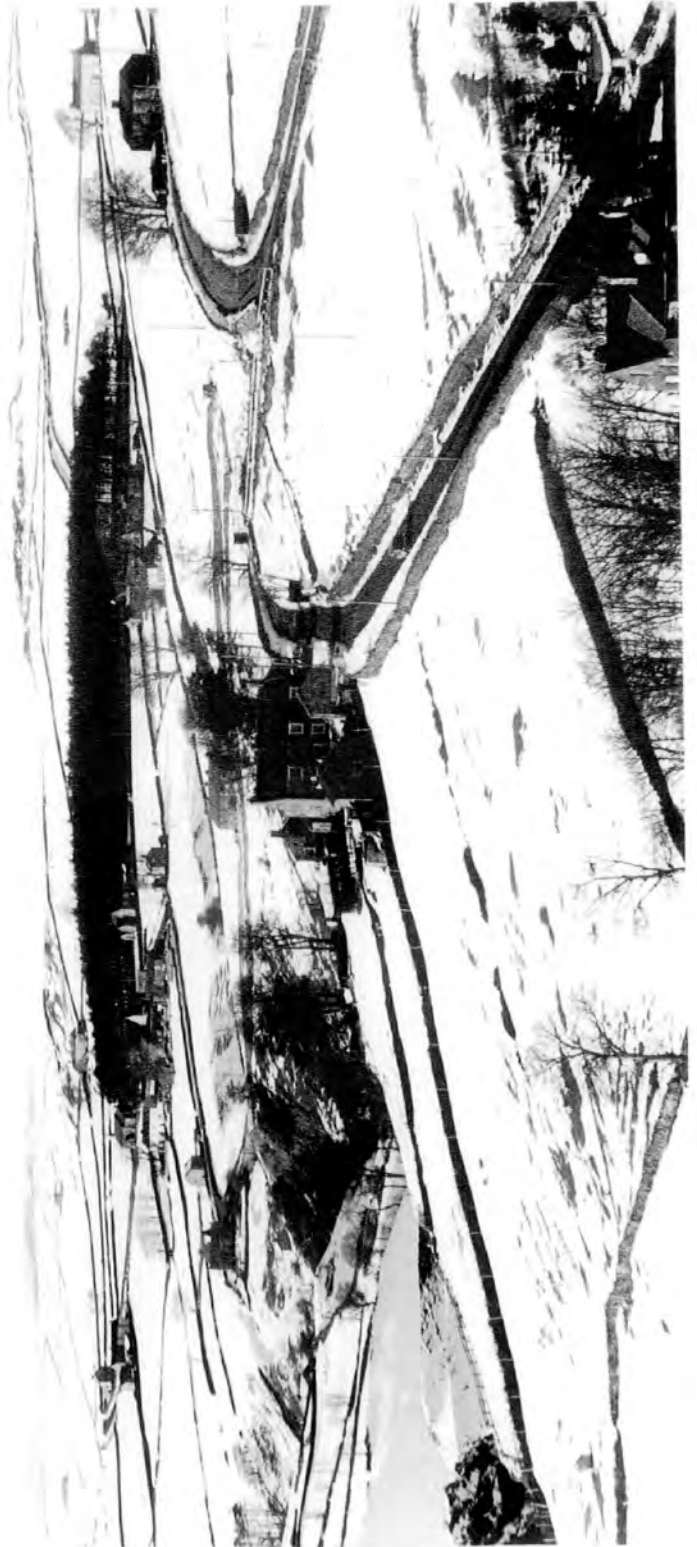
#### 2.1.2 Continuous observations at Lanehead

In the present work, an attempt has been made to make continuous measurements, over a long period of time, under all weather conditions. Observations were made of air-earth current, with an exposed collector, potential gradient, space charge and positive conductivity. When choosing the methods of measurement

it was hoped to use standard, tried-and-tested equipment, so as to spend no more time than was necessary in the design, construction and installation of the apparatus. Unfortunately, there was very little suitable equipment available, while, for potential gradient and air-earth current, there was none at all. The available equipment had been designed for intermittent use in fair weather, so that various modifications and additions were necessary. It was essential that the equipment should be reliable under all conditions, yet still sufficiently accurate for the purpose. The many problems associated with making continuous observations are discussed fully in Chapter 4. The data for both fair weather and disturbed weather have been analysed by statistical methods, bearing in mind the content of the preceding section.

### 2.1.3 Choice of the site

For many years, measurements of the atmospheric electric elements have been made, but only intermittently, in Durham at the University Observatory. In recent years, the increase in motor traffic and the greater building up of the area, have resulted in higher atmospheric pollution, although this is still low compared with that at the majority of towns and cities in this country. Recent space charge measurements have indicated that the extent of this pollution may have had an appreciable effect on the electric climate. There is no





View of Lanehead from East

The station is near the centre in front of the plantation of conifers. The gradual slope of the ground near the site can be seen.

evidence that the space charge content in the air has increased, yet its presence has made fine-weather measurements difficult to interpret. Heavy lorries passing within about 300 m of the Observatory provide a large proportion of the space charge. Domestic fires, and diesel locomotives on the nearby railway, must also have played some part. Negative space charges in fog have also been observed and attributed to insulation breakdown at the surrounding high voltage transmission lines (CHALMERS, 1952; BENT and HUTCHINSON, 1966). However the availability of a much less polluted site in upper Weardale, in the N. Pennines, made possible more extensive measurements, with which the present work is involved.

## 2.2 The Lanehead Field Station

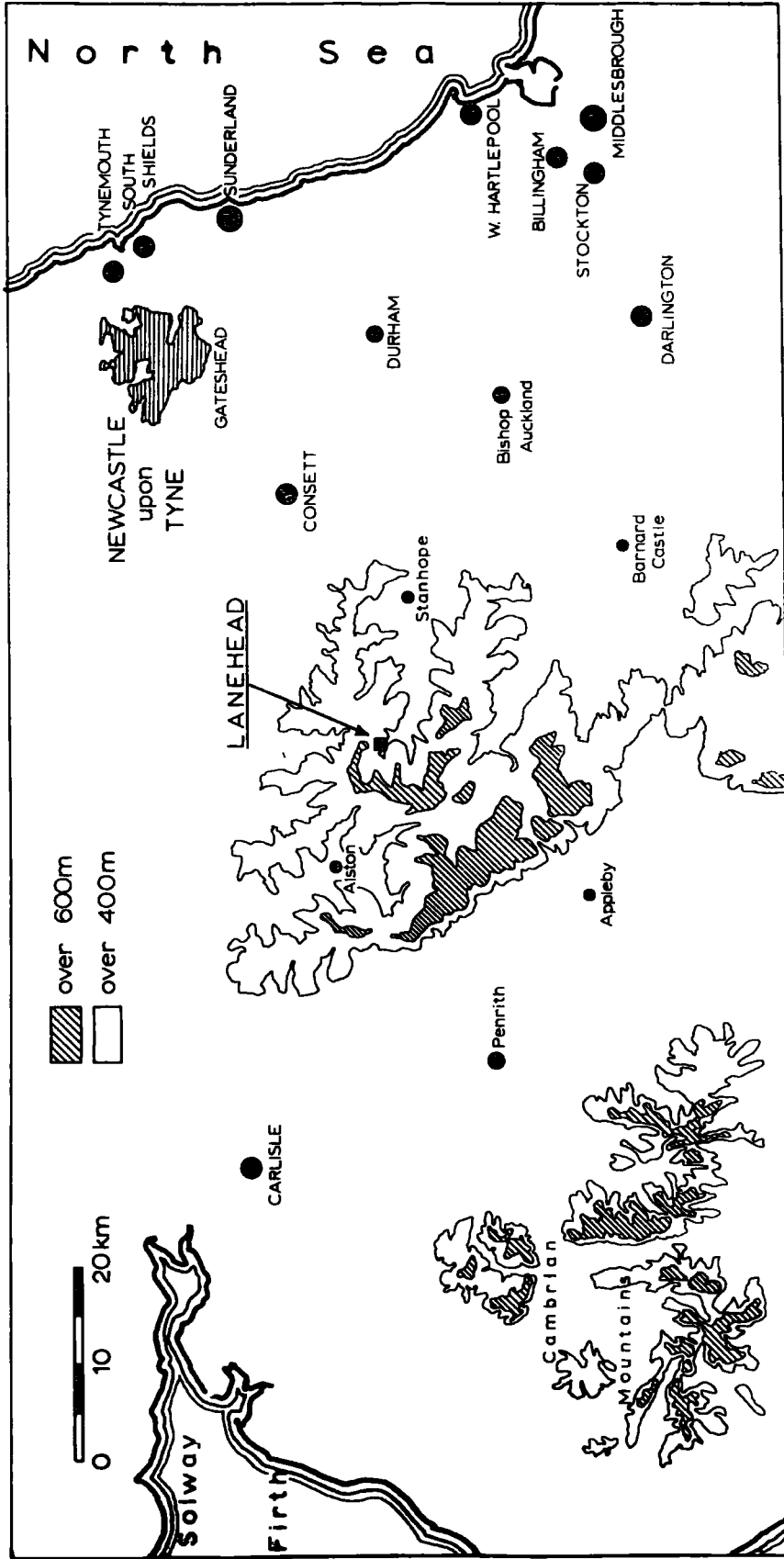
### 2.2.1 Introduction

Durham University Department of Geography has possessed the field station at Lanehead for a number of years, during which time a limited number of meteorological observations have been made there. It is mainly through the generosity of the Geography Department that the present work has been made possible. The field station is situated at a height of 440 m above sea level, part way up the North side of what may be described as a typical North Pennine basin. The ground rises gradually to a height of 630 m, about 2km to the North, while

the hills to the S and S.W. are of a similar height. Lanehead is a small hamlet with a total population of less than 20, who live in a few cottages within about 100 m of the station. Access to the station, from Durham, is by a class B road which continues on to Alston and from there to the Lake District. The traffic it carries is mostly light, except on some weekends and Bank Holidays during the summer. On the whole, though, the station is situated in very quiet surroundings.

Lanehead is probably as free from pollution as anywhere in the country, maintaining the necessary services and facilities. It is situated in an area of declining population, some distance from industry and other sources of pollution. Previous experiments have been performed there, by members of the Geography Department, to measure the amount of particulate pollution in the air. They were unable to find any pollution except when the wind was from the direction of the steel works at Consett. Another piece of evidence demonstrating the absence of pollution was the relatively slow rate of corrosion of exposed metal compared with Durham, where the air pollution is still only about 5 per cent of that in London. Within the last 3 years, the Weardale Cement Works have become operational, but are fortunately 11km away to the E, so that, with prevailing winds being from the W, any effects of pollution should be small. Space charge from lorries, passing through Lanehead, has been

FIG. 2.1 The North Pennines



detected on occasions, but, apart from these short periods, no overall effect was noticeable. The extent of artificial space charge from these and other sources of pollution could be ascertained only from the results of the investigation, and these are discussed in later Chapters.

### 2.2.2 General location of the site

Lanehead is situated in the middle of the North Pennines, about midway between East and West coasts and equidistant from both Newcastle-upon-Tyne and Carlisle. The surrounding area, with the more important towns and other land marks, is given in Fig.2.1. Table 2 gives a list of some of these towns together with their distances from Lanehead. It can be seen that the major sources of pollution, i.e. Consett steel works, Newcastle-upon-Tyne and Billingham, are all to the East, with nothing in the direction of the prevailing winds. For comparison with world-wide effects, the situation of Lanehead is at latitude  $54^{\circ} 39'$  N and longitude  $2^{\circ} 15'$  W from the Greenwich Meridian. Its map reference, from the Ordnance Survey, is 843417.

TABLE 2

<u>Landmark</u>	<u>Distance from Lanehead</u> ( <u>km</u> )	<u>Direction</u>
Durham	43	E
Consett	28	ENE
Newcastle	47	NE'E
Carlisle	47	WNW
Appleby	27	SW'S
Durham Coast	60	E
Eastgate cement works	11	E'S
Cowhill	2	SE
Allenheads	3.5	NNE
Summit	2	N

---

2.2.3 Description of the site

The field station building has been modified from its original use as a village school. Partitioning walls, electric power and cooking facilities have provided it with excellent accommodation. At the E end of the building, a large room has been put aside as a laboratory, while further to the E an area of coarse grass about 30 m by 20 m was bounded to the N and E by a substantially built stone wall, nearly 2 m high. This area was chosen in which to install the measuring apparatus, as it was conveniently close to the laboratory. To the North,



Fig. 2.2 Layout of Apparatus at Site

From left to right the instruments are: fan unit,  
air-earth current collector, Space charge collector,  
conductivity chamber, and field mill.



the plantation of tall conifers presented the problem of the electrostatic screening of the instruments. SCRASE (1934) used the criterion that, for negligible distortion of the electric field, nearby objects must subtend an angle of no more than  $30^\circ$  at the instrument concerned. Since the nearest trees were about 10 m high, then no instrument could be placed nearer than about 20 m to them. For the building, taking into account the sloping roof, the minimum distance was about 15 m. This left a sufficiently large area, about 7m by 12m, within which the apparatus was installed.

The grouping of the instruments is shown in Fig.2.2. They were spread out as far as possible to prevent interference between instruments. The space charge collector and field mill, which were raised above the ground, were kept well away from the other instruments so as not to disturb the electric field unnecessarily. Cables were kept out of harm's way in cable ducts, and suitable precautions were taken to protect the instruments from the weather.

## 2.3 Preliminary Work

### 2.3.1 Introduction

The Lanehead field station, although providing essential facilities, still needed much preparation before any instruments could be installed. Many generations of workers at the observatory

site in Durham have provided it with many facilities such as a mast, cable ducts, and an equipped laboratory. At Lanehead, though, the station was initially badly equipped. Its use as a Geography field centre had been limited mostly to the provision of accommodation. A fenced-off section of the surrounding ground contained a Stevenson screen and a few other instruments for meteorological observations. But none of these required the extra facilities which the present work has needed.

Certain basic requirements had to be met initially. Field drains were laid to prevent the surface of the ground becoming too wet, cable ducts were installed as well as concreted pits to house the instruments. The area was also fenced off to keep out stray animals from nearby farms. The laboratory was used to house the recording instruments and power supplies, as well as serving as a workshop. For this latter purpose a work-bench was constructed and a number of useful hand-tools added. It was later found that these workshop facilities were in almost constant use despite much major construction work being carried out in Durham.

### 2.3.2 The field drains and cable ducts

The ground at Lanehead slopes at a gradient of about 1 in 8 and comprises shallow top soil over clay and sandstone. As a result water from rainfall over higher ground runs down the hill so that the site would quickly become waterlogged unless

adequate drainage were provided. A system of field drains was laid with the lower end connected to an existing drainage system. A trench 2 feet deep and about 1 foot wide was dug to accommodate about 140 one-foot lengths of 4 inch unglazed pipes. These were covered with hard core and then topsoil. The reasonably dry Spring and early Summer of 1966 enabled this work to be carried out without too much difficulty.

The cable ducts, consisting of asbestos cement U-section gutting, of 5 inch by 6 inch cross-section, were installed over the field drains, with their tops flush with the ground. Timber blocks carried the cables above the wet bottom of the ducts, and concrete slabs protected them from above. Nearly all cables were carried for most of their length along these ducts where they were kept out of harms way.

### 2.3.3 Concrete pits and fences

The conductivity apparatus, air-earth current collector and upright field mill were all housed beneath ground level. For all three, holes were dug and lined with concrete. Drainage was provided by leading the water collected into the main drains. For the air-earth current collector a large concrete pipe 36 inches in diameter and 15 inches deep was lowered into a hole on to a previously concreted base. The other two pits were placed close to the cable ducts so as to aid drainage and to prevent cables being laid over the bare ground.

The site was originally fenced in on three sides, but not on the fourth. The necessity of fencing in this last side became obvious when a sheep and two calves were found grazing near the air-earth current collector. A p.v.c. covered chain-link fence, 3 feet high, was supported on deal posts concreted into the ground. A small gate in the middle allowed access to the instruments but kept out stray animals.

## CHAPTER 3

### APPARATUS FOR CONTINUOUS RECORDING

#### 3.1 Air-earth Current Collector

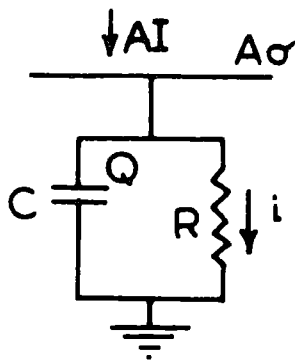
##### 3.1.1 Methods of measurement of air-earth current

There are two distinct methods by which the fair-weather air-earth current density may be measured, but these do not necessarily give the same result. By the direct method, a section of the earth's surface is isolated electrically and the current to it is measured. The indirect method requires the use of Ohm's Law to obtain the conduction current from simultaneous measurements of conductivity and potential gradient at the ground. As explained in Chapter 1, the total air-earth current may include convection currents as well as the conduction current. Since the total vertical current density should remain constant with height (see 1.1.4), the air-earth current density given by the direct method should be the more useful. The direct method requires compensation for displacement currents, but for fair-weather measurements this is not too difficult to achieve.

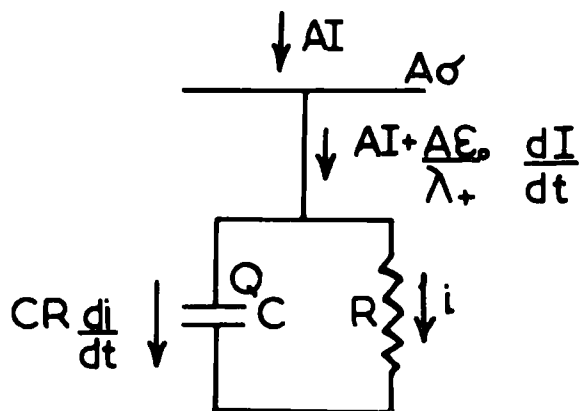
In precipitation there will be a further current component, that due to the rain itself. Here, convection currents can probably be ignored but there is still the problem that the exposed receiver measures the conduction, precipitation and also displacement currents, if these last have not been eliminated. The shielded

FIG.3.1. Method of compensation for displacement currents

(a) Steady conditions  $\left(\frac{dF}{dt} = 0\right)$



(b) Changing conditions  $\left(\frac{dF}{dt} \neq 0\right)$



receiver, which was mentioned in Chapter 1, excludes both conduction and displacement currents, but has its own disadvantages. For general purposes, it was decided to use a completely exposed collector, with suitable compensation for displacement currents. Such a collector would, it was hoped, provide better information of the total charge than that which measured only one component.

### 3.1.2 Compensation for displacement currents

The method of compensation due to KASEMIR (1955) was mentioned in 1.1.5. The circuit arrangement is shown in Fig. 3.1 which includes, diagrammatically, the collector of area A. In steady conditions there will be no current flowing through C, and the current through R will be the conduction current  $AI$ , which is equal to  $V/R$ , where  $I$  is the current density. Very close to the surface of the collector, from Ohm's Law,  $I = \lambda_+ F$ , where  $\lambda_+$  is the positive conductivity. A small change in  $I$  will produce similar changes in  $V$  and  $Q$ , so that the change in charge on the capacitor is

$$dQ = CdV$$

The instantaneous current through C is, therefore,

$$\frac{dQ}{dt} = C \frac{dV}{dt} = CR \frac{di}{dt}$$

The current,  $i$ , through R is equal to  $V/R$  so that the total current, through both C and R, is

$$i + \frac{dQ}{dt} = i + CR \frac{di}{dt}$$

If  $\lambda_+$  remains constant, the potential gradient will change proportionately to I, so that the resultant change in the bound charge,  $A\sigma$ , on the collector will give rise to a displacement current given by

$$A \frac{d\sigma}{dt} = -A\epsilon_0 \frac{dF}{dt} = \frac{-A\epsilon_0}{\lambda_+} \frac{dI}{dt}$$

where  $\sigma$  is the surface density of bound charge on the collector. The total current arriving at the collector will then be

$$AI + \frac{A\epsilon_0}{\lambda_+} \frac{dI}{dt}$$

Since the collector must not accumulate charge, this must equal the current leaving the collector through C and R.

$$i + CR \frac{di}{dt} = AI + A \frac{\epsilon_0}{\lambda_+} \frac{dI}{dt}$$

From this equation it can be seen that

$$i = AI \text{ and } CR = \epsilon_0/\lambda_+$$

This means that if  $CR = \epsilon_0/\lambda_+$ , the current through R is always equal to the air-earth conduction current. The main disadvantage with this method of compensation is that the conductivity does not remain constant so that, unless some means of maintaining CR equal to  $\epsilon_0/\lambda_+$  were devised, perfect compensation would not be possible.





Fig. 3.2 The Air-earth Current Collector

### 3.1.3 Construction of collector

A circular collector, of diameter 0.71 m, was constructed of aluminium. Fig. 3.2 illustrates the details of construction and installation. The conical bottom assisted drainage of rain water through a small hole in the centre. A cylinder 15 cm in diameter shielded the drainage hole sufficiently to prevent charged drops of water leaving before giving up their charge. Since the rest of the collector was made water-tight, water could escape only through this small hole. It was installed, filled with soil, with its top flush with the surrounding ground. A gap of about 2 cm was left between it and a surrounding guard ring positioned at the same level.

The insulators were made of polytetrafluorethylene (P.T.F.E.) because of its water-repellent properties. To support the weight of the collector and soil, 4 pairs of these insulators were used each insulator being  $1\frac{1}{8}$  inch long by 1 inch diam. Three grooves were cut round the circumference of each insulator, to increase the insulation path. A double shield arrangement and heater coils were provided, as shown in Fig. 3.3, to keep the insulators clean and dry. The insulators and shields, together with the V.R.E. head, were mounted on a rigid handy-angle frame, which in turn was positioned on a second frame concreted to the bottom of the pit in which the collector was installed. By means of brass locating pins, the collector was held on top of the insulators, and could easily be lifted off to provide access to the

FIG.3.3. Construction of insulators for air-earth current collector

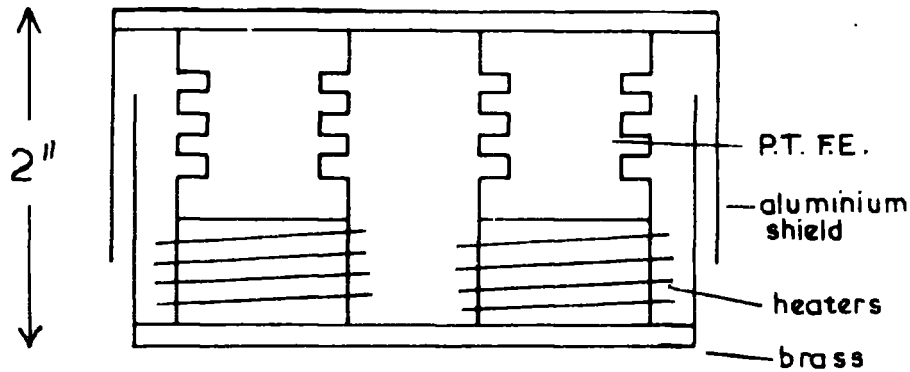
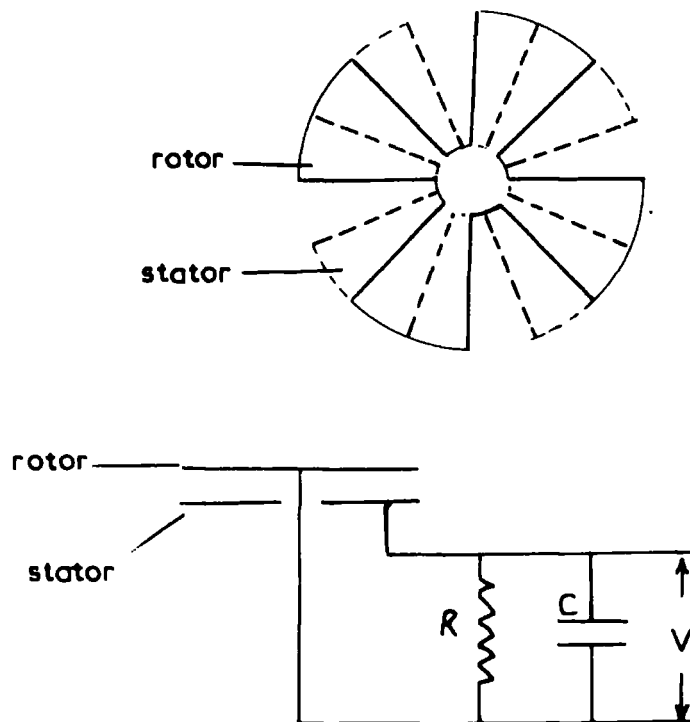


FIG.3.4. Principle of operation of field mill



insulators and V.R.E. head unit.

The surface area of the collector was  $0.4 \text{ m}^2$ , so that, with the  $10^{10} \Omega$  input resistor, an air-earth current density of  $2.5 \text{ pA m}^{-2}$  was registered as 10 mV on the V.R.E. This value is close to the average fair-weather value of current density, so that the range giving  $\pm 12.5 \text{ pA m}^{-2}$  was found to be suitable for both fair and some disturbed weather measurements. Compensation for displacement currents was achieved with a time constant of about 3 minutes. This is shorter than the value which would be given by KASEMIR's method, for fair-weather values of conductivity, but for conditions which change slowly the errors would be small.

### 3.2 The Field Mills

#### 3.2.1. Principle of operation

The field mill is one of a number of different types of field machines which have been used to measure the potential gradient at the ground from the bound charge. This is achieved by using a fixed plate which is alternately exposed to and shielded from the earth's electric field. The plate is connected to earth via a parallel combination of resistance and capacitance (Fig. 3.4). The alternate charging and discharging of this plate, and capacitance, produces an a.c. signal which can be amplified. If  $Q$  is the bound charge on the plate, when exposed, and  $C$  is the capacitance to earth of the plate and capacitor, then the potential  $V$  of the plate is  $Q/C$ . Therefore the alternating voltage produced across

the resistance R will have a peak to peak value of not greater than  $V = Q/C$ . The actual value of this voltage depends on whether the capacitor charges and discharges fully each cycle. A typical field mill comprises an earthed rotor which is divided into 8 equal segments, four of which are cut out. This rotates above a similar stator connected to an amplifier. The theory of the field mill has been given by MAPLESON and WHITLOCK (1955) and rederived by GROOM (1966), so that only a summary need be given here. If the effective area of the stator is A, the charge induced on it due to a potential gradient F, is

$$Q = A \sigma = -A \epsilon_0 F$$

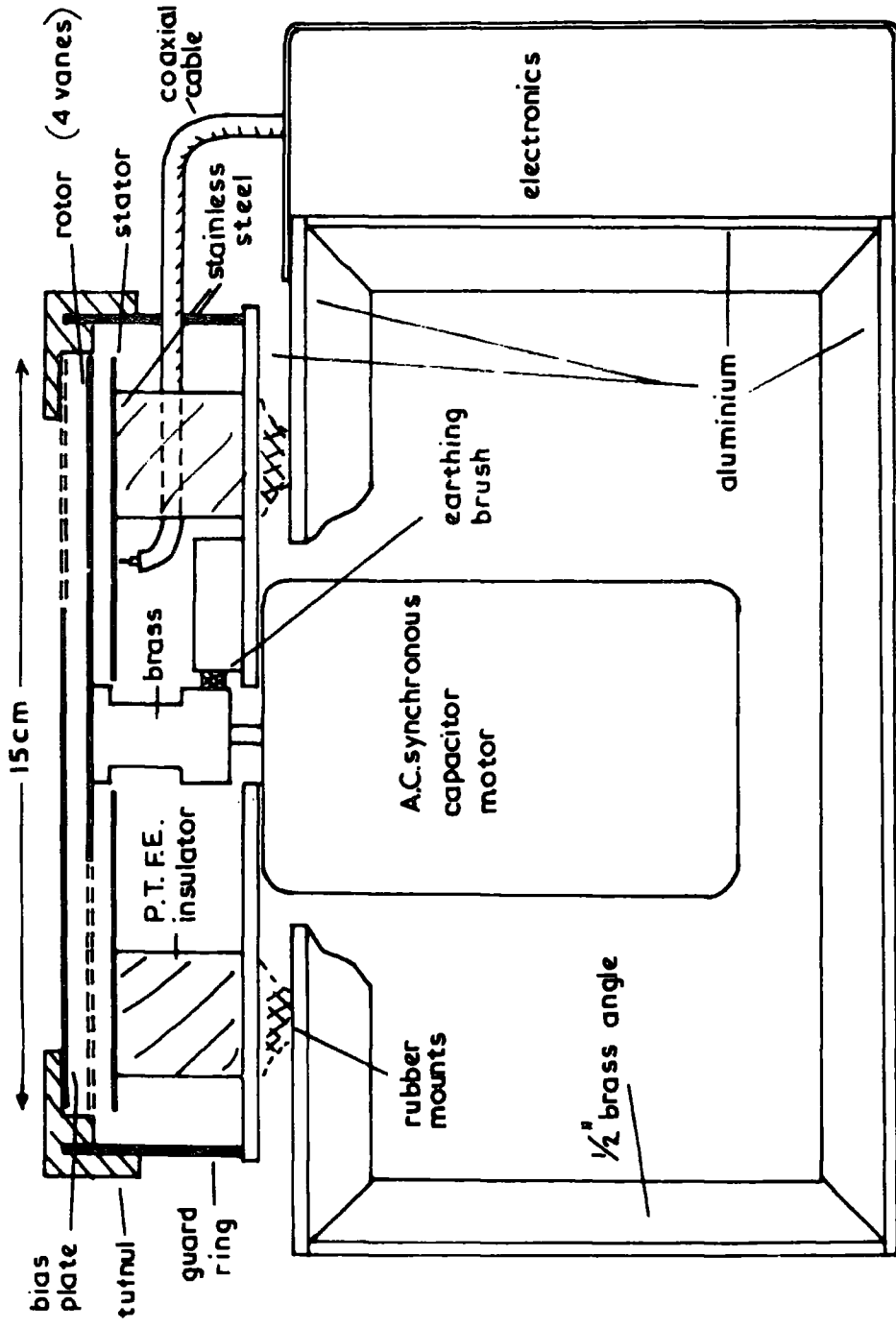
so that the maximum voltage is

$$V = \frac{-A \epsilon_0 F}{C}$$

The condition for V to be obtained depends on the values of C, R and the frequency, f, of the a.c. signal. The theory of the field mill shows that the a.c. voltage will equal V so long as  $2 fRC \gg 1$ . In practical terms the condition is satisfied for  $fRC > 1$ , since the error here is no greater than 1 part in about 500. That there should be no dependence on frequency is important if the speed of rotation is liable to vary.

This alternating signal may be amplified and the output signal, a.c. or rectified d.c., should be proportional to the magnitude of the potential gradient at the surface of the stator. However, the sign of the potential gradient will be unknown unless some means of

FIG.3.5. Construction of field mill



sign discrimination is used. The method employed here was to displace the zero reading of the mill, by applying an artificial, constant electric field. The details are discussed below.

### 3.2.2 Design and construction of the field mills

Both field mills were identical in design, which differed in certain essentials from the simple one described. The artificial field, to displace the zero, was applied by mounting a segmented bias plate above the rotor. This plate was maintained at a constant potential with respect to earth, so that the stator, which in this case was not segmented, could be exposed alternately to the artificial field and the earth's electric field. The output from the field mill was proportional to the difference between these two fields. In Fig. 3.5 can be seen the construction of the field mill, including the 3 plates, rotor and 2 stators, which are all 15 cm in diameter. An earthed, circular guard-ring supports the bias plate and provides electrical screening for the stator, which is supported on P.T.F.E. insulators and connected to the amplifier via coaxial cable. The guard-ring, and 3 plates are all of stainless steel to resist corrosion and reduce any effects of contact potentials.

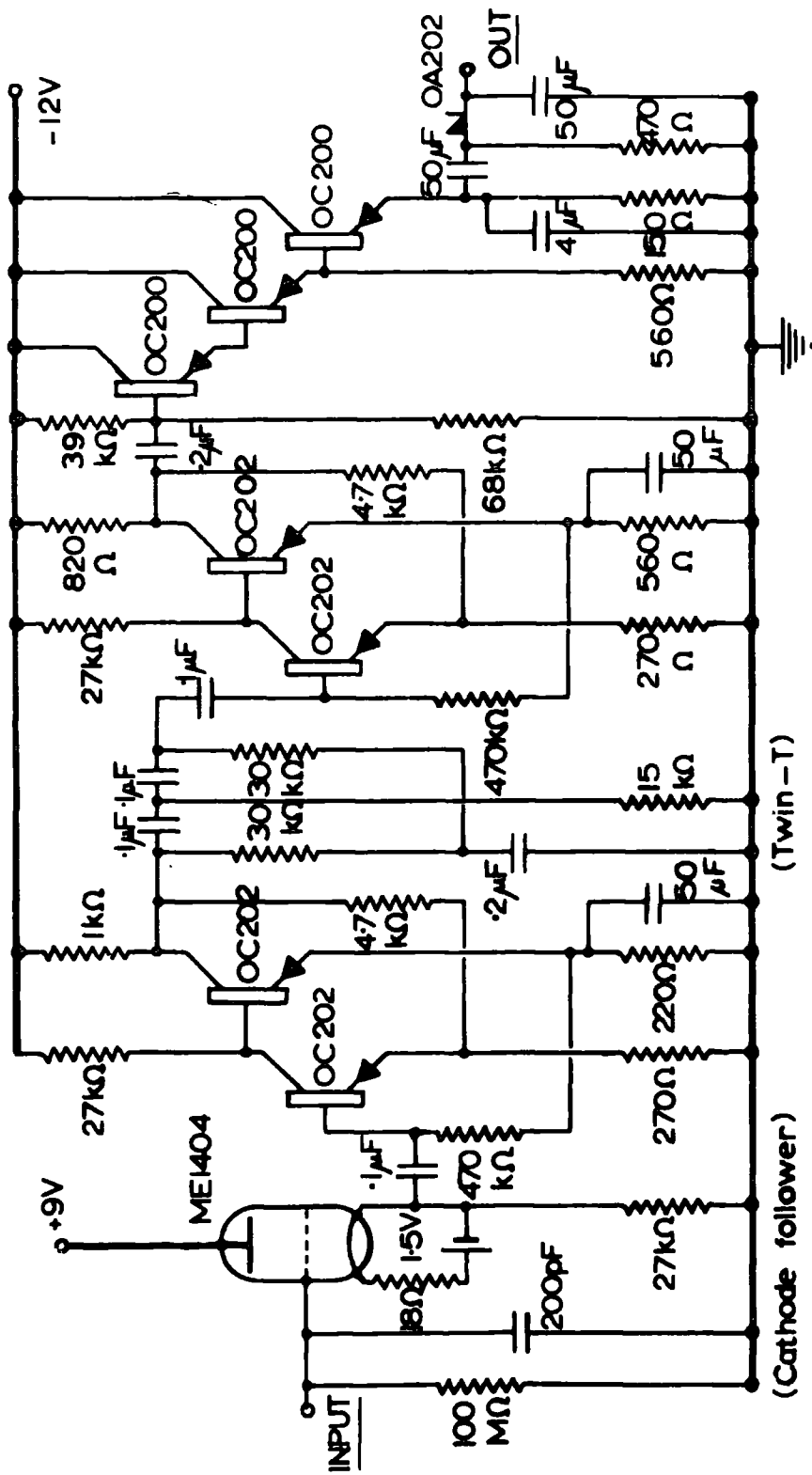
A mains-operated, synchronous, capacitor motor was used to drive the rotor. It was thought that mains pick-up could more easily be eliminated than interference from the commutator of a d.c. motor. At any rate, the use of an a.c. synchronous motor



was more convenient. The rotor was earthed via a carbon brush which made contact with the brass bush supporting the rotor. Both mills were quiet in operation, the moving parts having been carefully balanced by Mr. D. M. Smith, who also was responsible for the design and construction of the two field mills. The motor, plates and guard-ring were all mounted on an aluminium box, which was originally designed to house the electronics, by four rubber mounts. These further helped to reduce vibration.

The bias plate needed a stable d.c. voltage which could be set at an appropriate value for the range of potential gradient required. Conveniently, each V.R.E. had a spare power supply at -105V, stabilized to better than 1 per cent. The bias voltage was taken from this via a potential divider, the polarity being such that a positive potential gradient increased the output and a negative one decreased it. The bias plate was fixed 1 cm above the stator so that, since the stator had equal exposures to both fields, a range of  $\pm 500 \text{ V m}^{-1}$  required a bias voltage of -5 volts. Since the permanently-used field mill was to be used in all weather conditions, a choice of two ranges was provided. The mill was recalibrated several times but one pair of ranges used often was  $\pm 500 \text{ V m}^{-1}$  and  $\pm 5,000 \text{ V m}^{-1}$ , excluding the exposure factor. The change from one range to another was accomplished from inside the laboratory by means of a switch which changed both the bias voltage and amplifier sensitivity.

FIG. 3.6 The Field Mill Amplifier (Original design)



The zero stability was checked by shielding the field mill from the earth's electric field and adjusting the output to give half of full-scale deflection.

### 3.2.3 The electronics

Two completely different amplifier circuits were designed and constructed, although for the period of recording, from which the results were taken, only the second was in use. The first, shown in Fig. 3.6, employed an electrometer valve as first stage with p-n-p transistors for the later stages. Heavy negative feedback was used to increase the stability, but the amplifier suffered from being too cumbersome, especially since it needed 3 power supplies, and not sufficiently reliable for continuous measurements.

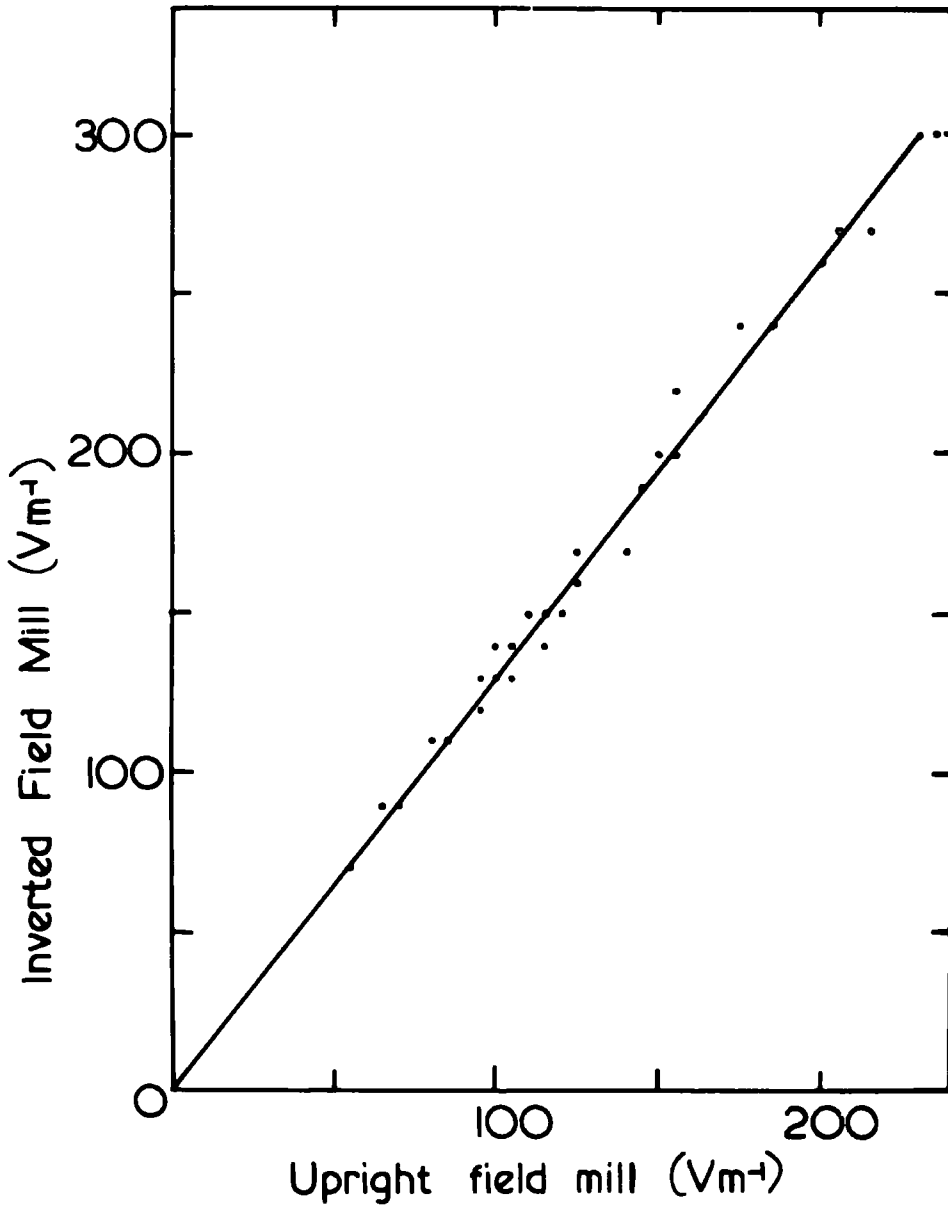
The second amplifier (Fig. 3.7) uses n-p-n silicon planar transistors throughout. The circuit is a modification of one designed by Mr. I.M. Stromberg. An input impedance of  $30M\Omega$  was obtained and this proved adequate for the purpose. The two amplifier stages, each employing negative feedback to control the gain, had an overall gain of 100. Since two ranges were provided a relay was employed so that the amplifier gain could be changed from inside the laboratory. The gain was changed by altering the amount of feed back in the second amplifier stage. For simplicity, the twin-T filter used in the earlier amplifier, in order to reduce mains pick-up, was omitted from the second design. Instead, the

pick-up was lessened by fixing the amplifier on the side of the field mill, and the connection to the stator was made with a short length of coaxial cable kept well away from the motor. This proved most satisfactory as the extent of the pickup was almost negligible. Connections to the amplifier were made via 6-way screened cable between the field mill and laboratory. Initially some trouble with earth loops was experienced, but this was avoided by reducing the current through the earth line and also by using an earth wire of lower resistance.

#### 3.2.4 Installation and calibration

Of the two mills which had been constructed only one was used permanently, the other serving as a spare. The permanent, all-weather field mill was mounted in an inverted position, with the plane of the stator 1 m above the ground. The second mill, when in use, was placed in a small concreted pit with its stator flush with the ground, so that its exposure factor would be very close to unity. In this position it was used to estimate the exposure factor of the inverted mill. Both mills were calibrated under identical conditions, as explained below, and their outputs recorded simultaneously for periods of several hours during fair weather, when the space charge concentration near the ground was low. The exposure factor represents the ratio of the potential gradient at the field mill to that over perfectly level ground. Space charge close to the inverted field mill will produce a different potential

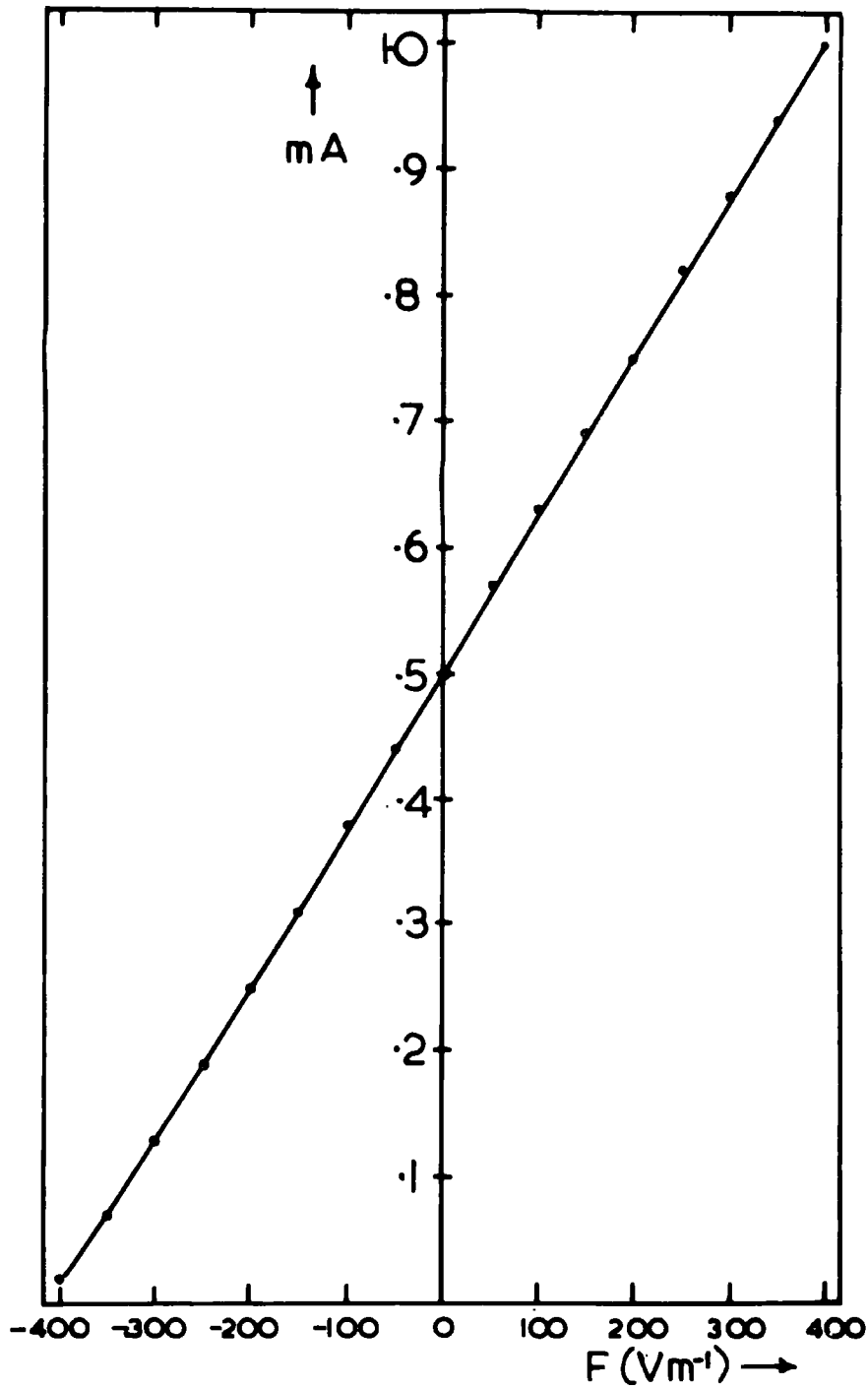
FIG.3.8. Comparison of Field Mill outputs-16h to  
21h Dec 11<sup>th</sup> 1967



gradient at the mill than space charge higher up, whereas over level ground, where the lines of force can be assumed vertical, there will be no difference. This means that the exposure factor of the mill can depend on the density of space charge between it and the ground. For this reason the exposure factor was estimated from the simultaneous records made over long periods of time, so as to average out space charge fluctuations as far as possible. The high correlation between the two records, shown in Fig. 3.8, indicates how little the exposure factor depends on changes in space charge density in fair weather. This implies that the estimated value of 1.3 is probably sufficiently accurate for fair-weather conditions.

Each mill was calibrated, in an upright position, by placing over it a calibration plate. A similar earthed plate, 60 cm square, was placed in the plane of the stator, a suitable circular hole having been cut for the field mill, and the calibration plate fixed 10 cm above it. Fig. 3.9 shows the result of a calibration for  $\pm 400 \text{ Vm}^{-1}$ . From time to time, slight modifications were made necessitating recalibration, sometimes for different ranges. They all, however, resembled the calibration curve shown, being nearly linear, although earlier calibrations showed a greater degree of flattening-off at the negative end due to the characteristic of the diode rectifier. The range of  $\pm 400 \text{ Vm}^{-1}$ , as calibrated, represents

FIG.3.9. Calibration curve for field mill-(exposure factor =1)



$\pm 308 \text{ Vm}^{-1}$  after correcting for the exposure factor. After June 30th 1968, the permanent mill was recalibrated for the two ranges  $\pm 8,200 \text{ Vm}^{-1}$  and  $\pm 900 \text{ Vm}^{-1}$ , after correcting for the exposure factor, so that measurements could be made in stormy weather.

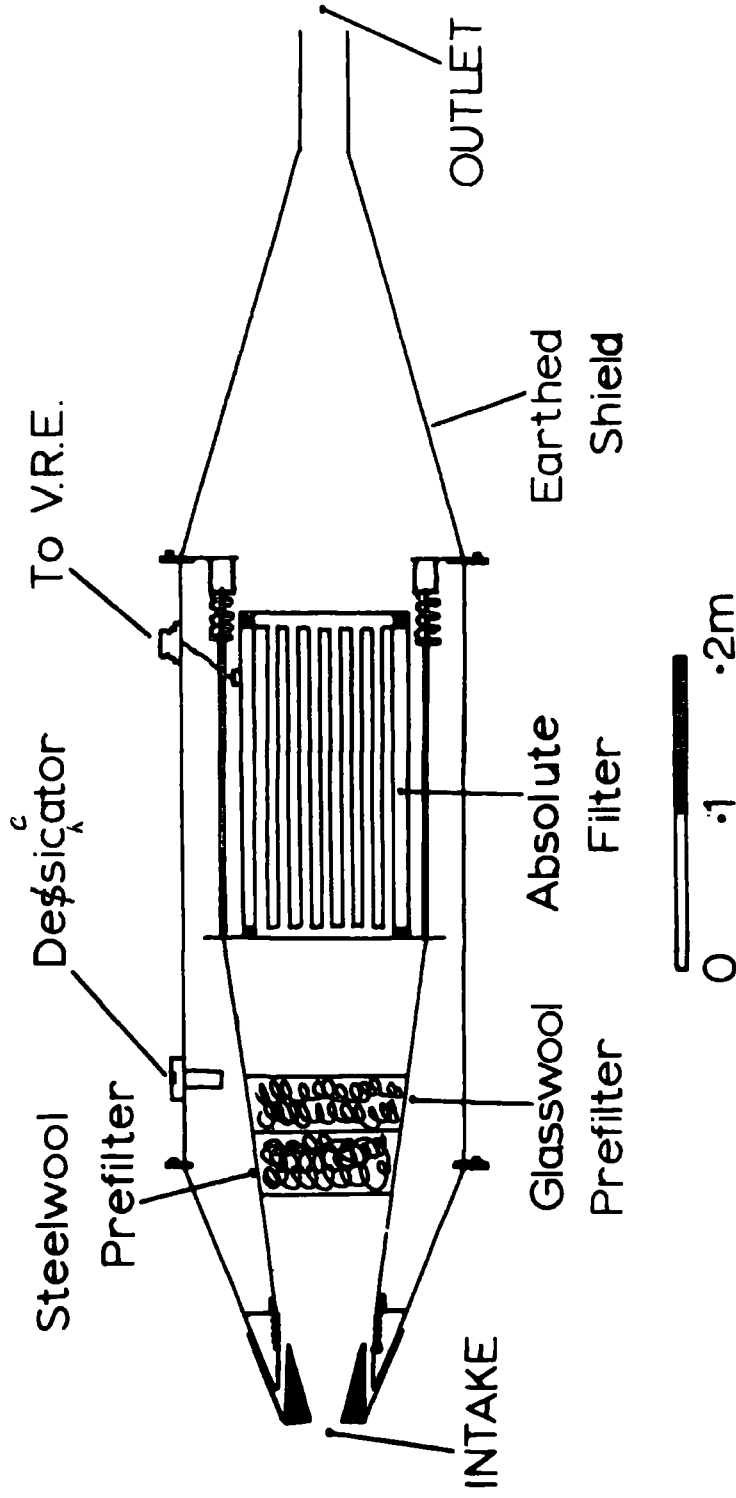
### 3.3 The Space Charge Collector

#### 3.3.1 Principle of operation

Methods of measurement of space charge density have included measuring the potential at a point inside an earthed cage containing the space charge (KAHLER, 1927), the double field mill method (SMIDDY and CHALMERS, 1958) and filtration methods. For the purpose of the present work a filtration apparatus, as used by BENT (1964) has been used. BENT describes this collector in detail, as well as giving the results of tests to determine the efficiency of two such collectors. The filter comprises a glass asbestos medium, described by the manufacturers as "absolute filter material", with fibres of approximately  $0.5 \mu$  diam. encased in an aluminium frame. It is manufactured by the Cambridge Filter Corporation, New York, who claim an efficiency of 99.97 per cent or better for the collection of  $0.3 \mu$  particles. BENT states that during the test, "negative small ions were produced artificially to a density of  $12,000 \text{ cm}^{-3}$  with a polonium ion-generator. Firstly with the collectors in tandem, then using an Ebert ion-counter, and finally in a conductivity



FIG. 3.10 The Space Charge Collector (from BENT, 1964)



test the results showed that the filter retained 99.8 per cent of the negative small ions with an air flow of 3 l/sec".

The construction of the collector is shown in Fig. 3.10. The absolute filter is mounted inside an inner Faraday cage together with pre-filters of stainless steel wool and glass fibre filaments to prevent larger particles damaging the absolute filter. P.T.F.E. was used for the insulators between the filter unit and outer casing, which was earthed to prevent any effects due to displacement currents. The filter unit was electrically connected to the input of a V.R.E. head unit, employing a  $10^{12} \Omega$  resistor. This required the insulation resistance between filter and outer casing to be better than  $10^{13} \Omega$ , so that some form of heating was necessary to keep the insulators dry. The filter element is almost non-conducting but this was no disadvantage since it is mounted inside a Faraday cage on which an equal and opposite charge is induced. Any net build-up of charge on the filter might inhibit the collection of ions of the same sign, but this should not be serious if the flow rate of air through the filter is high enough to overcome any electrostatic forces. With use, the resistance of the filter to the passage of air increases, so that, as commented by BENT, its excellent filtration properties should be maintained if not improved.



Fig. 3.11 Installation of Space Charge Collector

### 3.3.2 Installation

It was necessary to install the collector in such a way that it would operate reliably under all weather conditions. Some weather-proof housing was therefore required for the instrument. However, there was still the problem that rain, or at least water vapour, might be drawn into the collector, and cause insulation breakdown or possibly damage the filter. GROOM (1966) constructed a bad-weather collector, using a small piece of glass asbestos filter paper, which could readily be replaced when damaged. However, the smaller size of filter required a much more powerful fan to produce the considerable pressure drop needed across the filter. It was decided for the present work to use BENT's collector, and install it in such a way that the effects of rain could be minimized. A further problem was that vapour passing through the filter would cool and condense on the low pressure side, possibly with the formation of bubbles which could remove charge from the filter.

Initially the collector was mounted in an aluminium box with its inlet tube facing out horizontally. Heating was supplied by a 120 W heater coil wrapped round the collector. This arrangement suffered from insulation breakdown in rain. Finally a timber box, housing the collector in an inverted position, was mounted on a truncated pyramid of handy-angle concreted into the ground. Fig. 3.11 shows this arrangement with the inlet about 0.8 m above

the ground. Two pairs of lamps, wired in series, provided sufficient heat to keep the collector warm and so inhibit the condensation of water vapour. The box was made completely weatherproof, and provided good thermal insulation. The V.R.E. head unit was mounted close to the collector and connected via a short length of coaxial cable which had a rigid outer conductor. To eliminate small fluctuations the time constant of the measuring instrument was increased to about 1 min.

### 3.3.3 Fan Unit

A single fan was used to draw air through both the conductivity chamber and the space charge collector. Due to break-down the fan was replaced several times during the 18 months of use. Each fan was taken from a vacuum cleaner and rehoused in a brass cylindrical box, connected via rubber and plastic tubing to the two collectors. Gas meters were used to monitor the air flow, which could be adjusted by using a variable auto-transformer to vary the voltage to the fan. The fans were all rated at 500W or more for 240V, a.c. A timber box was constructed to house the fan unit and the two gas meters, and was placed downwind of the space charge collector, for prevailing winds. The fan was run at, normally, about 100V to 150V giving flow rates between 1 and 2 l s<sup>-1</sup>.

FIG.3.12. Principle of operation of Gerdien chamber

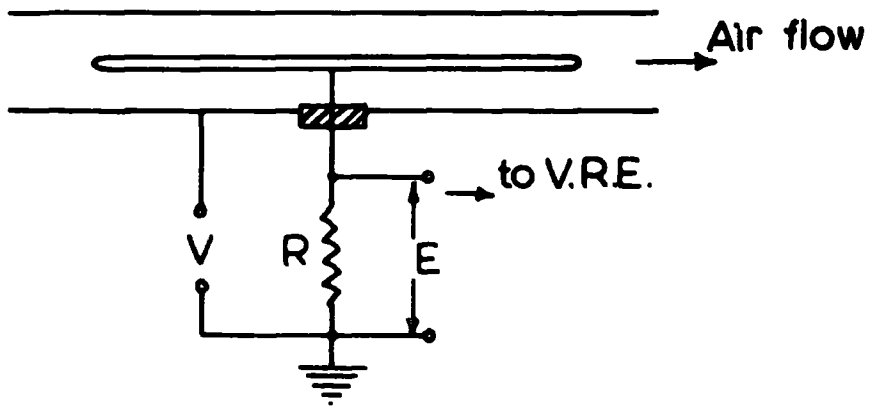
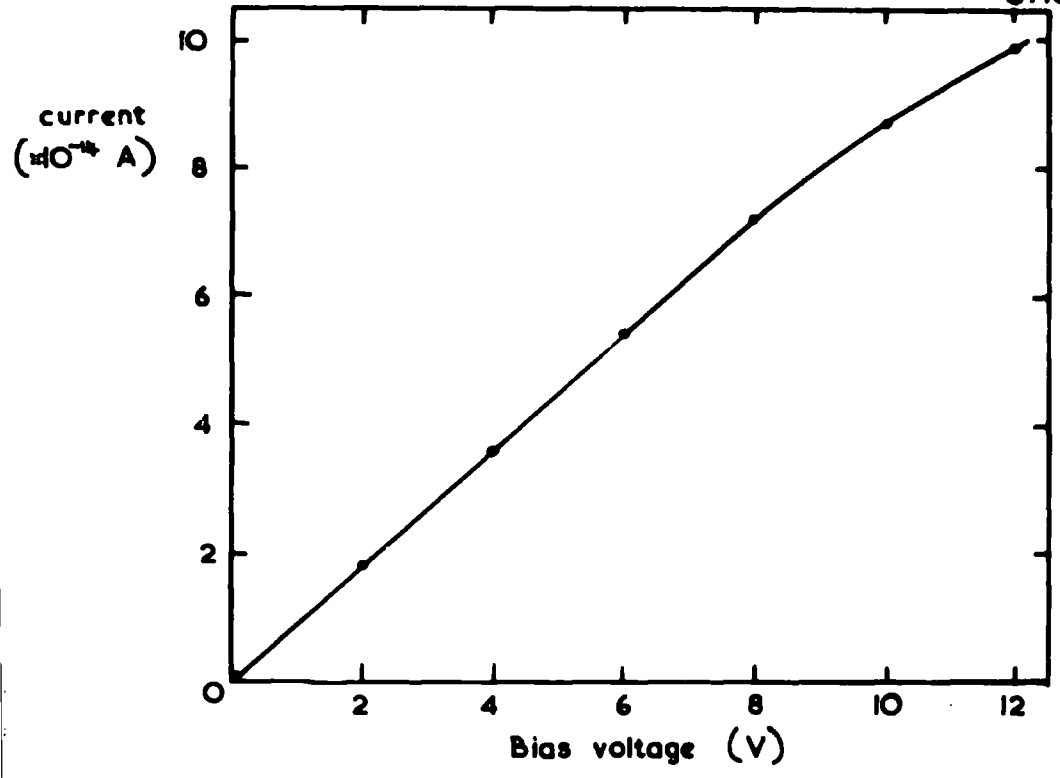


FIG. 3.13. Current-voltage characteristic of conductivity chamber



### 3.4 The Conductivity Chamber

#### 3.4.1 The Gerdien chamber

The cylindrical condenser method was first used by GERDIEN (1905) for the measurement of conductivity. The air, whose conductivity is to be measured, is sucked through the Gerdien chamber, which comprises two coaxial cylinders, one much smaller, in radius, than the other. Such a chamber is shown diagrammatically in Fig. 3.12. The two cylinders are insulated from each other, so that if a potential difference exists between them, small ions will move towards either cylinder. Those arriving at the central electrode will constitute a current which can be measured by a V.R.E. The arrangement of chamber, bias voltage, V.R.E. is shown in Fig. 3.12. The electric field at the outer cylinder will be much less than that at the inner cylinder, which will therefore collect more ions. The sign of the ions collected will depend on the polarity of the bias voltage so that for one instrument at any one time, the conductivity of only one sign will be measured.

For a particular Gerdien chamber the current measured by the V.R.E. will depend on both the conductivity of the air being measured, and on the bias voltage. The relation between voltage and ionic current will be linear, so long as the concentration of small ions in the chamber is not seriously depleted by the electric field. This requires a sufficiently high flow rate, otherwise, at the other extreme when all small ions are collected, the chamber



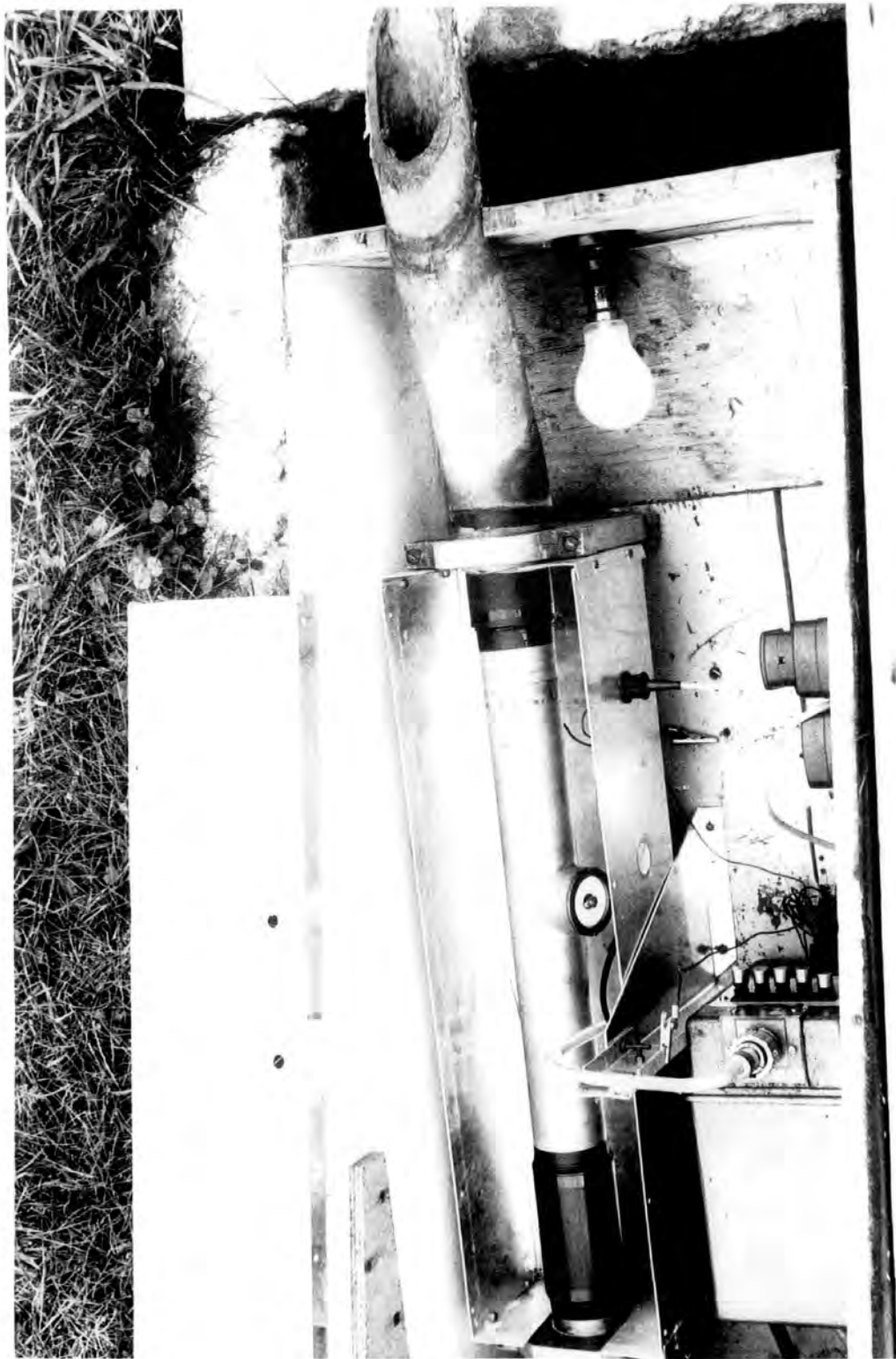


Fig. 3.14 Installation of Conductivity Chamber

behaves as an ion counter. For air of unipolar conductivity being drawn through a Gerdien chamber of capacitance C, the current collected from the centre electrode is given by

$$i = \frac{CV \lambda}{\epsilon_0}$$

where V is the bias voltage, which is limited to a maximum value depending on the flow rate. If now E is the voltage developed across the V.R.E. resistor R, the conductivity is given by:

$$\lambda = \frac{E \epsilon_0}{VCR} \quad (\text{see CHALMERS, 1967a, p61})$$

In Fig. 3.13 is shown the variation of E with V, for a flow rate of about  $21 \text{ l s}^{-1}$ , where for  $V < 10\text{V}$  the relation is linear. The bias voltage used throughout was + 6V for the positive conductivity.

### 3.4.2. Installation

The Gerdien chamber, as used and described by HIGAZI and CHALMERS (1966), was installed as shown in Fig. 3.14. The outer cylinder of brass was 5.4 cm in diam. by 35.6 cm long. The inner, solid cylinder, 8 mm in diam. and 25.4 cm long, was insulated from the outer cylinder by a circular disc of P.T.F.E. The capacitance of the complete cylindrical condenser was found by Higazi to be 8.51 pF. An earthed rectangular aluminium box provided electrical shielding, to eliminate any spurious effects from displacement currents, while the outer timber box protected the chamber and V.R.E. head unit from the weather. It was not possible to install the chamber vertically, as Higazi had done, and any sharp bends

would have reduced the measured conductivity, so the chamber was installed at an angle. The air was sucked through a wide cardboard tube with the inlet flush with the ground. Arrangements were made to drain the tube of any rain which entered, before it could be sucked into the chamber. However, some insulation breakdown was experienced after heavy rain, probably due to water vapour condensing on the insulator. The arrangement with the inlet flush with the ground reduced to a minimum any effect of distortion of the electric field, which might have reduced the measured conductivity, by preventing some of the ions from entering the chamber. However, at a later date (July, 1968) an earthed aluminium shield was placed over the inlet to provide added protection against heavy rain. The shield appeared to have an inappreciable effect on the measured conductivity but the performance in heavy rain was much improved.

The time constant of the V.R.E. was increased to about 1 min, so as to eliminate small fluctuations either in conductivity or, more especially, from instrumental effects. The V.R.E. head unit was mounted alongside the chamber, and connected to it via a coaxial cable inside a rigid length of aluminium tubing. For most of the time only the positive conductivity was measured since at ground level in fair weather, positive ions should predominate. HIGAZI, in Durham, found a ratio, for positive to negative conductivity, of 1.43 at ground level. From this it seemed that, of the two, the positive conductivity was the more important to

FIG. 3.15. Wind direction potentiometer & housing

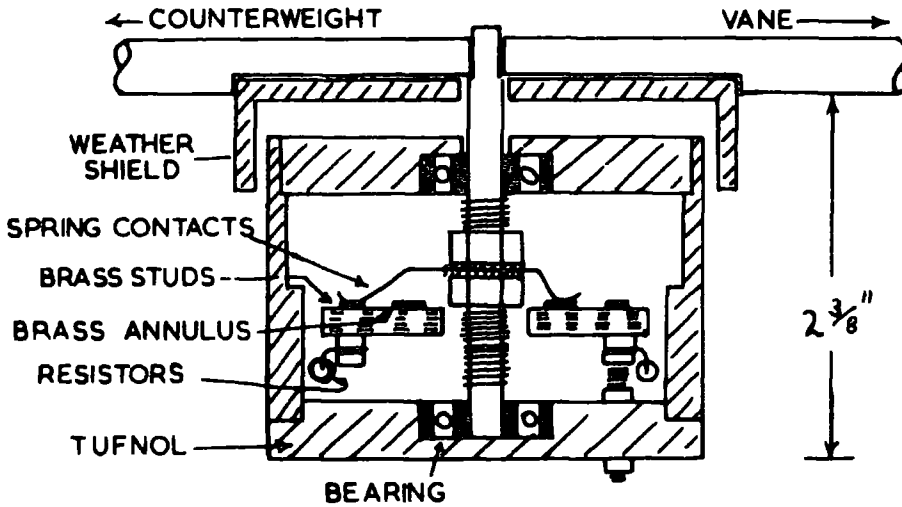
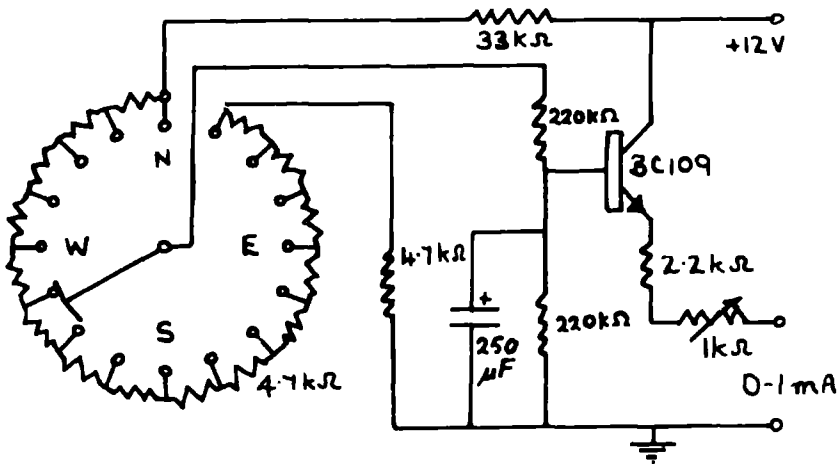


FIG.3.16. Wind-vane circuit diagram



measure. Initially an attempt was made to measure both signs by reversing the polarity of the bias voltage once every few minutes. However, the instrument required about 10 min or more to settle down after each reversal. Since some trouble was experienced in keeping the instrument working, it was not possible to spend more time on this attempt to measure both signs. In any case, it was thought that such an attempt would only have increased the chances of breakdown of the instrument.

### 3.5 The Wind Vane and Anemometer

#### 3.5.1 The wind vane

Measurements of both wind speed and direction were made in order to determine the effect, if any, these had on the atmospheric electric elements. In particular, certain wind directions might cause more pollution to be present than others. For the measurement of wind direction, a vertical shaft, supporting the vane, was allowed to rotate freely by means of two ball-race bearings, housed in a small cylindrical tufnol box, as shown in Fig. 3.15. Inside the box were 16 small brass studs equally spaced around a circle. Between adjacent pairs of these studs were soldered a total of 15 resistors, each  $4.7K\Omega$ . A brass brush, fixed to the shaft, made contact with one or other of these studs depending on its orientation. This potential divider was used to give an output voltage which, as can be seen from the circuit in Fig. 3.16, depended on

FIG.3.17. Construction of anemometer (less cups)

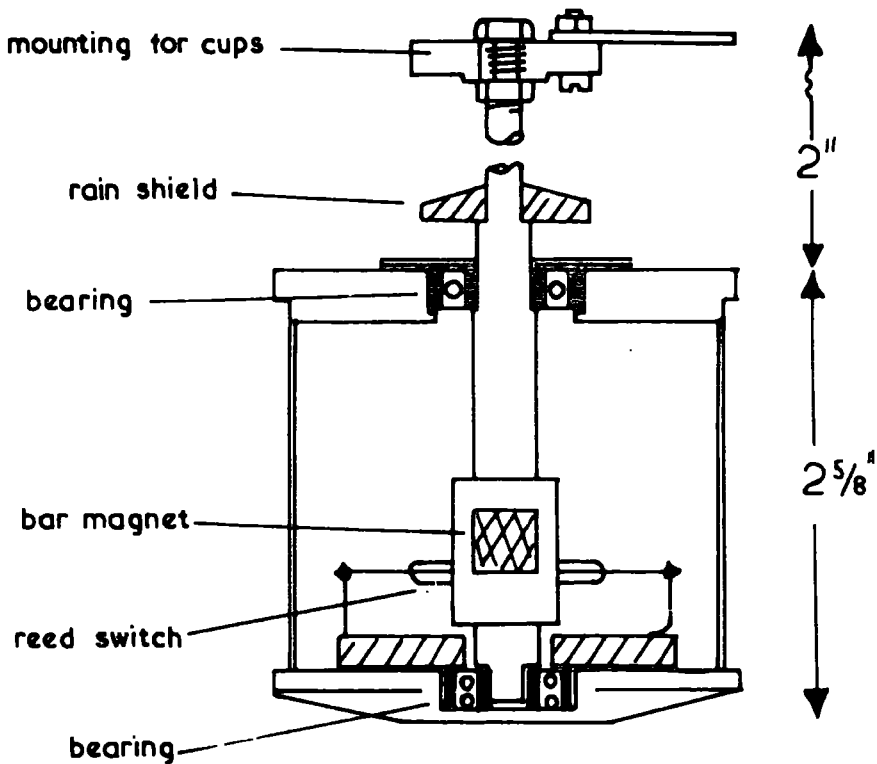
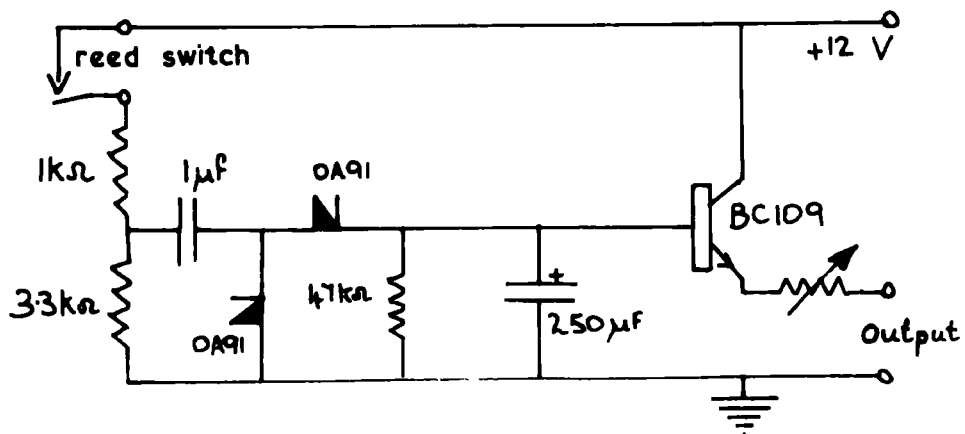


FIG.3.18. Circuit diagram for anemometer



the orientation of the vane.

### 3.5.2 The anemometer

A 3-cup anemometer was used, its speed of rotation being measured by converting it into electrical pulses. The bearings were both simple, self-aligning ball-races but care was taken to ensure that friction was reduced to a minimum. Fixed to the anemometer shaft was a small bar magnet which operated two reed switches, twice each revolution. One reed switch was used to supply pulses, of constant amplitude, to a simple diode-pump via a suitable differentiating circuit, while the other operated a counter which could be used to measure the run of wind. The construction details are shown in Fig. 3.17 and the circuitry in Fig. 3.18. Both wind vane and anemometer were adequately shielded from the weather and provided with small heater lamps wired in series and connected to the low voltage supply.

### 3.5.3 Installation

A steel mast, 13 feet long by  $1\frac{1}{2}$  inches dia. was erected, by means of U-bolts, on to a sturdy supporting bracket of spot-welded steel angle. This in turn was bolted to the outside of the N wall of the laboratory. The mast was stayed with 3 lines as a precaution against the possible effects of strong winds. Both wind vane and anemometer were mounted on a 30 inch length of 1 inch diam. steel tubing, secured to the top of the mast, as shown in Fig. 3.19. The wind vane was at a height of about 10 m



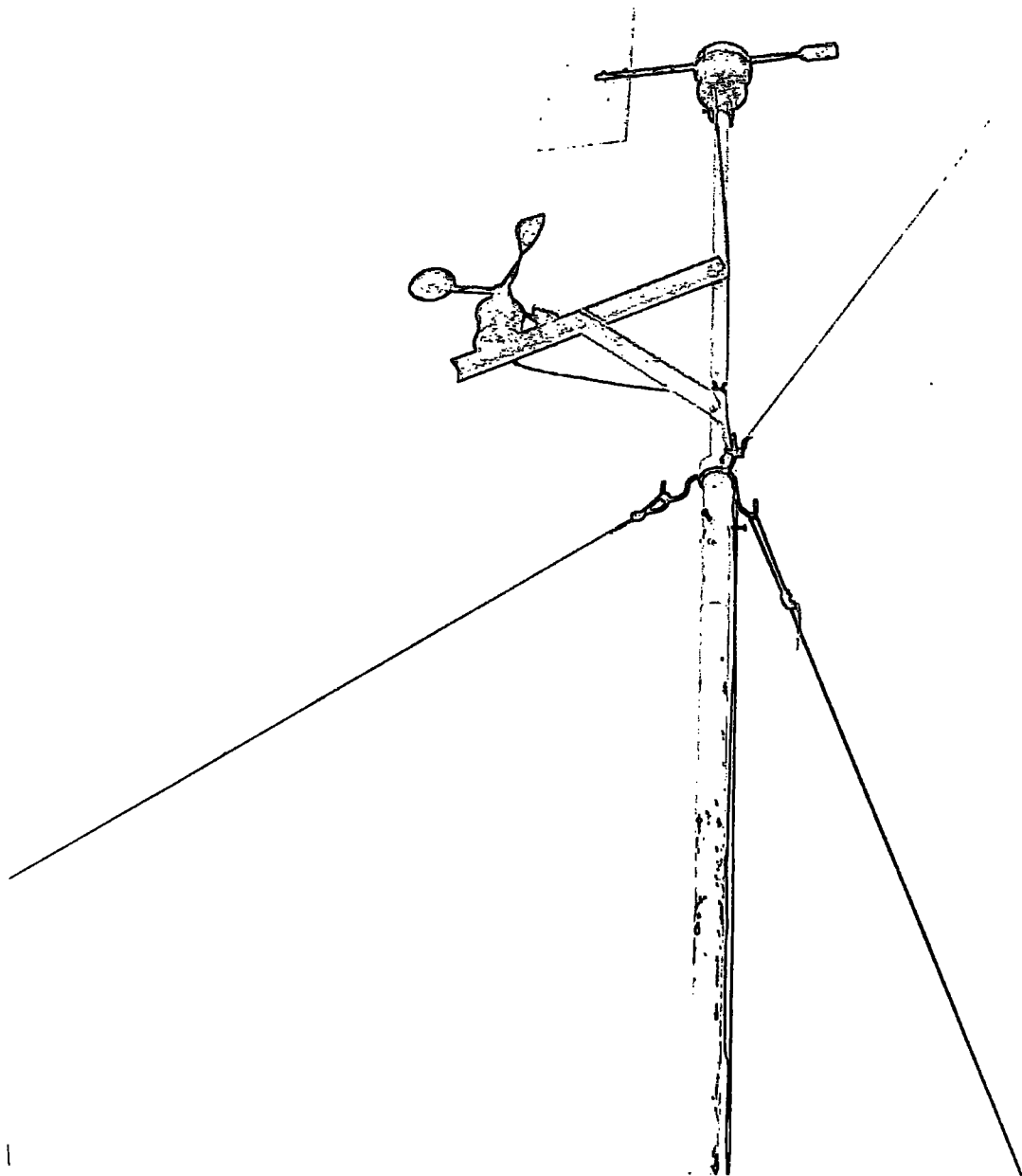


Fig. 3.19 Installation of Anemometer and Wind Vane

above the ground, and was sufficiently high for all but NW winds, where the trees nearby provided some shielding, although this was not thought to be serious.

### 3.6 Rate of Rainfall Measurement

#### 3.6.1 Existing methods of measurement

In meteorology most methods of measuring rate of rainfall are mechanical, and tend to be cumbersome, insensitive to small variations in rain-fall and need frequent chart changing. Usually, as in the tilting bucket method, the integrated rainfall is measured in steps of 0.01 inch. Direct measurements of rate of rainfall require large collecting areas and even then are not very sensitive. In a more sensitive method, the rain water is used as the dielectric of a condenser, so that either the rate of rainfall or the integrated rainfall can be measured. For rate of rainfall, the apparatus must be constructed in such a way that the volume of water which it contains is proportional to the rate of rainfall. This method was thought to be susceptible to unreliability when used continuously for long periods of time, so a simpler, more reliable method was used, and is described below.

#### 3.6.2 The acoustic rate of rainfall recorder

In the method used for measuring rate of rainfall, a microphone was placed under a thin aluminium sheet, so that the sound produced by rain drops striking the aluminium could be converted into an

FIG.3.20. Acoustic rate of rainfall recorder

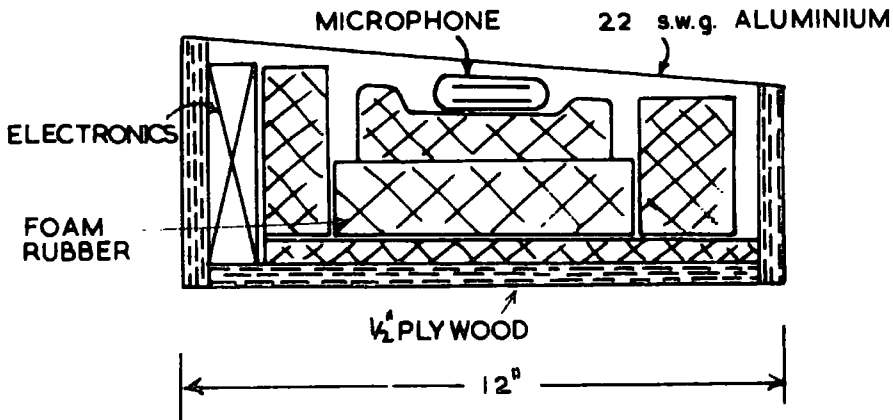
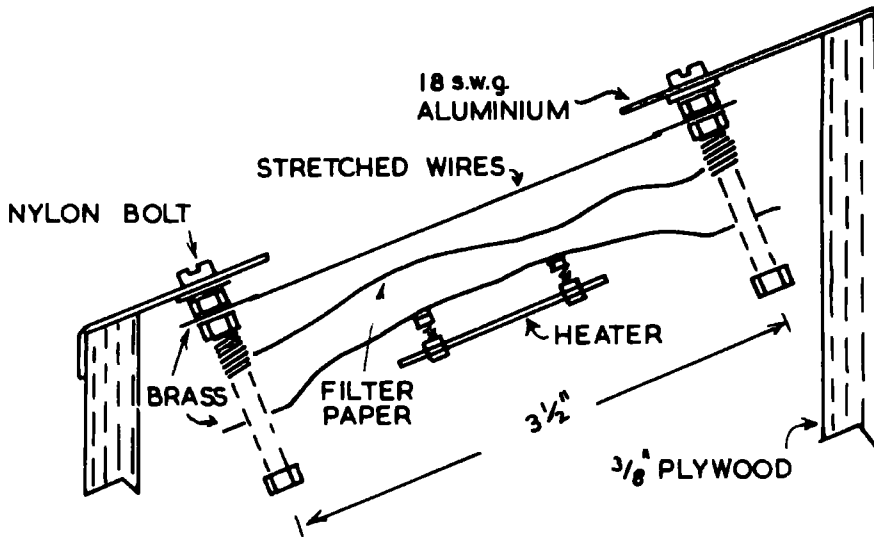


FIG.3.21. Construction of rain switch.



electrical signal, which, it was hoped, was dependent on the rate of rainfall. The microphone was placed on foam rubber to reduce noise from unwanted vibrations. A small timber box, 30 cm square, contained both microphone and electronics, and was covered with the aluminium sheet as can be seen in Fig. 3.20. A simple two stage amplifier with emitter follower output was used, and a time constant of about 1 min. employed to smooth out rapid fluctuations in rain intensity.

To prevent any ambiguity due to noise in non-raining conditions, a rain switch, described below, was incorporated to switch on the output to the recorder when rain commenced. By biasing the output, the rain switch was able to indicate the presence of rain, even when this was too light for the microphone to register it. Drops of rain shorted the switch, which, by means of a transistor, caused a reed switch to be closed. A small heater, dissipating about 8W kept the rain switch dry when no rain was falling and allowed it to switch off after the rain had ceased. The construction of the rain switch is shown in the exploded view in Fig. 3.21. A number of fine wires are stretched over a flat metal surface with a piece of filter paper sandwiched in between. Good insulation was maintained while the paper was dry, but the first drop of water caused a short and the output to the recorder was switched on. The lower plate was initially of aluminium but corrosion impaired its efficiency so it was replaced by brass. The complete circuit

FIG. 3.22 Rainfall Recorder Amplifier

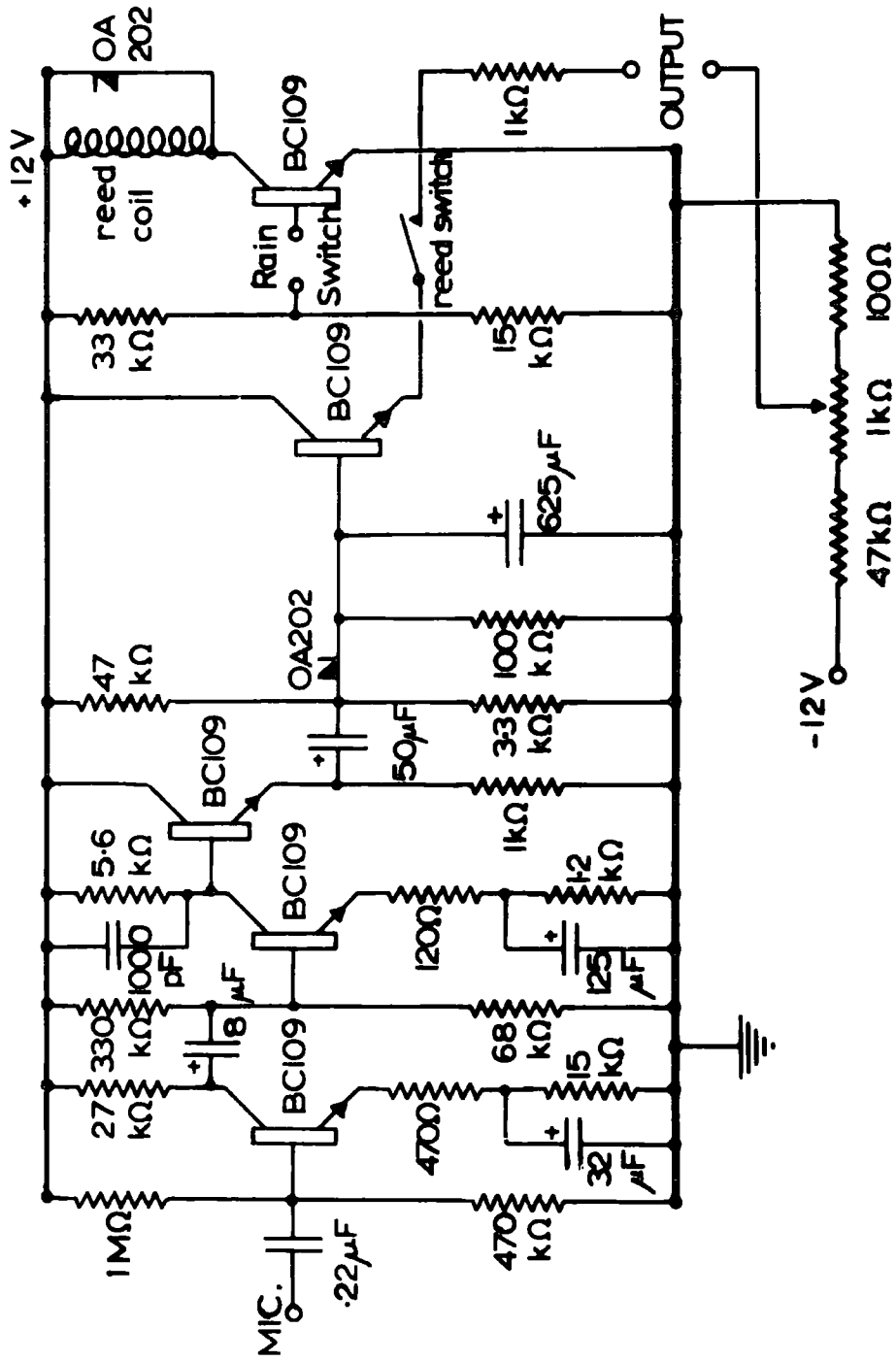
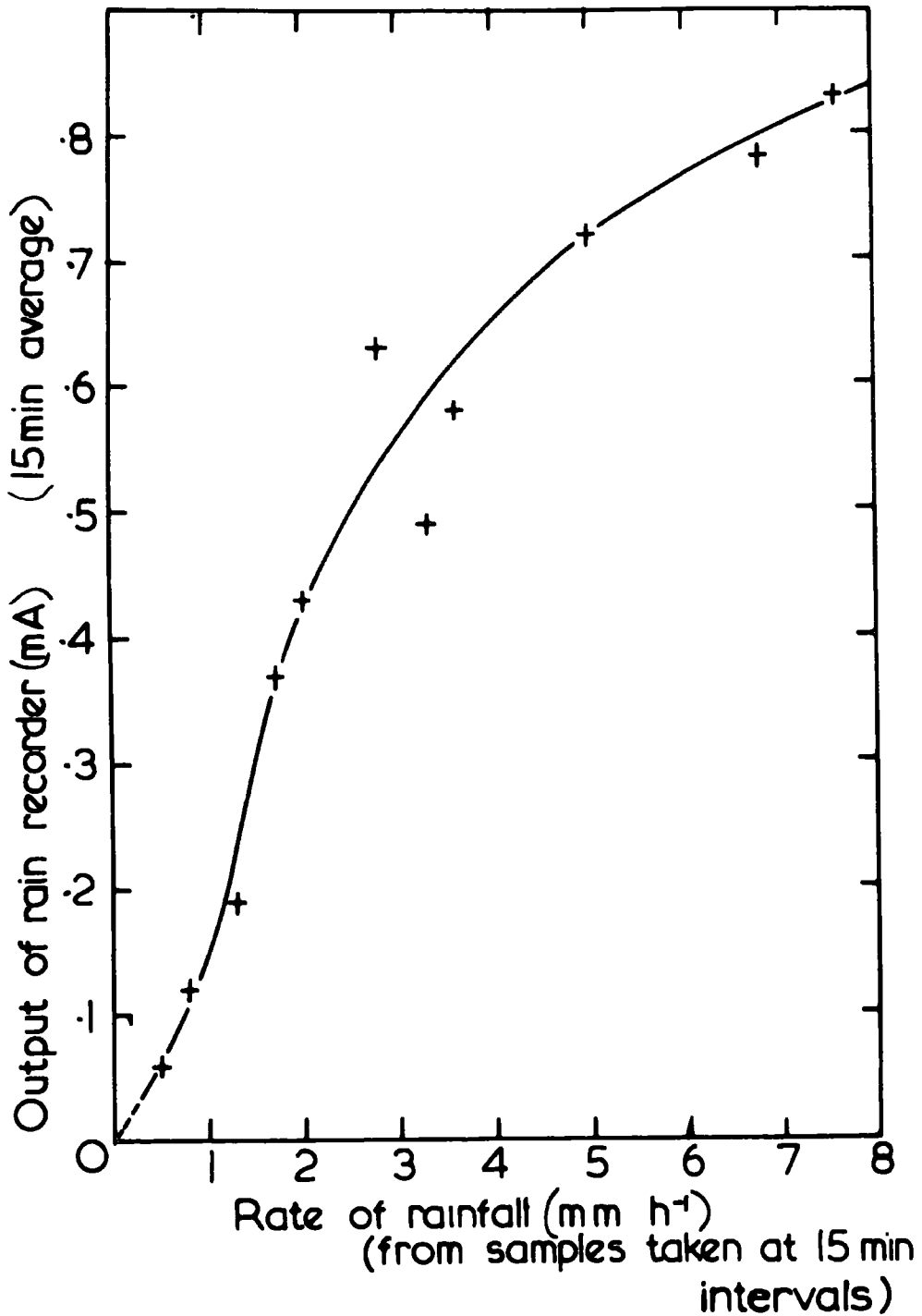


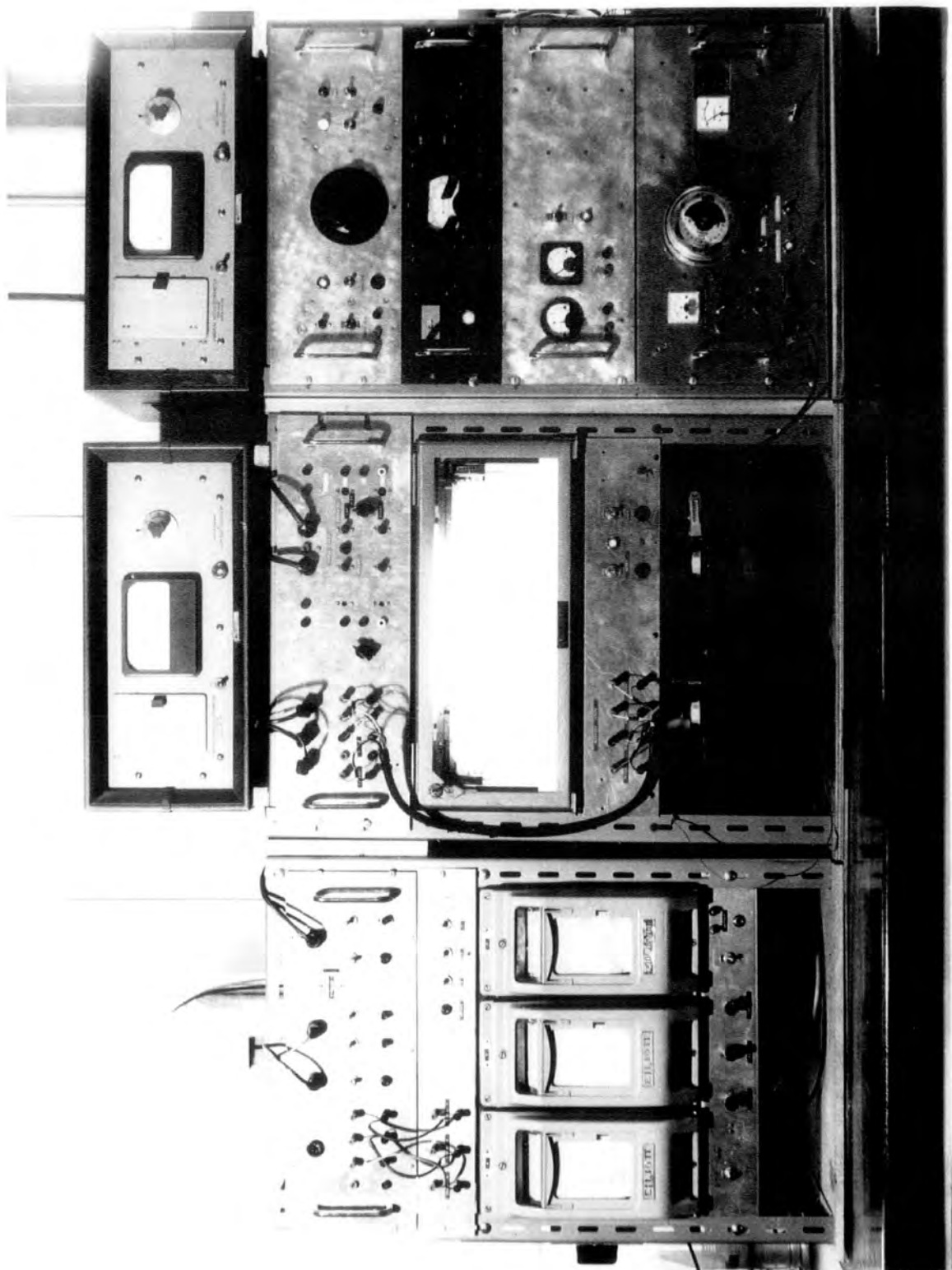
FIG.3.23. Calibration of rainfall recorder



for amplifier and rain switch is given in Fig. 3.22.

In Fig. 3.23 is a calibration curve obtained by measuring the volume of rain collected by a standard rain gauge in a given time, and averaging the output from the acoustic recorder, over the same period of time. The conditions were of mostly moderate to heavy rain during a number of periods separating a series of thunderstorms on July 1st to 3rd, 1968. In other conditions of rainfall, the calibration would probably be different, due to the different distribution of drop size. This type of rate of rainfall recorder worked reliably for long periods of time, with very little attention apart from periodic changing of the filter paper, and cleaning of the metal parts when corroded. The measurements are probably not very accurate except to indicate the type of rain, i.e. light, moderate or heavy. It does respond well to changes in rate of rainfall, and the time of commencement of rain can be accurately determined. Its lower limit of sensitivity, for the microphone, is probably about  $0,5 \text{ mm h}^{-1}$  or perhaps somewhat lower. Below this rate the threshold level for the switch to operate is determined mainly by the efficiency of the heater. Without this even dew would no doubt cause the switch to operate.





The Recording Instruments and Power Supplies

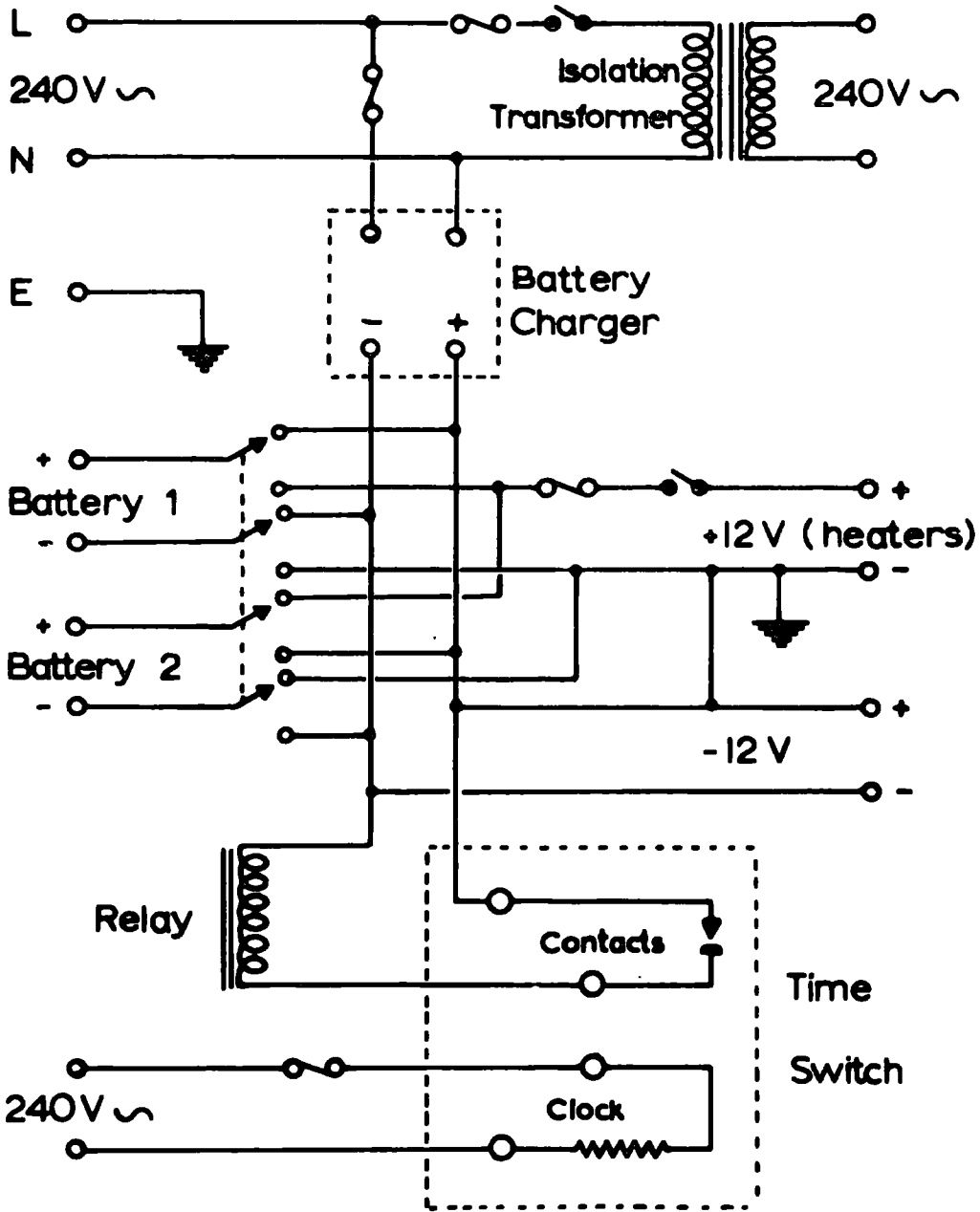
### 3.7 The Recording System and Power Supplies

#### 3.7.1 The pen recorder

The electric elements were recorded on an Elliot 4-channel pen recorder, each channel comprising a 0-1 mA, 500  $\Omega$  galvanometer. The wind and rain records were recorded separately on 3 single-channel pen recorders each 0-1mA, 1200  $\Omega$ . It was later realized that a superior system would have been a multi-channel potentiometric recorder, since the advantage of having all parameters on one chart would have out-weighed the disadvantage of possible confusion. Three channels of the Elliot recorder were centre-zeroed, so that both positive and negative values could be recorded. Due to the displaced zero, the channel for the field mill did not need to be centre-zeroed. The V.R.E's were designed to give 1mA for full scale deflection so that, with the centre zero, only half of full scale of each range was used. On all recorders the chart was divided into 50 divisions, 25 each way for the centre-zeroed channels. Readings were taken off at half-division intervals so that the accuracy of recording, neglecting instrumental inaccuracies, was 2 per cent of full scale each way.

The recording speeds were chosen for a suitable compromise between economy and being able to measure fast changes. For fair weather and many disturbed weather periods, it was decided that a speed of 2 inches per hour would be adequate. This required the changing of charts once every 15 days which was

FIG.3.24 Mains and Low Voltage Supplies



quite convenient. From July 1st 1968 onwards a chart speed of 6 inches per hour was used so as to be able to measure faster changes in stormy weather. This required charts to be changed every 5 days. For the single channel recorders a speed of 1 inch per hour was used throughout.

### 3.7.2 The power supplies

All the instruments were supplied directly or indirectly from the 240V, 50 Hz mains. For outdoor instruments an isolation transformer was used as a safety precaution. The output from this was stabilized at 240 V and its maximum rating of 500W was adequate for the purpose. The distribution box for mains was connected to this transformer by 20 yards of p.v.c. covered, copper sheathed, pyrotenax cable. The cable ducts with their concrete covers provided extra protection for the mains cables.

The low voltage heater supply, for the air-earth current collector, rainfall recorder, wind vane and anemometer, comprised a system of two 12V accumulators. By means of a time switch these were arranged to charge and discharge alternately, the change-overs occurring at 6 hour intervals. The circuit used to perform this changeover is shown in Fig. 3.24. The stabilized power supply was set at 12V and was used for all the transistor circuitry. Stabilization was claimed to 0.1 per cent or better, and in practice there appeared to be no appreciable voltage drift even over long periods of time.

CHAPTER 4.

THE INSTRUMENTAL PROBLEMS OF CONTINUOUS RECORDING

4.1 The General Problems

4.1.1 Maintenance and facilities

As mentioned in Chapter 2, the aim of the present work was to record continuously several of the atmospheric electric parameters. In Durham, previous workers had made observations only intermittently, and, since they were usually present at the time, were able to correct quickly any faults which developed. In the present work, the remoteness of the site has necessitated the use of continuous recording, which could operate reliably for long periods of time. The apparatus, at Lanehead, was subjected to the extremes of weather, so had to be constructed to withstand this. The reliability and endurance of the instruments could be ascertained only by experience, which showed that higher standards of durability were necessary for continuous recording.

During much of the Winter at Lanehead, temperatures were mostly below  $0^{\circ}\text{C}$ , and temperatures of  $-12^{\circ}\text{C}$  at night were not uncommon. For this reason, all instruments were equipped with heaters of sufficient power to prevent moisture from freezing inside the instruments. Despite these, heavy frosts during the early months of 1968 prevented access to the conductivity chamber, which remained out of action until the end of March. General maintenance

and repairs were further hampered by wind, snow and heavy rain, which, during the Winter, made it impossible to make proper repairs to the instruments. For some major repair work, the workshop facilities at Lanehead were often inadequate, so that the faulty instrument had to be returned to Durham, resulting in a loss of recording time. Visits to Lanehead were made about once or twice a week, so that changing of charts and maintenance could be carried out. Quite often, a minor fault, which was easily put right, caused instrumental breakdowns several days before a visit, so that some recording time was lost. Precautions were taken to prevent such breakdowns occurring, but it was impossible to eliminate them altogether. For most of the time, however, the apparatus functioned well and the amount of recording time lost was not too serious.

#### 4.1.2 Sensitivity of instruments

Continuous measurements of the electric properties of the atmosphere under all weather conditions required instruments capable of covering a sufficient range of values, while still retaining sufficient sensitivity for fine-weather recording. However, when one considers the enormous range of values that any one parameter may have, this is obviously not practicable on a single instrument, unless use were made of either a logarithmic amplifier or some means of automatically changing the sensitivity to a new range, to suit the conditions. Neither of these two

expedients proved practicable although the second one might have been possible, apart from the difficulties of suitably modifying the vibrating reed electrometers. It was not possible, either, to use more than one instrument for each parameter, as neither time nor resources were available, so that a compromise solution was used. The sensitivity of each instrument was chosen for a compromise between sufficient accuracy for fair-weather measurements and an adequate range for the majority of disturbed weather conditions.

## 4.2 Accuracy of Measurements

### 4.2.1 General

The overall accuracy of the measurements was affected by the long-term stability of the apparatus. For fair-weather results, random errors of this type could be reduced by taking an average of a large number of readings. The accuracy of individual observations, neglecting instrumental inaccuracies, was limited by the resolution of the pen recorders. Readings were taken from the chart records in steps of 2 per cent of full scale, positive or negative, so that this represented the limit in accuracy. All instruments were calibrated in conjunction with the pen recorders, which therefore introduced no errors greater than the 2 per cent of full scale. The instruments were all subject to some zero-drift during the long periods of continuous use. Frequent zero



checks were made on all instruments, so that for most of the time the zero errors were known to within 2 per cent of full scale.

All instruments were carefully calibrated and installed in such a way as to disturb the atmospheric electric conditions as little as possible. However, in the measurements made, it was difficult to determine the absolute values to a high degree of accuracy. Both field mill and space charge collector, unavoidably, disturbed the quantities which they were measuring. The calibration of each vibrating reed electrometer depended on the value of the input resistor, which had a tolerance of about  $\pm 10$  per cent. These instruments were calibrated against a known voltage, but the current measured depended also on the value of this resistor. To attempt to measure each resistor would have required disturbing the sensitive instruments unduly, not to mention the difficulties of measuring resistances of about  $10^{12} \Omega$  to better than 10 per cent accuracy. It was decided to leave well alone, so as not to interrupt the continuous recording and rely on the manufacturer's stated tolerance. Finally, the nature of the site as a whole would have introduced a further modification of the absolute values. If the instruments had been installed on flat horizontal ground instead, the results would, no doubt, have been different.

#### 4.2.2 Air-earth current

The long term stability of the air-earth current zero was normally well within  $\pm 2$  per cent of full scale. Zero checks were

made by placing a large earthed aluminium sheet above and very close to it. The long time constant (about 3 min.) prevented any short term fluctuations in the zero. The compensation for displacement currents proved to be adequate for fair-weather measurements as these were averaged over a long period of time. For disturbed weather, except in stormy conditions, there appeared to be no very serious inaccuracy from imperfect compensation. In rain, splashing would be limited mostly to the aluminium edge of the collector, but the effects of rain splashing out should have been compensated by a similar number of drops splashing in from the guard ring. For fair-weather measurements, a range of  $\pm 12.5 \text{ pA m}^{-2}$  was used mostly, so that 2 per cent of this gave an error of  $\pm 0.25 \text{ pA m}^{-2}$ , or about 10 per cent of the mean fair-weather value.

#### 4.2.3 Potential gradient

The displaced zero method of sign discrimination required high standards of stability of both amplifier gain and bias voltage. The latter could be maintained constant to within  $\pm 1$  per cent, but the stability of the amplifier depended on the variation of the supply voltage. With a stabilized power supply, the long term variations were mostly no more than 3 to 4 per cent of full scale positive or negative, so that with frequent zero checks the error in the known zero position was again, about 2 per cent. For the range most frequently used ( $\pm 380 \text{ Vm}^{-1}$ ), the error was about  $8 \text{ V m}^{-1}$ , or about 8 per cent of the mean fair-weather value. The error

in the estimate of the exposure factor of the mill would depend on the space charge density close to the ground. As explained in Chapter 3, it was hoped that in fair weather the exposure factor would remain sufficiently constant, and equal to the value calculated by the method explained in Chapter 3.

#### 4.2.4 Space charge

The accuracy of space charge measurements depends on the constancy of the rate of flow of air through the apparatus. This flow rate was measured and checked frequently, and found to be constant to within about  $\pm 5$  per cent. The power was taken from the stabilized output of the isolation transformer so that the variation in air flow would be mostly mechanical in origin. Zero checks indicated an error, for most of the time, of certainly not greater than 2 per cent full scale. This was occasionally exceeded during instances of partial insulation breakdown. For much of the time the ranges  $\pm 64 \text{ pC m}^{-3}$  and  $\pm 210 \text{ pC m}^{-3}$  were used, while later a change to  $\pm 135 \text{ pC m}^{-3}$  was made. This gave the accuracies of better than 10 per cent of the mean fair-weather value of space charge density.

#### 4.2.5 Conductivity

The zero stability of this instrument depended on the insulation properties of the Gerdien chamber. Due to the low conductivity of air, an insulation resistance of better than  $10^{15} \Omega$ .

was required, otherwise the bias voltage would cause a current to flow through this, resulting in a zero shift. Zero checks were made by switching off the air flow, so that the concentration of small ions in the Gerdien chamber could be reduced by the electric field between the cylinders. These ions are replaced only by diffusion, or possibly ionization in the chamber, so that the resultant ionic concentration is low, and any appreciable current flowing through the V.R.E. resistor is due to inadequate insulation. The design of the intake system was such that very few small ions should have been lost to the walls of the intake tube, so there should have been no great error introduced here. The overall accuracy of the instrument was about 2 to 3 per cent of full scale except during periods of heavy rain which often caused insulation breakdown. For the range of  $2.5 \times 10^{14} \Omega^{-1} \text{ m}^{-1}$ , this means an accuracy, again, of around 10 per cent of the mean value.

### 4.3 Reliability of Instruments

#### 4.3.1 The field mill

The prevailing weather conditions had less effect on the reliability of the field mill than on most other instruments. However, continuous use over a period of nearly two years, required the replacement of two motors which had burnt out, and the rubber mounts supporting the stator-rotor assembly perished after 18 months'

use and had to be replaced. Apart from these, the field mill proved, mechanically, sufficiently robust and reliable in all weather conditions, provided a spare supply of expendable parts was maintained. For most of the time, too, the electronics gave little trouble, except when, as a result of extreme cold or vibrations, a dry joint produced an intermittent fault. The earlier amplifier was less reliable due to the incorporation of the electrometer valve and the 3 power supplies.

#### 4.3.2 The Vibrating Reed Electrometers (V.R.E.)

The vibrating reed electrometers mostly gave no trouble provided the head units and connections were adequately protected from the weather. During the period of two years, two V.R.E's developed faults and required replacing. A few minor faults did develop as well but these were usually put right by the replacement of a valve. Long time constants were used to smooth out zero fluctuations and connections were made with rigid coaxial cable to decrease the effects of vibration, so that no trouble was experienced from piezo-electric effects due to wind or other sources of vibration.

#### 4.3.3 Insulation breakdown

For the apparatus using vibrating reed electrometers (V.R.E.) as measuring instruments, the insulation resistance to earth needed to be over ten times the value of the V.R.E. input resistor. The space charge collector required a  $10^{12} \Omega$  resistor in the V.R.E.

head unit so that an insulation resistance of better than  $10^{13} \Omega$  had to be maintained between the filter unit and the outer casing. As mentioned in Chapter 3, the problems of insulation breakdown were much reduced by pointing the inlet downwards and providing sufficient heat to keep the insulators dry.

The conductivity chamber also required a  $10^{12} \Omega$  V.R.E. input resistor, but, as described in 4.2.5, an insulation resistance of more than  $10^{15} \Omega$  was necessary. Insulation breakdown, due to moisture and dirt, put the conductivity chamber out of action from January until March 1968, when the apparatus was dismantled and thoroughly cleaned. Since then, no further trouble was experienced from insulation breakdown.

The insulators supporting the air-earth current collector provided adequate insulation for the  $10^{10} \Omega$  resistor, except when moisture was allowed to settle on them due to the heater supply being cut off. Other sources of insulation break down did occur from time to time. In Winter, heavy falls of snow completely covered the collector, making it inoperative until such time as it was possible to remove the snow. In the Summer, spiders' webs and blades of grass caused occasional breakdown but not to any great extent.

#### 4.3.4 The suction fan

The filter unit in the space charge collector required a high pressure suction fan to be used. For intermittent work,

the fan unit from an ordinary domestic vacuum cleaner has, in the past, been found suitable. In the present work, the shortcomings of using such a fan continuously became apparent after some months of use. Four such fans were rendered unusable in the course of about 18 months. These were all second hand as it proved difficult to obtain a new fan separate from its housing and without the irrelevant accessories. In the end a new fan, of 510W maximum rating, was extracted from a new vacuum cleaner, and, after taking every precaution to prolong its life, no deterioration of its performance was noticed over a period of about 2 months continuous use.

The breakdowns in the other fans were due to a number of causes. Firstly, these fans were not designed for continuous operation under the conditions imposed on them. The reduced voltage was intended to prevent too much wear and as a result of using a reduced voltage, the wear on both commutator and carbon brushes was increased, rather than decreased, due to the greater friction at lower speeds. In one extreme case, this brush wear was such that one fan required new brushes almost every week. The reduced air flow prevented adequate cooling of the bearings, which became slack from wear due to over-heating. These slack bearings increased both vibration and brush wear until eventually the bearings, through overheating, seized up and the windings burnt out.

A solution to the problem would have been to use a more robust

type of fan, with a separate motor and independent cooling facilities. Such a motor would have to be designed for continuous observations, and the fan capable of sucking air at the comparatively high pressures required and at a flow rate of at least  $3 \text{ l s}^{-1}$ . A fan of this type was not available, but as mentioned previously the new fan used at the end of the work was probably adequate for the purpose, provided care was taken to prolong its lifetime. The breakdowns occurred mostly during February and March 1968, during which time an appreciably amount of the space charge record was lost.



## CHAPTER 5

### THE ANALYSES OF THE RECORDED DATA

#### 5.1 Synopsis of Data

##### 5.1.1 Periods of recording

The air-earth current collector and field mill were installed by the end of the Summer of 1966, and recording commenced in November of that year. The first few months of recording were only trial periods, when insufficient data was collected for a worthwhile analysis. Until January, 1967, no attempt was made to compensate for displacement currents to the air-earth current collector, nor was the field mill operating reliably. The space charge measurements were added in April 1967 and the positive conductivity in about July 1967. The period from July 1967 to July 1968 inclusive was used to obtain the results given in the following chapters. During this period, the air-earth current, potential gradient and space charge were recorded continuously, except for the occasions when instrumental breakdowns occurred. The positive conductivity was recorded only occasionally until October 1967 while from December until March, 1968, the instrument was out of action. For the period July 1967 to June 1968, inclusive, these parameters were recorded at a chart speed of 2 inches per hour. From July 1st onwards this speed was increased to 6 inches per hour, so that there would be sufficient time resolution to measure the electric conditions in stormy weather.

### 5.1.2 Meteorological observations

Observations at the site were limited to records of rate of rainfall, wind speed and direction. The apparatus for rate of rainfall was installed initially in August 1967, but recording was made only intermittently until October when the 3 single-channel pen recorders were installed. At this time the recording of wind speed and direction were also commenced. The records of all three suffered from unreliable recorders, but otherwise were continuous.

Meteorological observations on a larger scale were obtained from the Meteorological Office Daily Weather Reports. The two nearest weather stations, Carlisle and Tynemouth, were about 50Km from Lanehead and less than 100m above sea level, so that it was difficult to infer the local weather conditions from the Weather Reports. However, they were useful in indicating the general weather situation in the area. Daily rainfall measurements at Burnhope reservoir, 2.5 Km from Lanehead and 50 m lower in altitude, were obtained from the Durham County Water Board, to supplement the data from the rainfall recorder at the site.

## 5.2 Analysis of the Data

### 5.2.1 Fair-weather diurnal variations

The problem, initially, was to find a method of choosing the fair-weather periods for analysis, since it was often not possible to determine, meteorologically, which were the fair-weather periods and which the disturbed. In Chapter 1 it was mentioned that ISRAËL<sup>11</sup>

and LAHMAYER (1948) proposed that every observation should be used unless precipitation was actually falling at the time. In practice, periods of precipitation could be seen by visual inspection of the records, while the available meteorological observations could be used to confirm this. This criterion was extended by excluding data recorded in fog, or other conditions which were obviously electrically disturbed, for example by space charge packets from passing vehicles.

For each calendar month of the 12-month period, the data of air-earth current, potential gradient and space charge were used to calculate the diurnal variations. Mean hourly values were calculated from readings taken at 15 minute intervals, so that for each hour on each undisturbed day, 4 readings were taken for each parameter. The positive conductivity data were analysed in the same way for the months of October, November, April, May and June. The monthly diurnal variations for each parameter were combined and the mean diurnal variation of each parameter for the whole year was calculated. The results of these analyses are presented in Chapter 6, which contains also the annual variation of the monthly mean values for each parameter.

The number of fair-weather periods in a month differed from month to month. The amount of data obtained in each month depended also on the reliability of the instruments. In September 1967, no recording took place for the whole of the first half of this month,

so that the number of observations was too small for the diurnal variations to be significant on their own. The diurnal variation of air-earth current for this month was singularly lacking in number of observations. For most other months, though, the number of observations was large enough to be significant.

### 5.2.2 Precipitation electricity data

Measurements in precipitation have usually involved determining the relation between precipitation current and potential gradient. As mentioned in Chapter 1 an inverse relation has often been found between precipitation current and potential gradient. Measurements of space charge in rain, however, are few in number. When the potential gradient is high enough for point-discharge to occur high space charge densities have been observed (ADKINS, 1959b) of opposite sign to the potential gradient. During quiet rain, with lower potential gradients, space charge densities have been found to be low (SMIDDY and CHALMERS 1960). It seems that very little importance has been attributed to the space charge near the ground during non-stormy rain, although ADKINS did point out the effect space charge has on the potential gradient at the ground.

A casual inspection of the records showed that, during conditions of continuous or intermittent rain-fall, there appeared to be an appreciable correlation between the space charge density and potential gradient, which were both usually negative. At the

same time the total air-earth current was mostly positive, implying a positive precipitation current greater, in magnitude, than the conduction current. It was therefore decided to attempt to discover a relation between space charge and potential gradient. If, as it seemed, the two were strongly correlated, the local space charge might be controlling the potential gradient. The statistical methods which were used for the analyses are discussed below and the results presented in Chapter 7.

The periods chosen for the analysis were all during non-stormy rain when conditions were reasonably steady. The length of time for each period depended on the length of rainfall, but was never less than an hour, nor more than 6 hours. The number of readings taken depended on the time resolution of the chart. In practice this limited the number of readings to 32 per hour. Since it was necessary to use some method of selection for the periods, the results might not have been completely representative of continuous rainfall. There were a few occasions, not included, where there was no apparent correlation, but this may have been due to faults such as instrumental breakdown. The periods normally chosen were those when conditions before and after were steady and undisturbed.

### 5.3 Statistical Methods

#### 5.3.1 Correlation coefficients

The purpose of this section is to outline the statistical methods used. The mathematical derivations of the expressions

used are too complex to be given here, but more details may be found in books such as BROOKS and CARRUTHERS (1953). For each period in rain which was analysed, the observations of space charge and potential gradient can be represented by a population of  $n$  pairs of variables,  $x$  and  $y$ . These pairs may be written as  $(x_1, y_1), (x_2, y_2), \dots, (x_i, y_i), \dots, (x_n, y_n)$ . In the analysis, the purpose is to discover whether or not there exists some functional relation between the two variables, i.e. if  $y = f(x)$ . This function, for a simple case, might be linear, so that any deviation of the observed points,  $(x_i, y_i)$  from the straight line, would be due to some disturbances or inaccuracies in measurement. For a linear relation, the correlation coefficient for the whole population is given by

$$r = \left[ \sum_{i=1}^n (x_i - \bar{x})(y_i - \bar{y}) \right] \frac{1}{n s_x s_y}$$

where the standard deviations  $s_x, s_y$  are given by

$$s_x^2 = \frac{1}{n} \sum_{i=1}^n (x_i - \bar{x})^2$$
$$s_y^2 = \frac{1}{n} \sum_{i=1}^n (y_i - \bar{y})^2$$

and  $\bar{x}, \bar{y}$  are the population means of  $x$  and  $y$  respectively.

For space charge density and potential gradient,  $y = f(x)$  and also  $y = y(t)$ ,  $x = x(t)$  i.e. both  $x$  and  $y$  are time dependent. Pairs of values of  $x$  and  $y$  are taken for the same value of  $t$ , i.e.  $(x(t), y(t))$ . If, however, there is a time lag or lead, the maximum correlation between the two may occur for pairs of values  $(x(t), y(t + l))$ , where  $l$  is the time, in the same units as  $t$ , by which  $y$  lags behind  $x$ . Rapid variations in  $x$  and  $y$  can have an appreciable affect on  $r$ . If  $x(t)$  and  $y(t)$  are periodic functions, the correlation coefficient is negative if they are  $\pi$  out of phase, and zero if  $\pi/2$  out of phase. By taking pairs of values separated in time by a constant amount, the above expression for  $r$  yields what is known as the cross-correlation coefficient.

In making the calculations, the time lag between the two variables was found first by inspection and then by trial and error, by finding the lag which gave the maximum cross-correlation coefficient. In all cases where a lag existed, it was always the space charge which lagged behind the potential gradient, due partly to the longer time constant in the space charge collector.

### 5.3.2 Lines of best fit

Once the correlation coefficient has been calculated, the next problem is to find the equation of the line of best fit. In the simple case, where either  $y$  or  $x$  can be assumed free from error, it is not difficult to calculate the appropriate regression

equation by the method of least squares. There are two possible regression lines for one population of pairs of observations, depending on which of  $x$  or  $y$  is free from error. For  $x$  free from error the regression line for  $y$  on  $x$  is given by:

$$y - \bar{y} = r \frac{s_y}{s_x} (x - \bar{x})$$

and for  $x$  on  $y$

$$x - \bar{x} = r \frac{s_x}{s_y} (y - \bar{y})$$

These two lines intersect at  $(\bar{x}, \bar{y})$  and the ratio of their slopes is  $r^2$ .

In the present analysis, neither  $x$  nor  $y$  is free from error. For this case MORGAN (1960) gives the following equation for the line of best fit:

$$y - \bar{y} = c \frac{s_y}{s_x} (x - \bar{x})$$

where  $c$  lies between  $r$  and  $1/r$  and can be obtained from the following expressions:

$$(k + 2)c^2 - 2r(k + 1)c + k = 0$$

The value of  $k$  is given by

$$k = \frac{-e_x}{e_y} \quad \text{when } 0 < \frac{e_x}{e_y} \leq 1$$

$$k = \frac{e_y}{e_x} - 2 \quad \text{when } 0 < \frac{e_y}{e_x} \leq 1$$

where  $e_x, e_y$  are the relative errors in  $x, y$ . It can be seen that



k must lie between 0 and -2, at which extremes c is equal to r and  $1/r$  respectively. The relative errors are given by

$$e_x = \frac{e'_x}{s_x}$$

$$\text{and } e_y = \frac{e'_y}{s_y}$$

$e'_x$ ,  $e'_y$  are the average absolute errors in each of the individual values x and y, so that each value is given by

$$x \pm e'_x$$

$$\text{and } y \pm e'_y$$

For space charge density and potential gradient, the observations were taken down in terms of the variables x and y which, on the chart, had equal units. Each x or y had an integral value between 0 and 100, the readings being taken every half division. Now, as mentioned in Chapter 4, the error in the reading of each parameter was probably about half a division, so that

$$e_x = e_y \approx 1$$

Since more than one range was used for each of space charge and potential gradient, it was therefore more convenient to calculate the equation of the line of best fit in terms of x and y, and then convert to  $\phi$  and F. The relative errors in x, y are therefore given by

$$e_x = 1/s_x$$

$$e_y = 1/s_y$$

If the line of best fit is represented by

$$y = ax + b$$

this can easily be converted into the form

$$F = A/c + B$$

The constants, A and B were calculated for each set of records, the value of c being obtained from the table by MORGAN. The results of the analysis are set out in Chapter 7.

### 5.3.3 Tests of significance

In many cases it is necessary to test the significance of the observed value of the correlation coefficient. Even if this value is not zero, and the number of pairs of readings is small, it is still not necessarily justifiable to assume a functional relation between the two variables. Instead, it is necessary to calculate the probability of such a correlation coefficient occurring with an uncorrelated population. This probability  $P(r)$  of obtaining such a value  $r$  depends on the number of degrees of freedom,  $(n - 2)$ . If  $P(r) = 0.05$ , the 95 per cent level of significance,  $r$ , the observed coefficient, is significant only if

$$r > r'$$

In Table 5 are given some values of  $r'$  for corresponding values of  $n$  between 10 and 100, and for 4 levels of significance taken

from BROOKS and CARRUTHERS. For the correlation of space charge the minimum value of  $n$  was 30, so that, at the 95 per cent level, the minimum correlation coefficient which is significant is 0.361; at the 99.9 per cent level this value becomes 0.570.

Table 5

Values of  $r'$  from an uncorrelated population

n	Significance level (per cent)			
	90	95	99	99.9
10	549	632	765	872
12	497	576	708	823
14	457	532	661	780
16	426	497	623	742
18	400	468	590	708
20	378	444	561	679
25	337	396	505	618
30	306	361	463	570
35	283	334	429	532
40	264	312	403	501
45	248	294	380	474
50	235	279	361	452
60	214	254	330	414
70	198	235	306	385
80	185	220	286	361
90	175	207	270	341
100	165	197	256	324

CHAPTER 6

THE FAIR WEATHER DIURNAL VARIATIONS

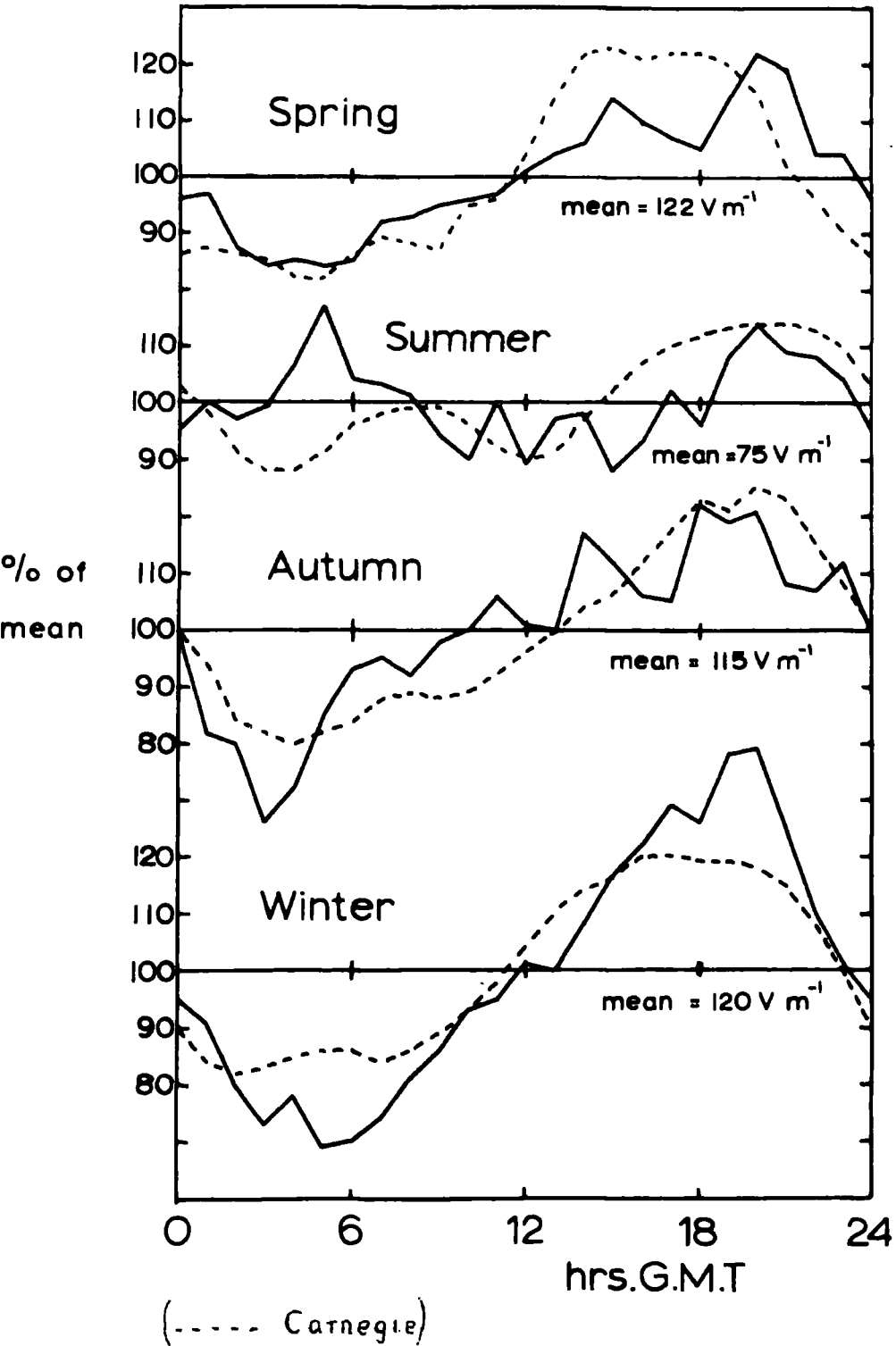
6.1 General Results

6.1.1 The average diurnal variations for the full year

The fair-weather data obtained during the one-year period July 1967 to June 1968 were divided according to the 12 calendar months and the analysis carried out as described in Chapter 5. The total diurnal variations for the full year were obtained from averaging the absolute values for each month. These total diurnal variations, for air-earth current, potential gradient and space charge are given in Fig. 6.1. In neither these curves nor the monthly diurnal variations was any attempt made at smoothing, since this procedure leads to distortion, and may also eliminate certain important details. The raw data from which these variations were obtained comprised a total of some 32,000 individual readings, for all three parameters.

From Fig. 6.1 it can be seen that both air-earth current and space charge vary more widely than potential gradient. The variations of air-earth current and space charge both show a minimum in the early afternoon, but the times of maxima are different. For air-earth current density, the maximum value of  $3.2 \text{ pA m}^{-2}$  occurs at 7h G.M.T., while for space charge density the maximum value of  $40.4 \text{ pC m}^{-3}$  occurs at 21h, followed by a section which is nearly a plateau at  $37 \text{ pC m}^{-3}$ . The minima,

FIG. 6.2 Diurnal variations of Potential gradient



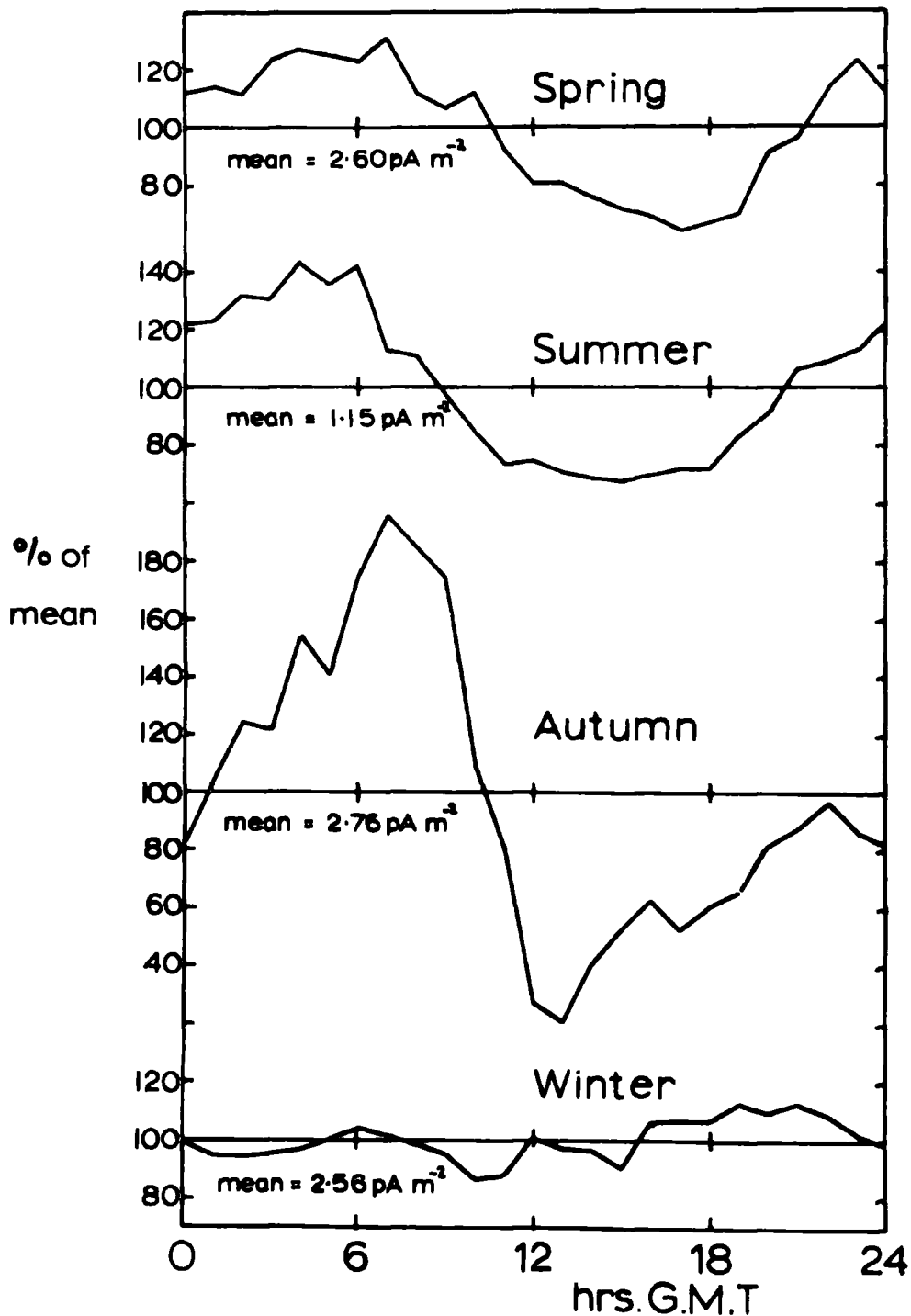
which are closer, occur at 13h ( $1.49 \text{ pA m}^{-2}$ ) and 14h ( $20 \text{ pC m}^{-3}$ ) respectively. The general shapes of both curves are similar, as are the magnitudes of the variations, and will be discussed later in the Chapter.

The diurnal variation of potential gradient, on the other hand, is notably different. Its maximum and minimum values occur at 20h ( $135 \text{ Vm}^{-1}$ ) and at 3h ( $85 \text{ Vm}^{-1}$ ) respectively. Its minimum coincides roughly with the maximum of air-earth current, but its maximum value occurs only an hour before that of the space charge. The mean values of the 3 parameters were found to be  $2.28 \text{ pA m}^{-2}$ ,  $108 \text{ Vm}^{-1}$  and  $30.3 \text{ pC m}^{-3}$  respectively. The first two are close to the values of  $2.4 \text{ pA m}^{-2}$  and  $130 \text{ Vm}^{-1}$ , for an average land station, given by CHALMERS (1967a), but the value for space charge density is a factor of 3 greater than that given by CHALMERS. However, values of space charge density, as given in Chapter 1, vary widely from place to place far more than do either air-earth current density or potential gradient.

#### 6.1.2 The seasonal diurnal variations

The diurnal variations for each of the three consecutive months of each season were averaged to obtain the diurnal variation for the season. The months were grouped, for convenience, so that Spring consists of February to April, Summer of May to July etc. The diurnal variations for all four seasons are shown in Figs. 6.2 to 6.4 for each of air-earth current, potential gradient and space charge. In Fig. 6.2, for potential gradient,

FIG. 6.3 Diurnal variations of Air-earth current

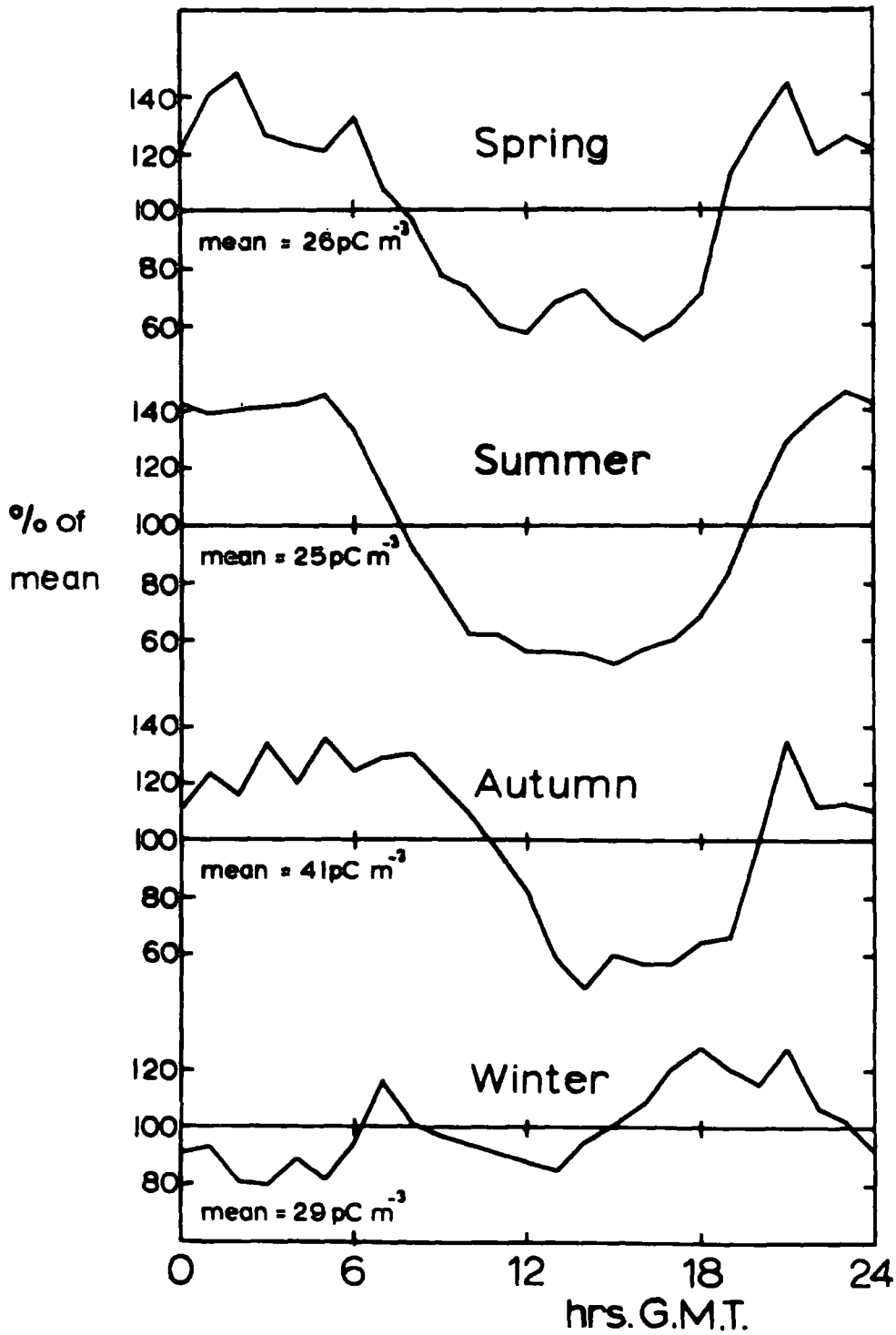


are included the equivalent diurnal variations, also plotted against G.M.T, from measurements on board the Carnegie (PARKINSON and TORRESON, 1931). There is some similarity in general shape between each pair of variations, but those from Lanehead are less smooth. In Spring, Autumn and Winter all variations have minima in the morning and maxima in the afternoon. In summer there are semi-diurnal components in both, but the first maxima do not coincide. For Lanehead the first maximum occurs at 5h while the Carnegie maximum occurs at about 8h and is less pronounced. The later maximum in both variations occurs at about 20h. The Winter variation, for Lanehead, has the greatest amplitude, being nearly 40 per cent either way, with the minimum amplitude in Summer. The Carnegie variations remain about 20 per cent either way for most of the year, with the exception of Summer which shows a slightly smaller variation.

The diurnal variations of air-earth current and space charge, for the four seasons, are shown in Fig. 6.3 and 6.4. The scale in both cases is reduced to accommodate the appreciably larger variation compared with that of the potential gradient. For air-earth current the very large amplitude exceeds any other by 2 or 3 and Winter by nearly 10. For the first three seasons the times of maximum and minimum are similar, but in Winter there are 3 maxima and 3 minima. It is interesting to note that the minimum variation of air-earth current coincides with the



FIG.6.4 Diurnal variations of Space charge



maximum variation of potential gradient. The diurnal variations of space charge are mostly similar to those of air-earth current. For Spring, Summer and Autumn there is a morning maximum and afternoon minimum for each variation. There are also maxima in the evening, especially for Spring and Autumn where they both occur at 21 h. The Winter variation has some features similar to the variations of potential gradient. The maximum occurs at 18h to 21h with a minimum at 3h, but there are also secondary maximum and minimum at 7h and 13h respectively.

#### 6.1.3 The monthly diurnal variations

From Fig. 6.5 to 6.16, comparisons can be made between the diurnal variations of all parameters for each month. For any parameter, the difference between the monthly diurnal variations for each season is often less than the difference between the seasonal diurnal variations. An exception to this occurs for space charge in January. Individual days within a month do, however, differ from the monthly average, sometimes by a large amount. By taking a large number of days, the disturbances on individual days should cancel out so long as they occur randomly. Comparing the monthly diurnal variations with those for the full year demonstrates the necessity of obtaining a large number of readings for a sufficiently smooth variation. The diurnal variations of positive conductivity have been included for those months for which data was available.

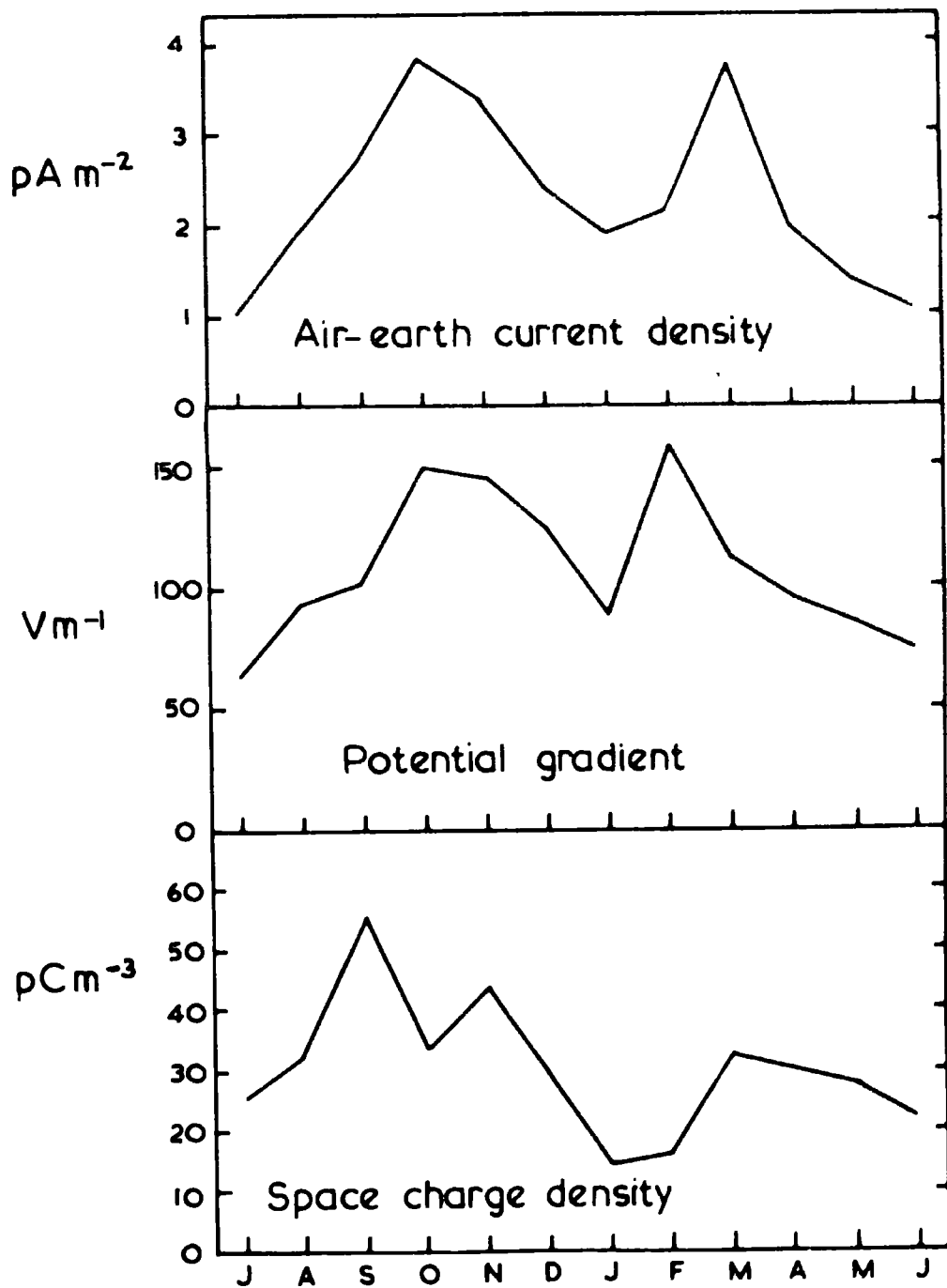
During the months March to October inclusive the air-earth current and space charge variations have similar shapes, but for the rest of the year there is little similarity. During the Winter the current variation is less and the space charge more nearly follows the variation of potential gradient. In December the variations for potential gradient and space charge are similar. Each variation has a minimum at 5h to 6h and a maximum at 18h to 20h, and they both have similar magnitudes of variation. On the other hand there is virtually no similarity between the two for January.

The diurnal variations of positive conductivity for April, May and June are similar in form, with maxima in the morning at around sunrise, or a little later, and minima in the late afternoon or evening. The similarity between positive conductivity and air-earth current is less than between space charge and the latter. For October and November, the maximum is later in the day and close to mid-day, with minima in the early evening.

#### 6.1.4 The annual variation

The mean value of the diurnal variation of each parameter for each month was used to find the annual variation of the monthly means, which, for air-earth current, potential gradient and space charge are shown in Fig. 6.17. All parameters have low values in Summer with secondary minima in January. The range of variation of air-earth current density lies between  $1.04 \text{ pA m}^{-2}$  for July and

FIG.6.17 Annual variation of the monthly means  
July 1967 - June 1968



3.84 pA m<sup>-2</sup> for October. For potential gradient the corresponding values for these months are 64 Vm<sup>-1</sup> and 150Vm<sup>-1</sup> although the maximum, 158 Vm<sup>-1</sup>, occurs in February. The space charge density has a maximum in September of 55.5 pCm<sup>-3</sup> with a minimum value of 14.4 pC m<sup>-3</sup> in January.

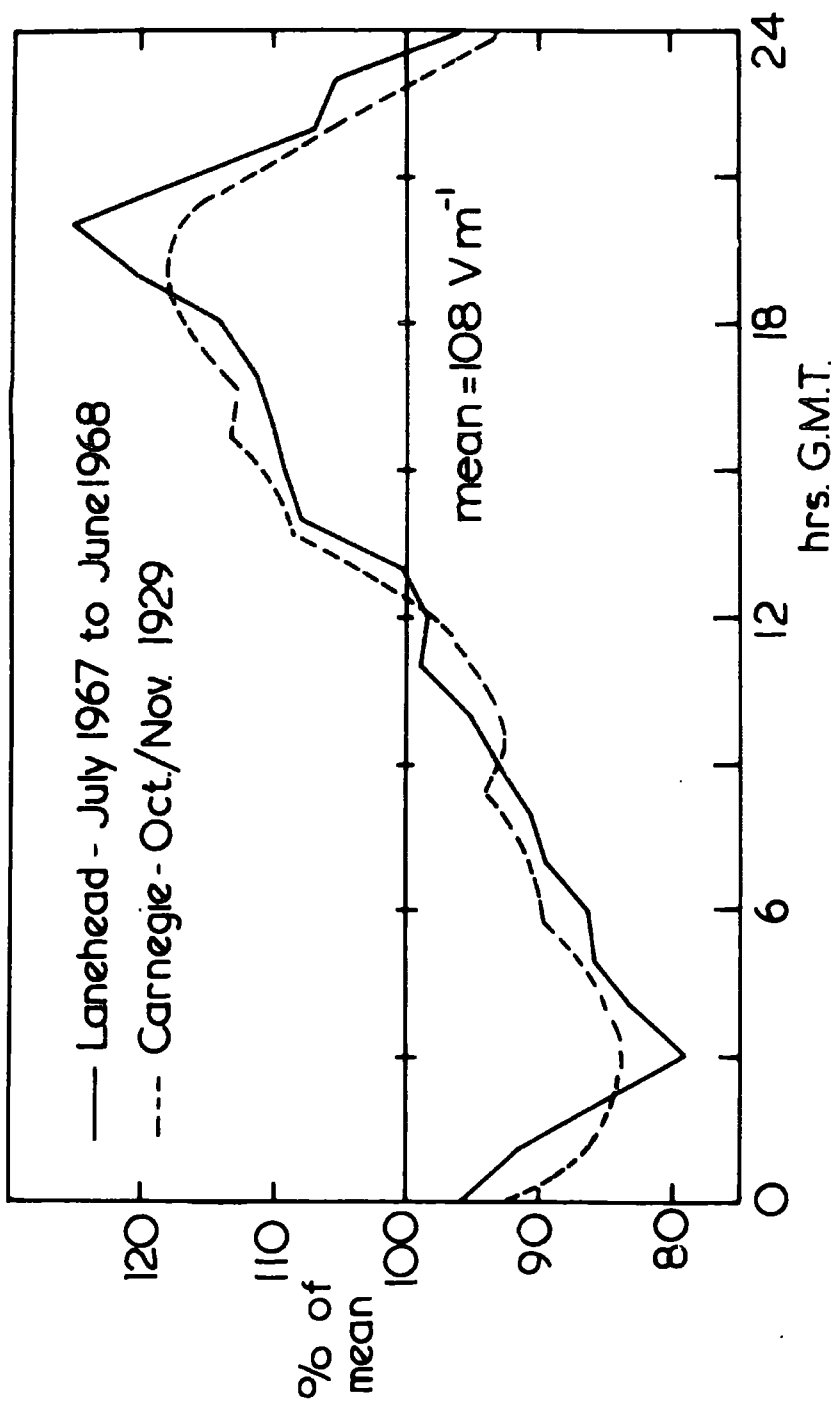
The values of all parameters for July 1967 and June 1968 are sufficiently close both to confirm the stability of the instrumental calibrations, and to imply that the annual variations shown in Fig. 6.17 may be reproducible to within the limits of measurement. There is no sharp discontinuity between June and July, especially for the air-earth current density with values of 1.06 and 1.04 pA m<sup>-2</sup> respectively. For potential gradient these values are 75 and 64 Vm<sup>-1</sup> and, for space charge, 22.1 and 25.9 pC m<sup>-3</sup> respectively.

## 6.2 The Total Diurnal Variations

### 6.2.1 The potential gradient

The diurnal variation of potential gradient for the whole year is shown, as a percentage of the mean, in Fig. 6.18, together with the results of the measurements on board the Carnegie during October and November, 1929 (TORRESON et.al. 1946). The close similarity between the two curves is striking considering the different conditions under which the two sets of results were obtained. The Carnegie measurements were made in the Central Pacific, one third of the way round the World from Lanehead

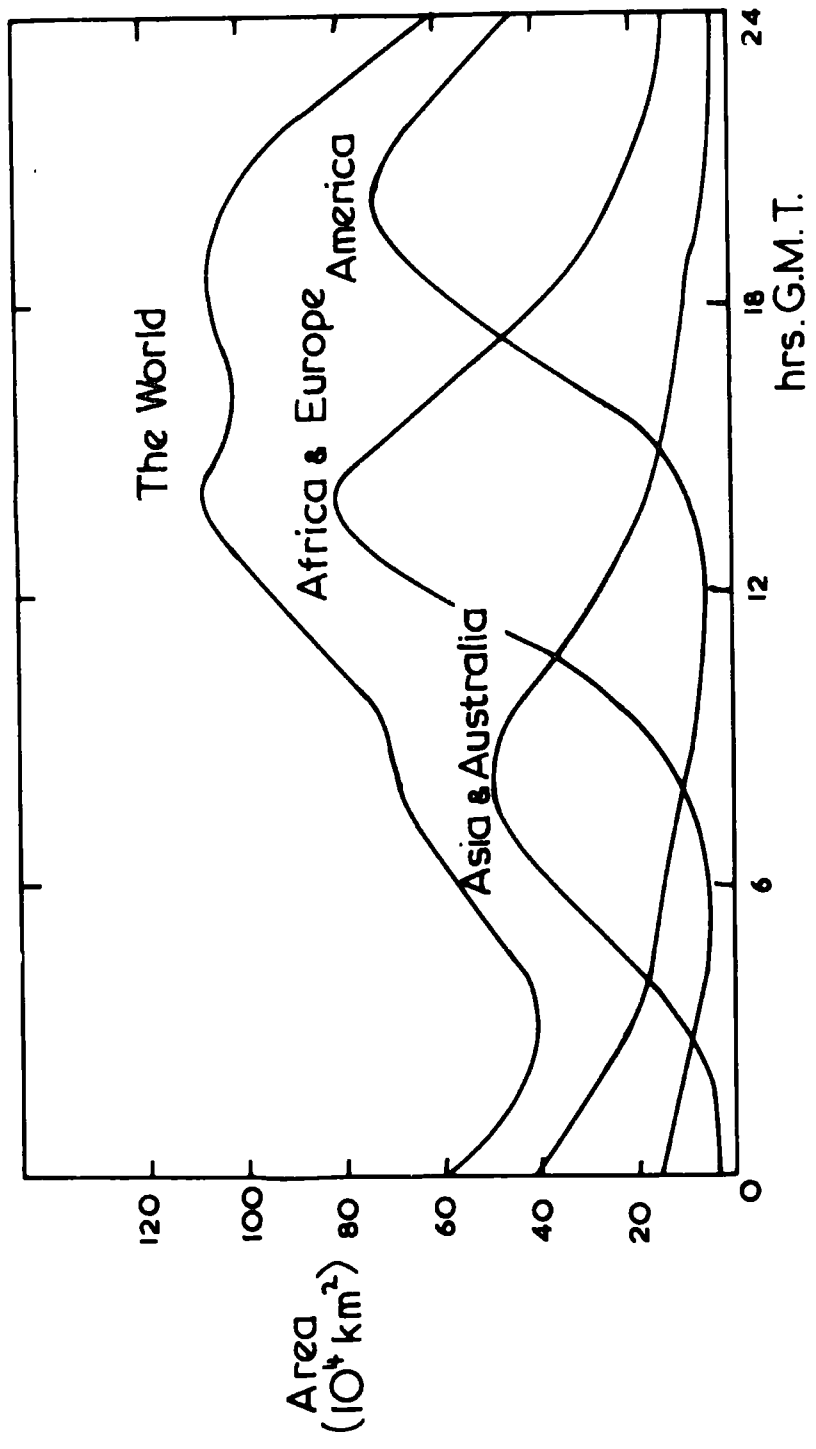
FIG.6.18 Diurnal variation of Potential gradient - July 1967 to June 1968



and 38 years ago. The connection between the diurnal variations of potential gradient and the World thunderstorm activity has been mentioned in Chapter 1, so that, for comparison, the diurnal variation of World thunderstorm activity, from WHIPPLE and SCRASE (1936), is given in Fig. 6.19. At any given time, the thunderstorm area includes all those places where thunder was audible in the interval from 60 min before to 60 min after the specified time. The thunderstorm areas from land masses only are included, there being no evidence of a diurnal variation of thunderstorm activity over the oceans. A direct comparison between the total thunderstorm area and the potential gradient depends on the thunderstorm activity, at any one time, being proportional to the area experiencing thunderstorms at that time. If the charge transfer per unit thunderstorm area varies from continent to continent, the shape of the total diurnal variation of thunderstorm activity will be different from that of the thunderstorm area. This would explain the greater emphasis on the peak at 19h to 20h, due to America, as opposed to that at 14h on the potential gradient curves.

The World thunderstorm curves show maxima at 8h, 14h and 20h GMT for the 3 different land masses at different latitudes. The resultant curve has a minimum at 3h with a maximum at 14h, due to Africa and Europe, and subsidiary maximum at 19h with an inflexion at 8h. The Carnegie curve has a minimum at about 3h

FIG. 6.19. Diurnal variation of land thunder areas





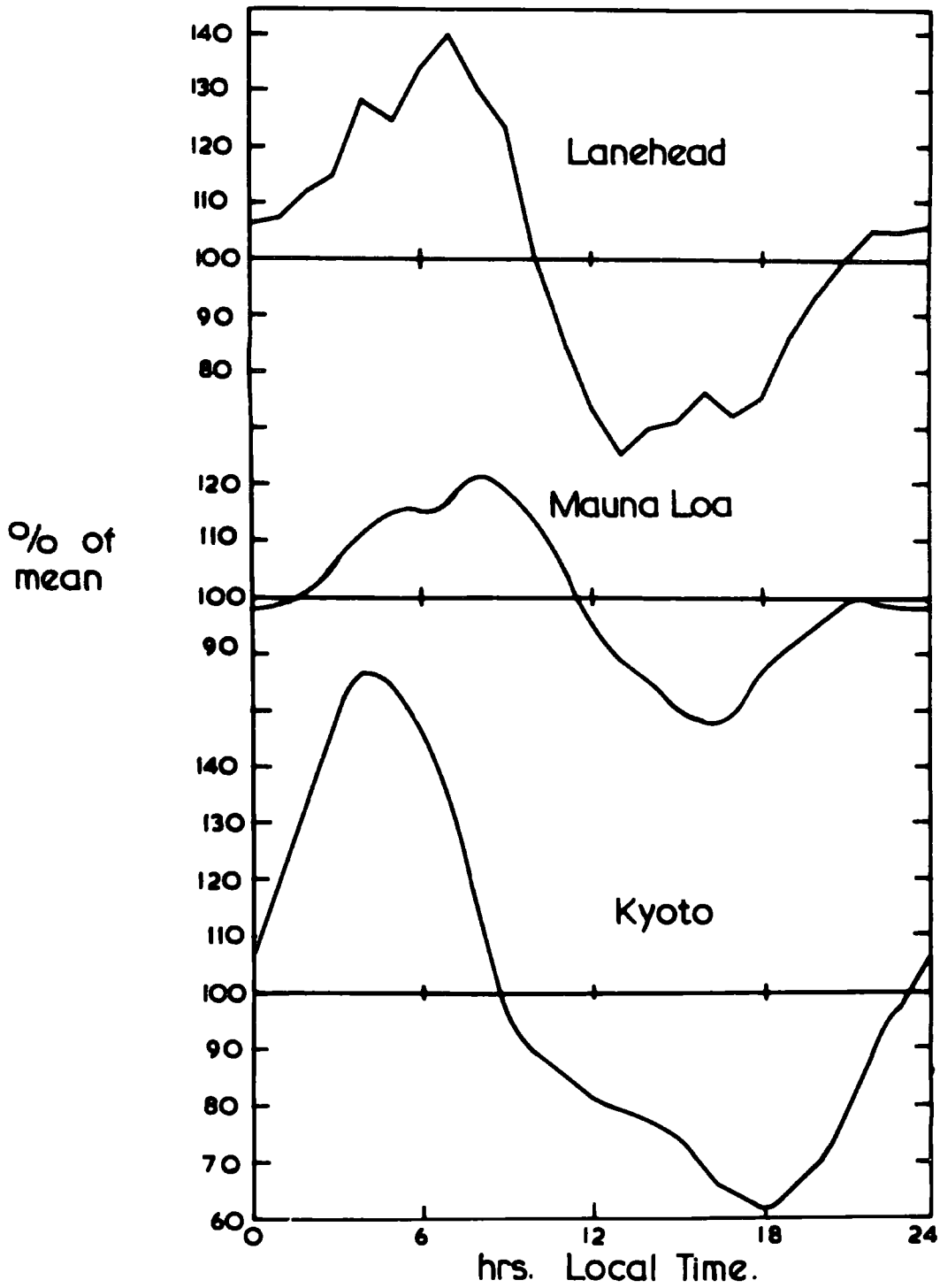
and a maximum at 19h. For Lanehead the minimum also occurs at 3h but the maximum is at about 20h. It seems that both diurnal variations of potential gradient are influenced more by thunderstorms in America than those in other continents. For Lanehead, both maximum and minimum are more pronounced than for the Carnegie variation, but apart from these, they both have a similar percentage range of variation. The Lanehead variation also seems to lag by about half an hour behind the Carnegie curve. On the whole, though, considering the comparatively large departures of the monthly variations from the average, the agreement is remarkable.

#### 6.2.2 Air-earth current and space charge

For the purpose of direct comparison, the diurnal variations of air-earth current and space charge are reproduced, as percentages of the means, in Fig. 6.20. The shapes are basically similar but with obvious differences. In the morning the variation of air-earth current exceeds that of space charge, while in the evening the opposite is true. The two curves are closest during the afternoon, but for the rest of the day the space charge appears to lag behind the air-earth current by 1 or 2 hours.

Neither the space charge nor air-earth current variations appear to have any similarity to the World-wide effects. However, for the air-earth current, comparisons can be made with other results when considering the variations with respect to local time. Fig. 6.21 shows two diurnal variations which, in this way, are

FIG.621. Diurnal variations of air-earth current

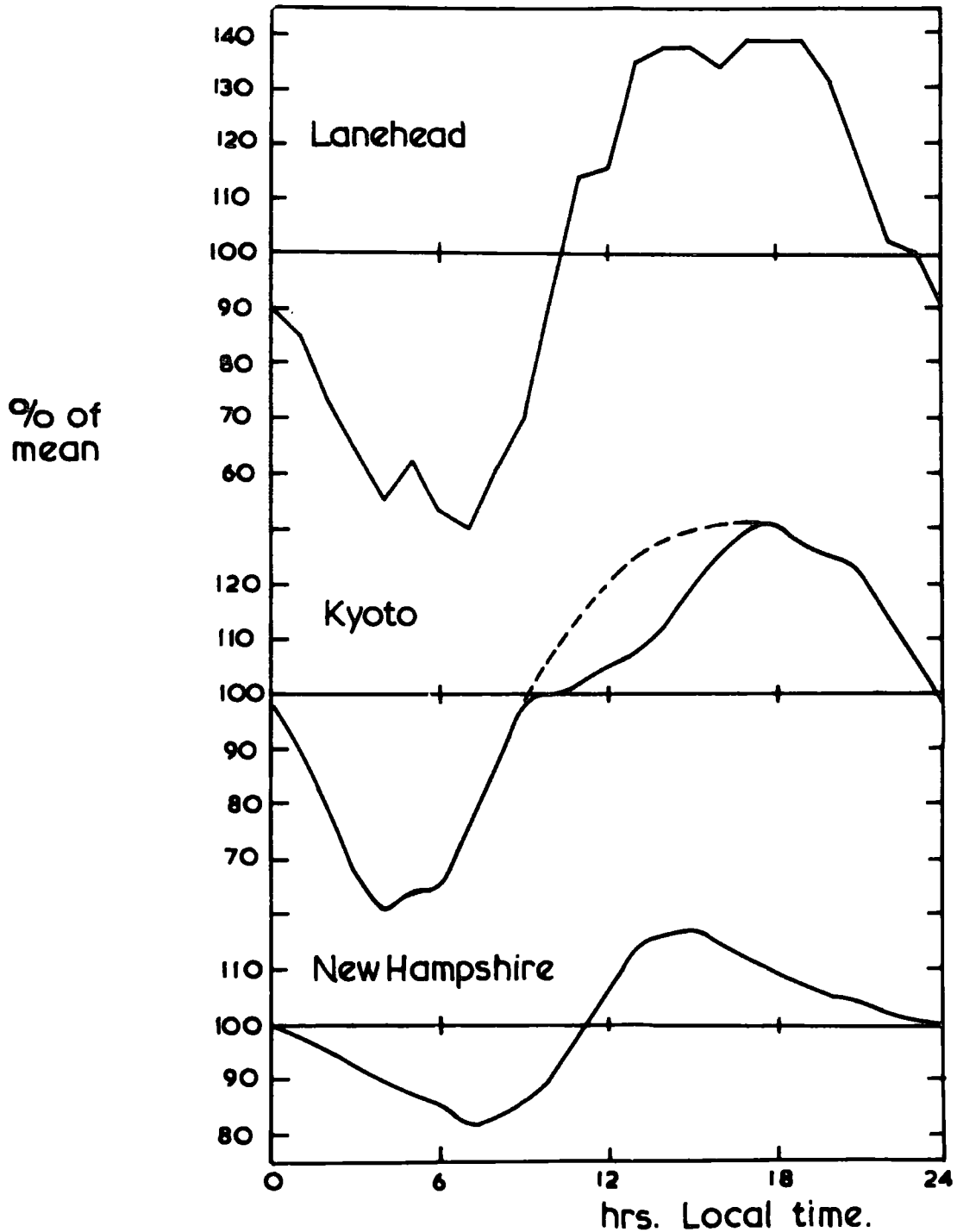


similar to that found at Lanehead. The diurnal variation of air-earth current was found at Mauna Loa (COBB and PHILLIPS, 1962) from direct measurements for a period of one year. The curve is taken from COBB (1968) and is similar to the Lanehead variation in shape but not in amplitude. The double peak in the morning occurs in both curves, although for Mauna Loa it is an hour later. The times of minima differ, but the short plateau just before midnight is common to both. The variation from Kyoto (OGAWA, 1960) was obtained by the indirect method of measurement in an area most probably suffering appreciably more from pollution than Lanehead. This curve shows less similarity with either of the first two, but is included because of the connection with columnar resistance discussed below. An interesting fact about the Mauna Loa curve is that, in GMT, it agrees well with the Carnegie results of air-earth current and the World thunderstorm activity.

### 6.2.3 The columnar resistance

In Chapter 1 it was argued that the air-earth current, and not the potential gradient, is more likely to follow the variation of world thunderstorm activity. The argument relied on the columnar resistance,  $R$ , varying little. However, if the variation in  $R$  is greater than the variation of  $V$ , the potential of the electrosphere, this will determine the variation of  $I$ . From Chapter 1, the air-earth current density may be written as,

FIG.622. Diurnal variations of Columnar resistance



$$I = \frac{V}{R}$$

which can be differentiated, assuming all three to be functions of time, to give,

$$\frac{dI}{dt} = \frac{1}{R} \frac{dV}{dt} - \frac{V}{R^2} \frac{dR}{dt}$$

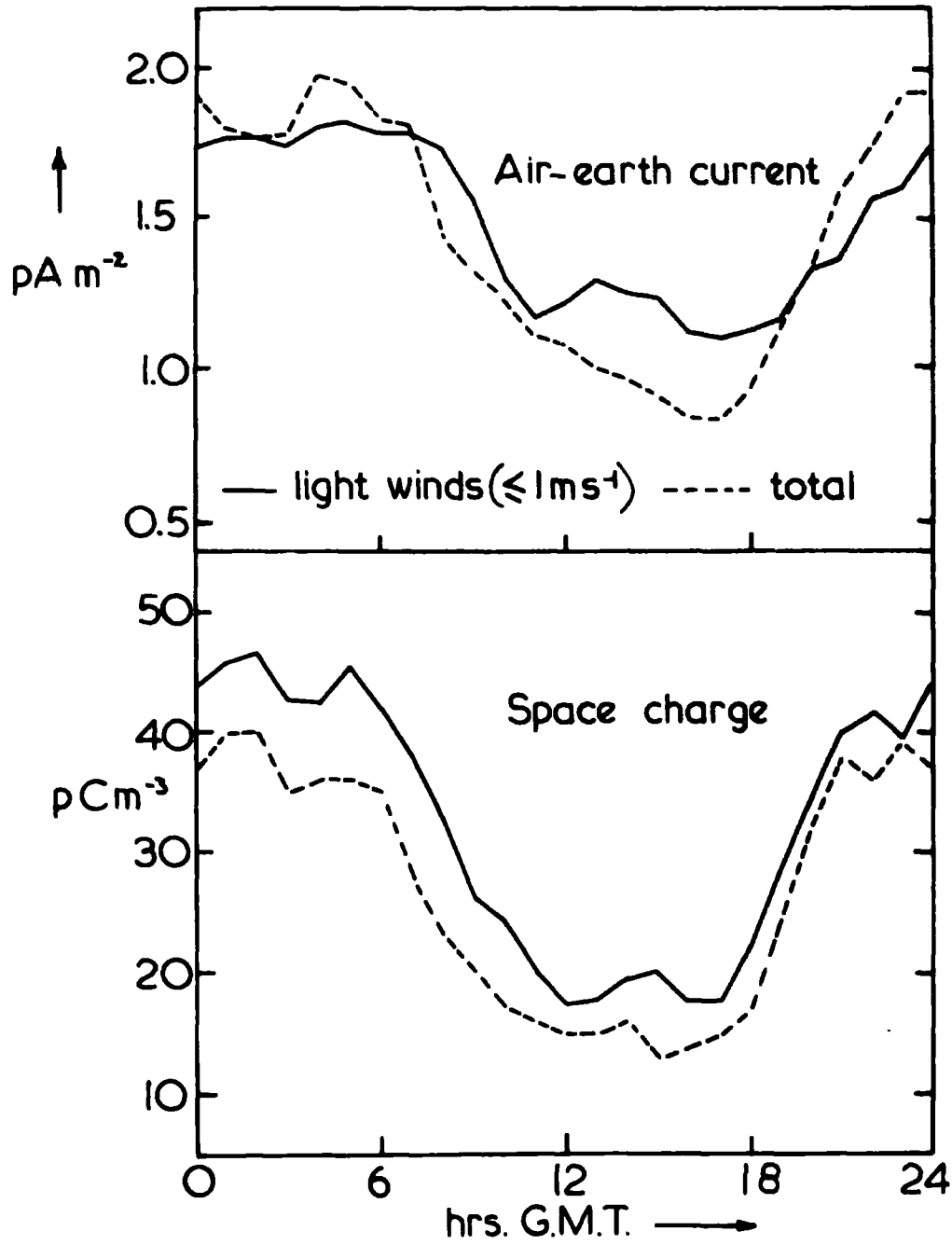
Multiplying through by  $R/V$  and using  $I = V/R$  this gives:

$$\frac{1}{R} \frac{dR}{dt} = \frac{1}{V} \frac{dV}{dt} - \frac{1}{I} \frac{dI}{dt}$$

Therefore the percentage variation of  $R$  is given by the difference between the percentage variations of  $V$  and  $I$ . Since the variation of potential gradient measured at Lanehead agrees well with the World thunderstorm activity, it may be reasonable to assume that it reflects, also, the variation in  $V$ . Since the variation of  $I$  is also known, the variation of  $R$  can be estimated.

This estimated diurnal variation of the columnar resistance at Lanehead is given in Fig. 6.22. OGAWA (1960) used similar arguments to obtain the variation of columnar resistance at Kyoto from his air-earth current results and the potential gradient variation from the Carnegie. The broken line represents the estimated values when no horizontal diffusion of nuclei occurs. Both curves are plotted against local time, since the variation of columnar resistance is a local effect. The third curve in Fig. 6.22 represents the local time variation of columnar resistance over New Hampshire (SAGALYN and FAUCHER, 1956) obtained directly from conductivity measurements at heights up to 5 km. All

FIG. 6.23 Effect of wind on diurnal variations (APRIL - JUNE)



three curves are similar in shape although the directly measured variation, over New Hampshire, varies only about half as much as the other two.

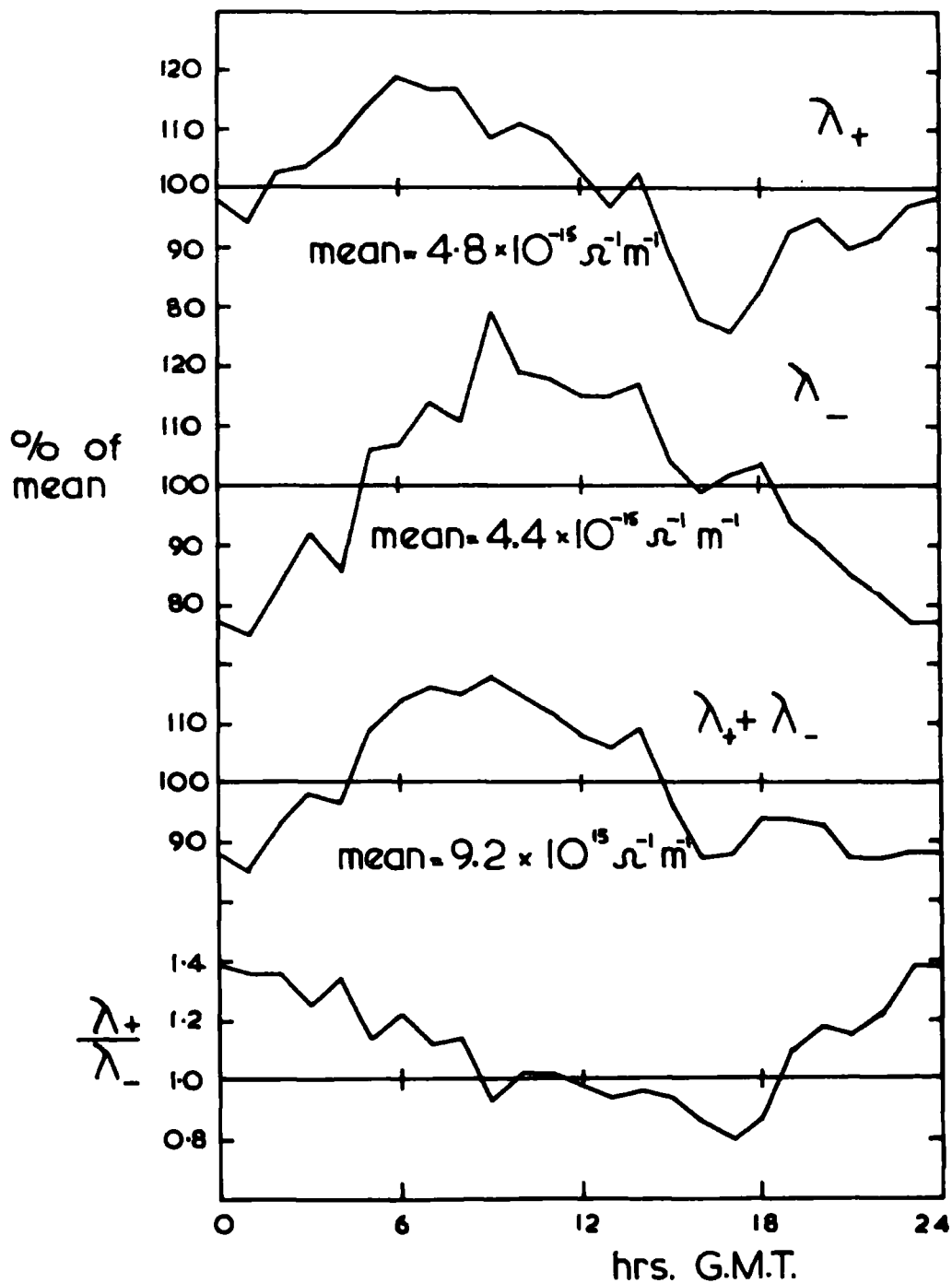
### 6.3 Some Further Results

#### 6.3.1 The effect of wind

The similarity between the diurnal variations of air-earth current and space charge can imply that changes in space charge density produce similar changes in air-earth current density. Since the potential gradient variation is different from both these variations it is possible that the space charge could affect the air-earth current by means of convection or turbulent transfer processes. Both of these would depend on the wind velocity, among other things, so an attempt was made to test the affect of the windspeed on the diurnal variations of air-earth current and space charge. The fair-weather data for the three months of April to June were used for the purpose. From this data, for wind speeds less than about  $1 \text{ m s}^{-1}$ , the diurnal variations of air-earth current and space charge were calculated. Even for these three months there was insufficient data for low windspeeds during day time to obtain a smooth variation. It was necessary therefore, to use a method of smoothing by taking overlapping means of 3 consecutive points.

The smoothed diurnal variations, together with the total variations for the same three months, are shown in Fig. 6.23. In neither case, considering the small amount of data, is there a

FIG. 6.24. Diurnal variations of conductivity — JULY 1968



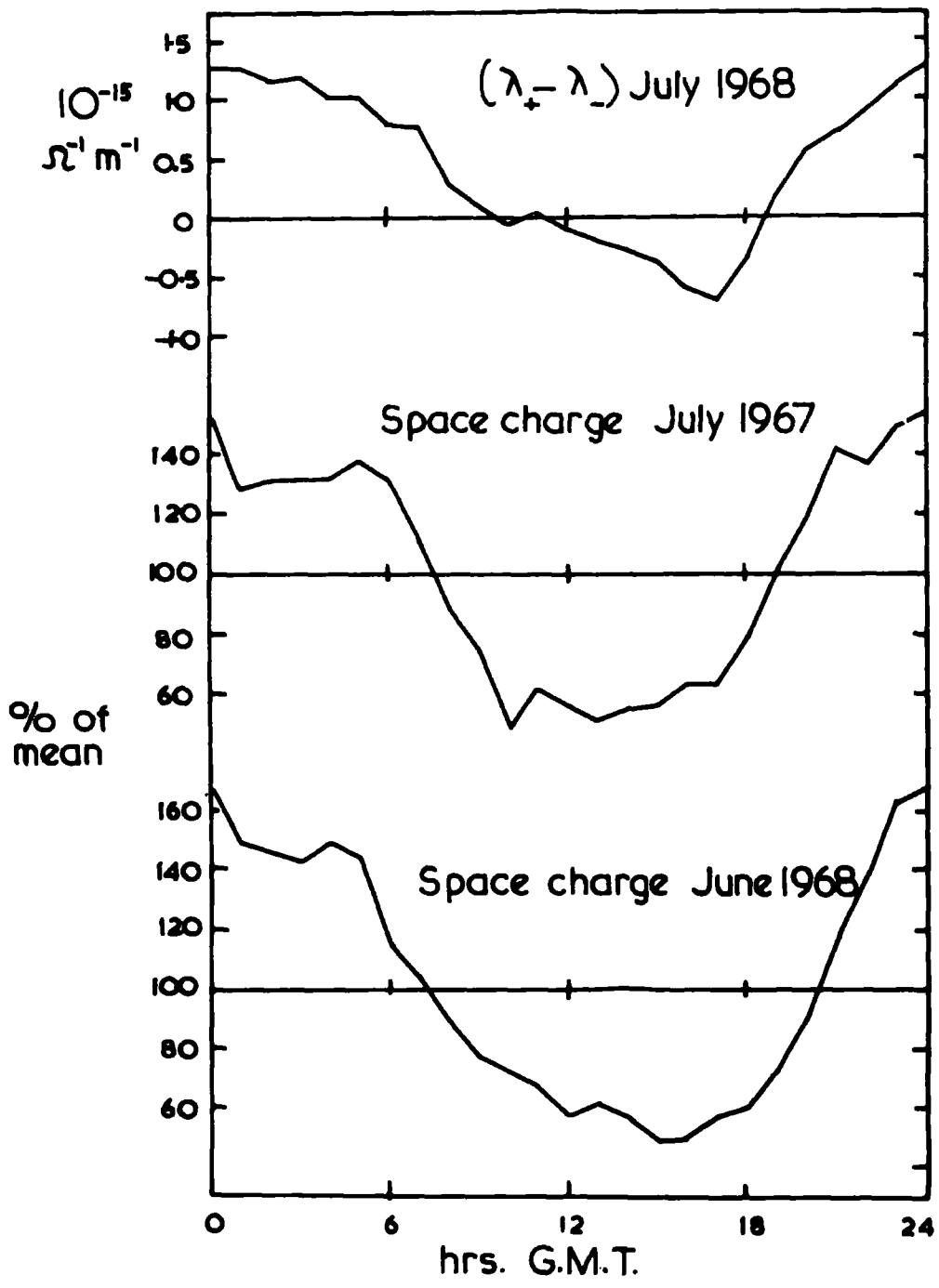


significant difference between the two variations. For air-earth current density the mean value, for light winds, is  $1.47 \text{ pA m}^{-2}$ , while for the total it is  $1.43 \text{ pA m}^{-2}$ . The only real difference appears to be in the amplitudes of the variation, which is less for light winds. For space charge density the mean values are  $32 \text{ pC m}^{-3}$  and  $26.5 \text{ pC m}^{-3}$ . The variation for low wind speeds is almost the same as the total variation in shape and amplitude but with a different mean value. From this limited evidence it seems that wind has an almost negligible effect on space charge density, except to raise its mean value, but slightly reduces the amplitude of the diurnal variation of air-earth current, without significantly affecting the mean value.

### 6.3.2 Diurnal variation of conductivity for July

For the month of July, 1968, after the one-year period discussed previously, the positive and negative conductivities were recorded alternately. The polarity reversal was performed manually every 5 days, to give 17 days of positive conductivity record and 12 days of negative conductivity. The diurnal variations of both polar conductivities together with the total conductivity are shown in Fig. 6.24. The times of maximum and minimum differ for the two conductivities. For the positive conductivity these are at 6h and 17h respectively, and, for the negative conductivity, 9h and 1h. Both conductivities vary by some 20 per cent either side of the mean value. The different variations for the two conductivities

FIG.6.25. Conductivity and space charge



imply a variation in the ratio of positive to negative conductivities. The mean ratio is 1.1, but the ratio varies between 1.4 at 0h to 2h and 0.8 at 17h. HIGAZI and CHALMERS (1966), in Durham, found a ratio of 1.43 close to the ground, while NOLAN and De SACHY (1927) found a value of 1.22.

Since the ratio of positive to negative conductivities varies with time of day, it follows that the space charge density due to small ions will have a similar variation, assuming that the corresponding mobilities vary little. The estimated variation of space charge due to small ions ( $\lambda_+ - \lambda_-$ ) is shown in Fig. 6.25 together with diurnal variations of space charge for July 1967 and June 1968. The variation of the difference between the two conductivities had to be smoothed. The similarity between the variations can be seen but, due to limited data, may not be significant.

## CHAPTER 7

### SPACE CHARGE AND POTENTIAL GRADIENT IN PRECIPITATION

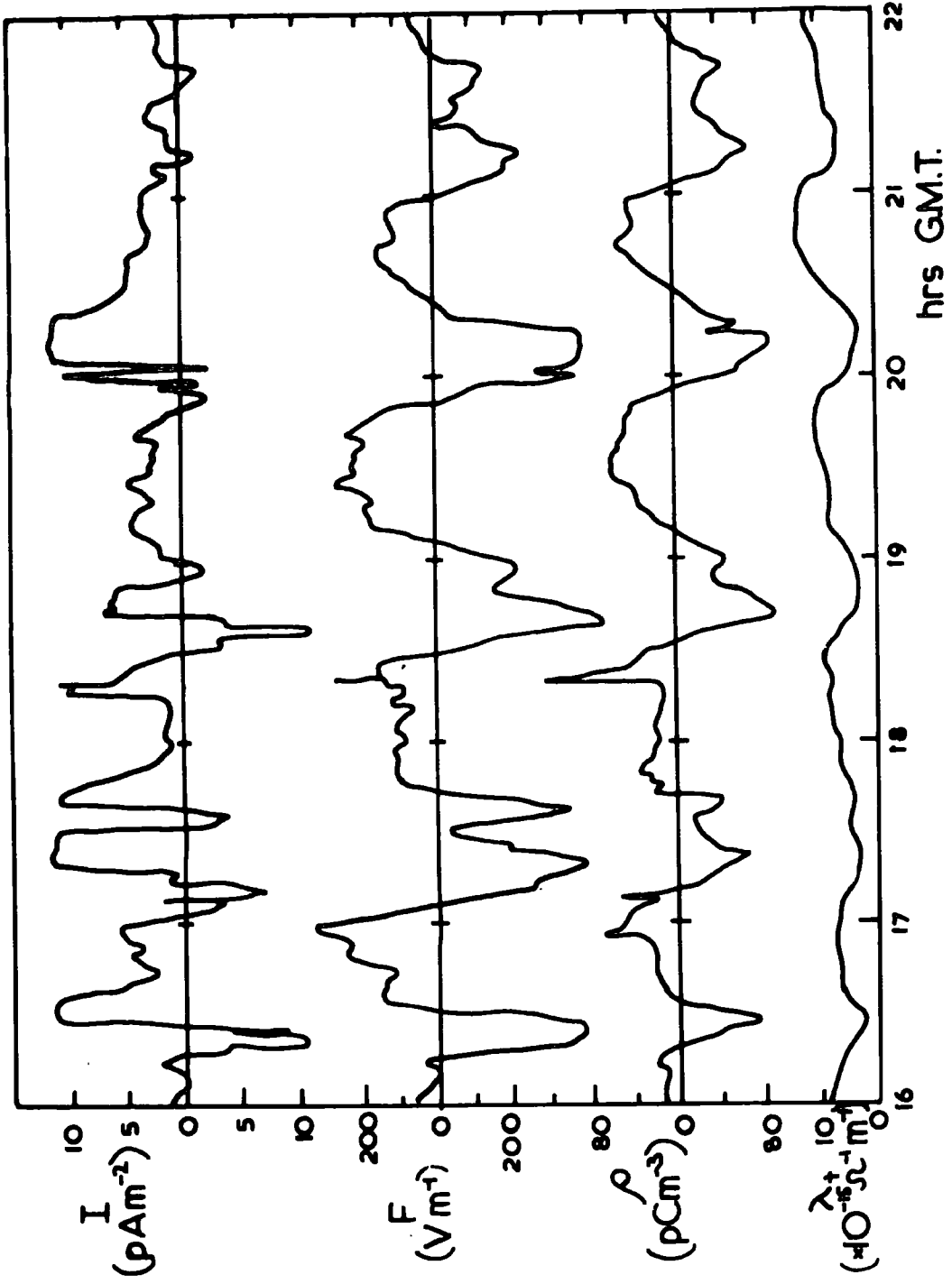
#### 7.1 General Observations of Precipitation Electricity

##### 7.1.1 Introduction

This Chapter is mostly concerned with the results of a quantitative treatment of measurements of space charge density and potential gradient. The measurements of the air-earth current were not included in the analysis partly due to the difficulty of interpreting measurements of the total current and because the values of current density often exceeded the range of the instrument ( $\pm 12.5 \text{ pA m}^{-2}$ ). With the data available it was not possible to attempt to determine the relation between potential gradient and precipitation current density. Instead, the close correlation between the records of space charge density and potential gradient prompted the analysis which led to the results given later in this Chapter.

The apparatus was subjected to precipitation of all types and magnitude, during the period of recording, from light drizzle to heavy showers and hailstorms. It was, therefore, not possible to cover the entire range of values of any parameter with a single instrument. The comparatively slow chart speed limited the resolution, so that only steady precipitation could be considered. However, the instrumental ranges used enabled both fair-weather and

FIG. 7.1. Intermittent rain - May 10th, 1968 - record 191

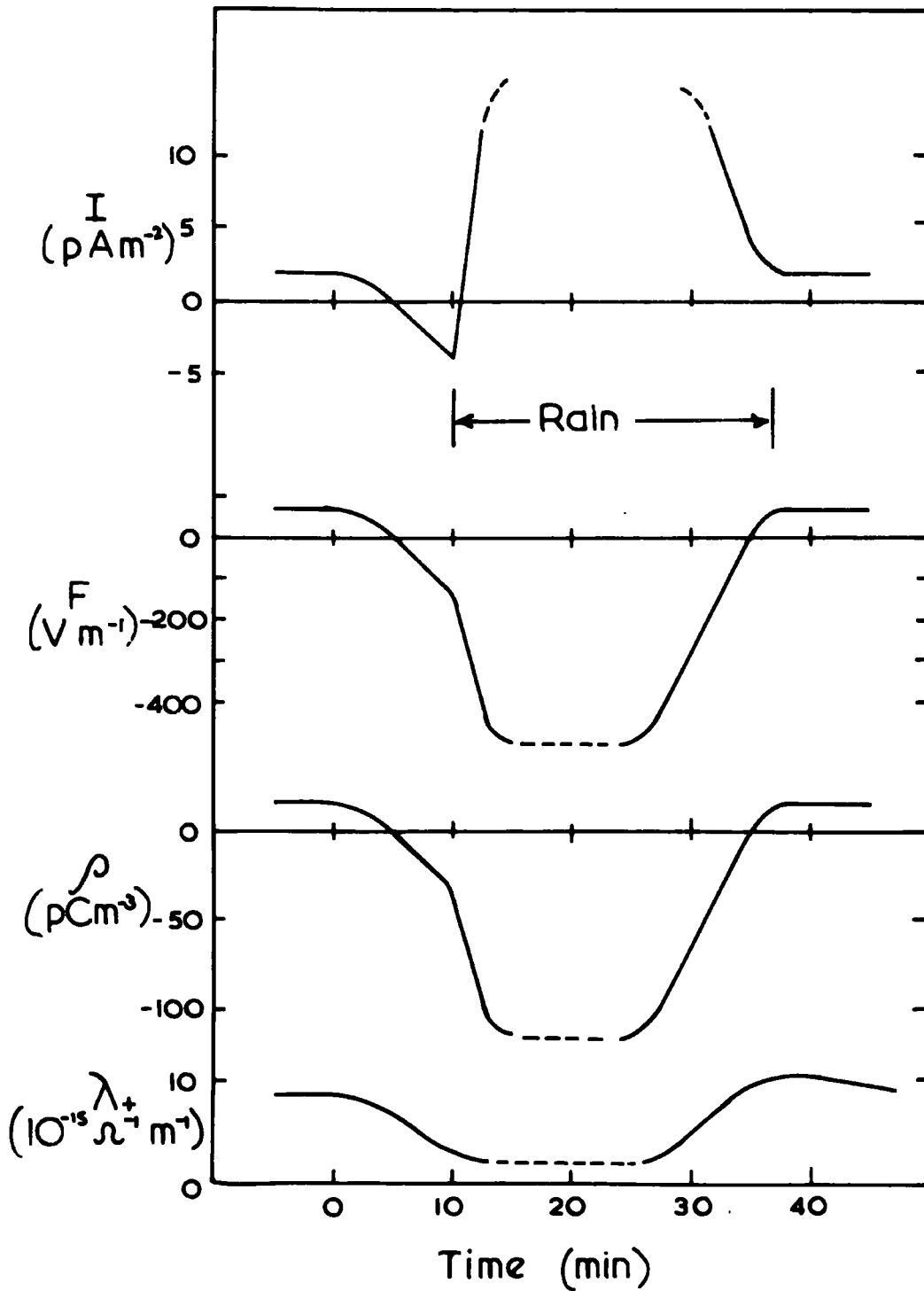


steady precipitation to be recorded without the need for changing ranges. The chart speed, 2 inches per hour, proved just adequate for the conditions during precipitation from nimbo-stratus.

#### 7.1.2 Light precipitation

An example of the electrical conditions prevailing during light rain is shown in Fig. 7.1, which comprises the records of the total air-earth current density, potential gradient, space charge density and positive conductivity. This intermittent rain, possibly associated with a warm front, lasted for about 6 hours from 16h to 22h on May 10th, 1968. The values of all parameters are changing slowly compared with stormy conditions. The total current is mostly positive, while the potential gradient and therefore conduction current are mostly negative, implying a precipitation current which is positive and mostly greater in magnitude than the conduction current. This total current for part of the time exceeds the fullscale value of  $+12\text{pA m}^{-2}$ , so that on the record it appears less positive than it would actually have been. The current is negative during periods when, presumably, the precipitation current is low and the conduction current negative. The space charge and potential gradient are both mostly negative, reaching minimum values when the current is going positive, so implying an inverse relation between precipitation current and potential gradient, as found by previous workers. Both space charge and potential gradient decrease and become negative before

FIG.7.2. Idealised record in light rain



the onset of rain, which is characterized by the rapid increase of total current from negative to high positive values.

The maximum values of total air-earth current density exceed  $12 \text{ pA m}^{-2}$ , whilst the minimum values only reach about  $-11 \text{ pA m}^{-2}$ . The values of potential gradient lie within  $\pm 500 \text{ Vm}^{-1}$  i.e. about 5 times the magnitude of the fair-weather value. For space charge the range is  $\pm 120 \text{ pC m}^{-3}$  compared with a value of about  $30 \text{ pC m}^{-3}$  for fair weather. The positive values of both are mostly not very much greater than the fair-weather values, with the exception of the occasional peak, and occur during breaks in the precipitation.

For most of the records considered the duration of the rain was less than 6 hours, but the parameters varied in much the same way. At or just before the commencement of rain all three parameters decrease and become negative simultaneously. As the rain commences or becomes heavier the precipitation current rapidly increases so that the total current soon becomes positive. At the same time the potential gradient and space charge decrease more rapidly. The positive conductivity also decreases to a fraction of its normal value, in a similar way to the space charge. In Fig. 7.2 is shown an idealized example demonstrating the main features, but in practice, as seen from Fig. 7.1, the variations are more complex. As the rain eases off all four parameters slowly return to their fair weather values when the rain finally stops.



## 7.2 Correlation of Space Charge and Potential Gradient

### 7.2.1 The recording periods

The data from 43 periods of light precipitation, including some snow, for potential gradient and space charge density were analysed and the correlation coefficients calculated. The lengths of the periods varied from about 1 hour to 6 hours, with numbers of pairs of readings varying from 30 to 192, the average being about 60. Isolated periods of precipitation of appreciably less than an hour in duration were not included due to insufficient data. The readings were taken at intervals of about 2 minutes, there being 32 readings per hour, as this was a convenient fraction of the smallest time division on the chart.

In the majority of these periods the total current was mostly positive and the potential gradient and space charge mostly negative. On a few occasions the total current was of the same sign as the potential gradient, and changed sign with both potential gradient and space charge. At these times the precipitation current must have been low so that the space charge was perhaps due to rain near, but not at, the site. At other times there was sometimes no apparent correlation between space charge and potential gradient, but this was usually due to other disturbances, such as point discharge, or to an instrumental fault. The periods analysed represent the majority of occasions of light rain, when no other large disturbances were occurring either just before or at the time of the record.

Table 7.1

Record Number	Date	Time (G.M.T)		n	r	lag (min)	Potential gradient ( $V m^{-1}$ )		Space Charge ( $\mu C m^{-3}$ )	
		Start	Finish				Mean	Std. devn	Mean	Std. devn
1.1	3. 7.67	1100	1300	64	0.89	0	-19	90	-3	18.5
3.1	5. 8.67	1100	1230	48	0.92	0	-49	112	-21	32.6
4.1	22. 8.67	2215	2415	64	0.87	0	+29	48	-8	15.7
4.2	23. 8.67	0045	0245	56	0.70	2	-47	115	-14	22.9
4.3	23. 8.67	1500	1700	64	0.37	0	-75	44	-9	6.7
5.1	22.10.67	2015	2215	63	0.77	2	-44	36	+9	53.4
7.1	30.10.67	1615	1915	62	0.90	2	-37	51	-56	79.0
7.2	3.11.67	0045	0400	62	0.95	2	+207	267	-55	66.3
7.3	3.11.67	0500	0700	63	0.96	2	-177	161	-48	40.5
8.1	28/29. 11.67									
		2300	0130	62	0.95	2	-209	190	-45	33.4
9.1a	5.12.67	1515	1715	62	0.87	4	-278	359	-103	78.7
9.1b	5.12.67	1715	1915	62	0.97	4	-169	196	-57	52.1
9.2	9.12.67	0215	0415	63	0.96	2	+15	90	+10	34.2
9.3	10.12.67	0200	0315	38	0.84	4	-222	530	-14	52.6
9.4	11.12.67	1030	1130	32	0.79	0	-27	55	-24	23.9

Table 7.1 (contd.)

Record Number	Date	Time (G.M.T)		n	r	lag (min)	Potential gradient ( $V m^{-1}$ )		Space Charge ( $\mu C m^{-2}$ )	
		Start	Finish				Mean	Std. devn	Mean	Std. devn
9.5	11.12.67	1430	2030	192	0.91	0	-193	215	-105	80
10.1	23.12.67	1500	1630	47	0.97	2	-12	144	-7	29.4
10.2	23.12.67	1815	1915	31	0.97	2	-12	145	-5	33.3
10.3	26.12.67	0445	0645	63	0.97	2	-12	151	+1	37.8
11.1	14. 1.68	0030	0215	55	0.94	2	-54	89	+10	10
11.2a	14. 1.68	1230	1430	62	0.76	4	-141	123	-19	7.5
11.2b	14. 1.68	1430	1630	62	0.94	4	-76	148	-10	9.1
11.2c	14. 1.68	1630	1830	63	0.80	2	-89	99	-16	7.3
12.1	25. 1.68	0045	0215	47	0.75	2	-55	60	-22	17.0
12.2	28. 1.68	1545	1715	47	0.91	2	+35	117	-10	26.1
18.1	6. 5.68	0830	1030	63	0.96	2	+65	433	+18	63.2
18.2	10. 5.68	1200	1400	63	0.97	2	-261	320	-48	48.3
19.1	10. 5.68	1600	2200	191	0.93	2	-30	189	-3	40
19.2	11. 5.68	0345	0545	63	0.88	2	-189	50	-31	13.7
19.3	11. 5.68	0615	0730	38	0.94	4	-192	274	-47	62.1

Table 7 (contd.)

Record Number	Date	Time (G.M.T)		n	r	lag (min.)	Potential gradient ( $V m^{-1}$ )		Space Charge ( $\mu C m^{-3}$ )	
		Start	Finish				Mean	Std. devn	Mean	Std. devn
19.4	17. 5.68	1845	1945	32	0.59	0	+60	250	-1	44.5
19.5	21. 5.68	1200	1600	127	0.98	2	-13	130	-12	30
20.1	27. 5.68	0700	0800	32	0.88	0	-30	125	-16	29.1
20.2	4. 6.68	0200	0400	32	0.85	0	+49	211	+5	18
21.1	6. 6.68	0045	0245	62	0.96	4	-317	514	-53	59.4
21.2a	6/7.6.68	2300	0100	30	0.97	4	-135	252	-22	41.4
21.2b	7. 6.68	0100	0300	30	0.90	4	+4	94	+12	23.6
21.4	15. 6.68	0545	0645	31	0.81	2	+4	70	+5	16.9
22.1a	25. 6.68	1930	2130	30	0.90	4	-50	188	-15	34.8
22.1b	25. 6.68	2130	2330	32	0.86	0	-24	176	+6	41.2
23.1	3. 7.68	1655	1735	30	0.89	2.5	-804	255	-110	41.7
23.2	3. 7.68	1830	1910	32	0.81	0	-820	594	0	45.1
23.3	3. 7.68	1937	2017	27	0.87	6	-1180	589	+94	126

### 7.2.2. Correlation coefficients

The correlation coefficient for each period is given in Table 7.1, together with the number of pairs of readings used to compute it. Without exception the correlation coefficients are positive. For many records the correlation coefficients are about 0.9 or higher, while only one has a coefficient less than 0.7. The record 4.3 has a coefficient as low as 0.37, but this was found to be due to a wide divergence between the records of space charge and potential gradient for part of the period. The reason for this was not apparent from the charts, but appeared not to be an instrumental fault.

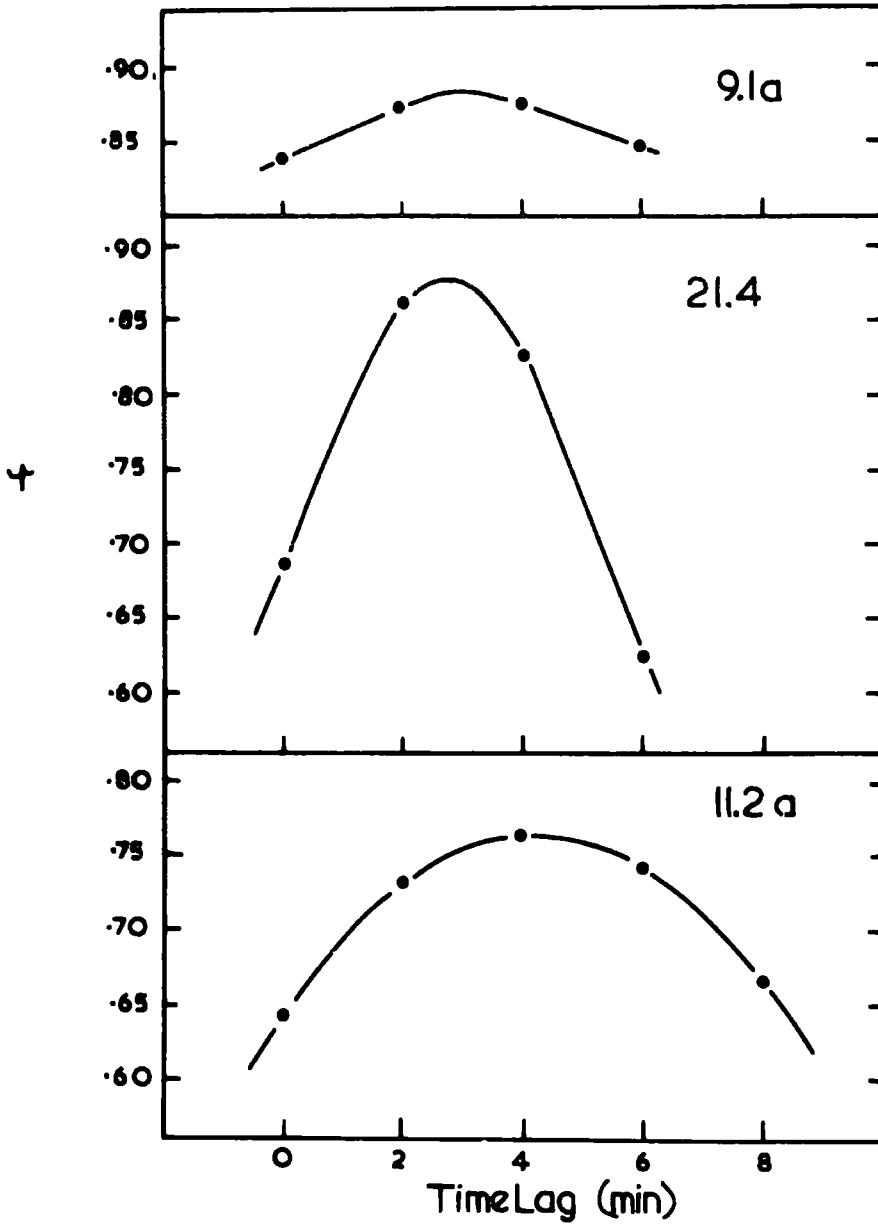
The significance of a correlation coefficient was discussed in Chapter 5, and was shown to rely on the number of degrees of freedom. If all pairs of readings are independent, the number of degrees of freedom is  $n - 2$ , as given in Chapter 5. However, if the record has a memory which is longer than the time interval between readings, the number of degrees of freedom will be less than  $n - 2$ . The length of this memory may be found from the auto-correlation of members of the time series. GROOM (1966) assumes a value of 5 min for this memory. Taking this value, the number of degrees of freedom will be reduced to  $0.4(n - 2)$ . Applying this to the present records, a significance test may be applied to the correlation coefficients. From Table 5, for record 4.3 where the number of degrees of freedom,  $\nu$  is about 25, the correlation coefficient is significant at the 90 per cent level

but not at the 95 per cent level. For the next lowest correlation coefficient, 0.7 for record 4.2,  $\nu \simeq 22$  so that the coefficient is just significant at the 99.9 per cent level. For record 23.3, which has the lowest value of  $n$ ,  $\nu = 10$ ,  $r = 0.87$  so that it is significant at the 99 per cent level but only barely significant at the 99.9 per cent level. As a further example, in record 21.4,  $\nu = 12$ ,  $r = 0.81$ , which is significant at the 99 per cent level but not quite at the 99.9 per cent level. For all the records, except 4.3, the correlation coefficients are significant at the 99 per cent level at least, and most at the 99.9 per cent level.

### 7.2.3 Mean values and standard deviations

In Table 7.1 are given, also, the mean values and standard deviations of space charge density and potential gradient. For potential gradient, the mean values are predominately negative, with only a few positive values. The largest positive value, for 7.2, is  $207 \text{ Vm}^{-1}$ , whereas the corresponding value of space charge is  $-55 \text{ pC m}^{-3}$ . The largest negative mean value of potential gradient is  $-1180 \text{ Vm}^{-1}$ , for 23.3, though the field mill range was  $\pm 8,000 \text{ Vm}^{-1}$  to allow for the larger variation in potential gradient. There was, however, in this record no evidence of point discharge occurring. The standard deviations indicate the spread of the readings, although in most cases the distribution is not symmetrical, there being more lower than higher values.

FIG.7.3. Variation of Cross-correlation coefficient with time lag.



The mean values of space charge are also mostly negative with the largest negative value of  $-110 \text{ pC m}^{-3}$  occurring in 23.1, although this is similar to 23.3 mentioned above. Similar values occur in 9.1a and 9.5, both for snow, but most other values are within  $\pm 50 \text{ pC m}^{-3}$ .

### 7.2.3 Time lags

The time lag of space charge behind potential gradient was taken to be that which gave the maximum cross-correlation coefficient. These time lags are shown in Table 7.1, given as an integral multiple of the time interval between readings. They are all seen to be either zero or positive implying that the potential gradient leads the space charge. The time lag can be partly accounted for by the time constant of the space charge collector being about 1 min and greater than that of the field mill.

There may be errors in the calculated values of the cross-correlation coefficient, if the true correlation coefficient corresponds to a time lag which is not an integral multiple of the time interval. With a time interval of as long as 2 min the errors introduced may not be negligible and need to be considered. Fig. 7.3 shows the variation of the cross-correlation coefficient with time lag for each of 3 records. In the first, 9.1a, the time lag lies about midway between two points, so that the maximum correlation coefficient is about 1 per cent higher than the calculated coefficient, which corresponds to a lag of 4 min.





Table 7.2

Values of constants for lines:  $F = A\rho + B$

Record Number	r	k	c	A ( $V\ m^{-1}$ per $pC\ m^{-3}$ )	B ( $V\ m^{-1}$ )
1.1	0.89	-1.35	1.04	5.04	-4
3.1	0.92	-0.69	0.97	3.32	20
4.1	0.87	-1.47	1.07	10.2	50
4.2	0.70	-1.02	1.00	5.06	32
6.1	0.77	-0.44	0.87	5.87	490
7.1	0.90	-0.42	0.94	6.10	63
7.2	0.95	-1.25	1.02	4.08	16
7.3	0.96	-1.24	1.01	4.02	14
8.1	0.95	-1.48	1.03	5.92	55
9.1a	0.87	-1.35	1.05	4.80	220
9.1b	0.97	-1.37	1.01	4.59	78
9.2	0.96	-0.89	0.99	2.61	-10
9.3	0.84	-0.34	0.90	9.07	-98
9.4	0.79	-0.75	0.93	1.92	18
9.5	0.91	-0.97	1.00	2.68	88
10.1	0.97	-0.79	0.99	4.83	22
10.2	0.97	-0.70	0.99	4.32	11
10.3	0.97	-0.65	0.98	3.93	-17
11.1	0.94	-1.33	1.02	9.08	38
11.2a	0.76	-1.64	1.18	19.3	217
11.2b	0.94	-1.63	1.03	16.7	99
11.2c	0.80	-1.56	1.12	15.2	153
12.1	0.75	-0.57	0.89	3.15	13
12.2	0.91	-0.72	0.97	4.36	78
18.1	0.96	-1.58	1.03	7.05	-59
18.2	0.97	-1.57	1.02	6.74	62
19.1	0.93	-1.40	1.03	4.87	-15

Table 7.2 contd.

Record Number	r	k	c	A $V\ m^{-1}$ per $pC\ m^{-3}$	B $V\ m^{-1}$
19.2	0.88	-1.40	1.04	4.88	-16
19.3	0.94	-1.35	1.02	4.51	22
19.4	0.99	-1.15	1.00	5.61	-53
19.5	0.98	-0.91	1.00	4.33	39
20.1	0.88	-1.33	1.04	4.45	40
20.2	0.85	-1.75	1.13	14.6	-21
21.1	0.96	-1.67	1.04	7.14	59
21.2a	0.97	-1.53	1.02	4.98	-24
21.2b	0.90	-1.25	1.02	3.10	-33
21.4	0.81	-1.55	1.09	4.03	15
22.1a	0.90	-1.66	1.07	5.80	38
22.1b	0.86	-1.56	1.09	4.66	-51
23.1	0.89	-0.34	0.93	5.68	-180
23.2	0.81	-0.72	0.94	12.4	-820
23.3	0.87	-0.28	0.91	4.58	-300

In 21.4 both potential gradient and space charge vary more rapidly, so the resulting error is about 2 per cent. The third, record 11.2a, shows an optimum case where the time lag is very nearly an integral multiple of the time interval, so that the error is negligible. In all cases, the error in the calculated coefficient will lead to an underestimate rather than an overestimate of the true value. It is probable that the error in all cases is not more than 2 per cent.

### 7.3 The Relation between Space Charge and Potential Gradient

#### 7.3.1 The lines of best fit

The high values obtained for the correlation coefficients implied that a linear relation should exist between potential gradient and space charge density. The line of best fit for each record was obtained by the method due to MORGAN (1960) as described in Chapter 5. The potential gradient,  $F$ , was presumably due to the presence of the space charge,  $\rho$ , so the lines of best fit were obtained in the form:

$$F = A\rho + B$$

In Table 7.2 the values of  $A$  and  $B$  are given for each of 42 records. Record 4.3 was not included because the low correlation coefficient was not significant at the 95 per cent level. The corresponding correlation coefficients are repeated in Table 7.2, and the values of  $k$ , obtained from the relative errors of  $x$  and  $y$ , and  $c$  also included. The values of  $c$  can be seen to be mostly close

to unity due to the high correlation coefficients. The values of A, in  $Vm^{-1}$  per  $pC m^{-3}$ , are all positive, whereas the values of B, in  $Vm^{-1}$ , are both positive and negative. B represents the potential gradient which should exist above the region of space charge which is controlling F.

A scatter diagram, showing both the regression lines with the line of best fit, is given in Fig. 7.4, which is taken from record 9.1a. The slope of the line of best fit lies between the slopes of the regression lines. The distribution of points is not even, but grouped at the negative end. In Fig. 7.5, which is for record 19.1, the scatter is less and the distribution more even. The correlation coefficients for these two records are 0.87 and 0.93 respectively.

### 7.3.2 Distribution of slopes of lines

For most of the records the high correlation coefficients mean that any inaccuracy in the slope of the line, from the assumptions associated with the use of MORGAN's method, should be relatively small. Therefore, a meaningful comparison may be made between the values of slope. A distribution of the slopes of the lines should reflect a physical distribution rather than just a distribution due to the random errors of measurement. To obtain a smooth distribution a large number of records is essential. Although not large, statistically, it was hoped that the number, 42, of records would provide an indication of the distribution of the

FIG.7.6. Frequency distribution of A – for  $F = Ap + B$

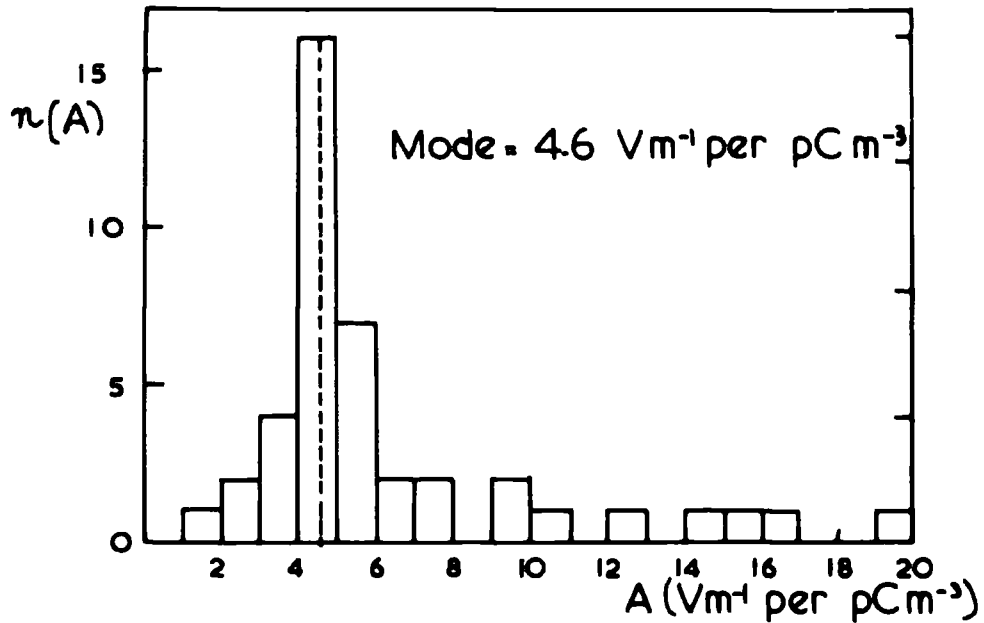
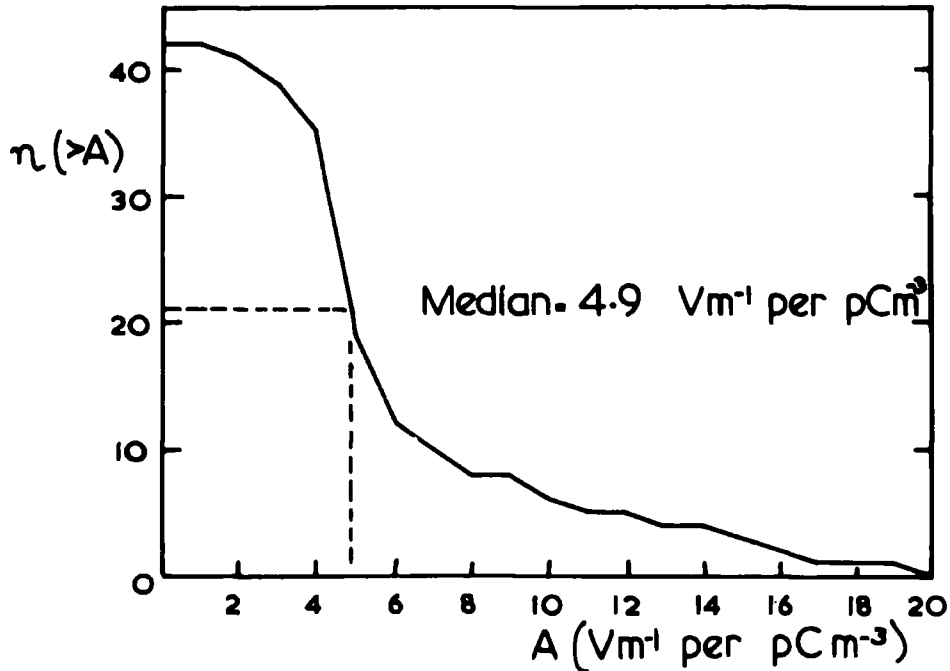


FIG.7.7. Cumulative frequency distribution of A



values of A.

In Table 7.2, the values of A can be seen to range from about 2 to  $19 \text{ Vm}^{-1}$  per  $\text{pC m}^{-3}$ , i.e. by a factor of about 10. Closer inspection, however, reveals a predominance of values 4 to  $5 \text{ Vm}^{-1}$  per  $\text{pC m}^{-3}$ , implying that there is a preferred value between these limits. The distribution of A is shown in Fig. 7.6 as a histogram with the class interval chosen to be  $1 \text{ Vm}^{-1}$  per  $\text{pC m}^{-3}$ . Within the class 4 to  $5 \text{ Vm}^{-1}$  per  $\text{pC m}^{-3}$  the frequency of occurrence is 16, i.e. 38 per cent of the total. Between 3 and  $6 \text{ Vm}^{-1}$  per  $\text{pC m}^{-3}$ , the number is 27 or 64 per cent of the total. This implies that a typical value lies between 3 and  $6 \text{ Vm}^{-1}$  per  $\text{pC m}^{-3}$ , or that there will be a 2 in 3 chance of a value lying between these limits. The distribution is not symmetrical about its highest point, but squashed up against its lower limit of zero, while on the other side of the distribution there is no such limit. For such a distribution the mean, median and mode will not all coincide. The mode will lie between 4 and 5 but the high values of up to  $19 \text{ Vm}^{-1}$  per  $\text{pC m}^{-3}$  will cause the mean to move outside this limit.

For all 42 records the mean value was calculated as:

$$\bar{A}_1 = 6.32 \text{ Vm}^{-1} \text{ pC m}^{-3}$$

with standard deviation:

$$S_{A_1} = 3.84 \text{ Vm}^{-1} \text{ per pCm}^{-3}$$

By excluding all values of A for which the frequencies of

occurrence is less than 2, the mean and standard deviation become:

$$\bar{A}_2 = 5.01 \text{ Vm}^{-1} \text{ per pC m}^{-3}$$

$$S_{A_2} = 0.83 \text{ Vm}^{-1} \text{ per pC m}^{-3}$$

The mode of the distribution, i.e. the most frequent value, is about  $4.6 \text{ Vm}^{-1} \text{ per pC m}^{-3}$ . In Fig. 7.7 the cumulative frequency, taken from the histogram, has been plotted. The ordinate,  $n(> A)$ , is the frequency of occurrence of values greater than A. The point of maximum negative slope coincides with the mode, but this is more conveniently obtained from the histogram. The median, that value which divides the population into two equal parts, can be obtained conveniently from Fig. 7.7 as shown. The value, about  $4.9 \text{ Vm}^{-1} \text{ per pC m}^{-3}$ , is a little higher than the mode but lower than either of the means.

### 7.3.3 Estimate of height of space charge

It is necessary now to consider the physical implications of the preceding analysis and its results. Firstly, the relations found are between potential gradient and space charge density, both measured at the ground. A simple calculation shows that for the measured space charge densities to produce the required potential gradients, the space charge must extend upwards for several tens of metres. Also, the variations in space charge density must be similar at all heights to produce the high degree of correlation between it and potential gradient. Poisson's equation can be used to determine the space charge necessary to produce the

required potential gradient, and can be written as

$$\frac{dF}{dz} = -\frac{\rho}{\epsilon_0}$$

$$\text{or } dF = -\frac{\rho}{\epsilon_0} dz \quad \text{--- 1}$$

For simplicity, it is convenient to assume that the space charge density,  $\rho$ , remains constant with height,  $z$ . Equation 1 can then be integrated over the region from  $z = 0$  (ground level) to  $z = h$  (the top of the region of space charge) where the potential gradient  $F_h$  is considered constant over the period considered, and due to charges in clouds and higher in the atmosphere, including those on the electrosphere. By integrating equation 1:

$$F_h - F = -\frac{\rho}{\epsilon_0} h \quad \text{..... 2}$$

If  $h$  is now kept constant and the variation of  $\rho$  and  $F$  with time is considered, equation 2 can be differentiated so that:

$$-\frac{dF}{d\rho} = -\frac{h}{\epsilon_0}$$

$$\text{which gives } h = \epsilon_0 \frac{dF}{d\rho} \quad \text{..... 3}$$

Since  $dF/d\rho$  is the slope of the line relating  $F$  and  $\rho$ , equation 3 may be rewritten as:

$$h = \epsilon_0 A \quad \text{..... 4}$$

Alternatively, equation 2 may be compared with the equation of the line of best fit. These two equations may be written:

$$F = \frac{h}{\epsilon_0} \rho + F_h$$

$$\text{and } F = A\rho + B$$



By comparing coefficients the following are obtained:

$$F_h = B \quad \dots\dots\dots 5$$

$$\frac{h}{\epsilon_0} = A$$

which leads to  $h = \epsilon_0 A$ , which is identical to equation 4.

Considering the units of A,  $Vm^{-1}$  per  $pC m^{-3}$ ,  $\epsilon_0$  must be expressed in  $pF m^{-1}$ , and so h can be calculated. Substituting the value of  $\epsilon_0$  with these units equation 4 becomes:

$$h = 8.854 A$$

For each of the mean values of A the following values of h were found:

$$h_1 = 56m$$

$$h_2 = 44.4m$$

The work of COLLIN, RAISBECK and CHALMERS (1963) was mentioned in Chapter 1. They obtained 3 empirical relations in the form  $F = a \Delta f + b$ , where  $\Delta f$  was the difference between the potential gradient at the level of the top of a 25m mast and at the ground, and F was the potential gradient at the ground. They obtained the following relations from 3 sets of results:

$$F = 3.5 \Delta f - 9.4$$

$$F = 2.3 \Delta f + 59$$

$$F = 4.0 \Delta f + 110$$

The total height of space charge may be calculated from these, assuming constant space charge density with height. The height h is given directly from

$$h = 25a$$

since the height of the mast was 25 m. From the mean value of a,

FIG.7.8. Frequency distribution of  $B$  — for  $F = Ap + B$

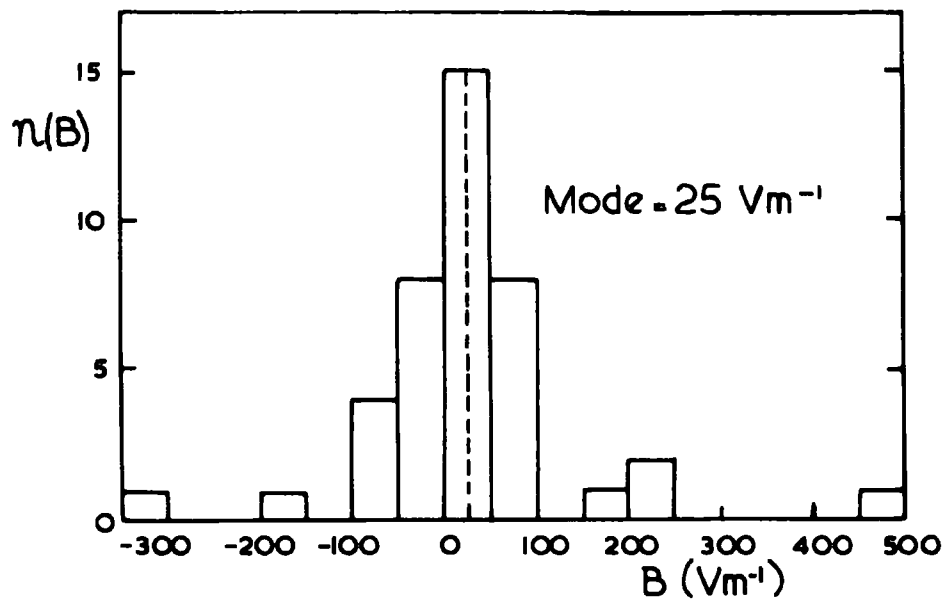
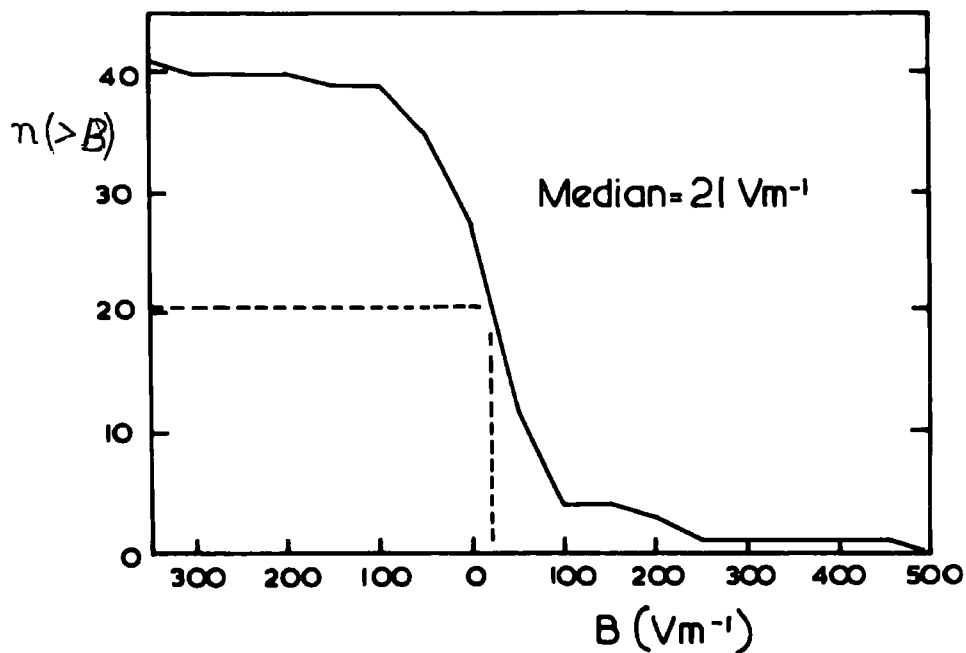


FIG.7.9. Cumulative frequency distribution of  $B$



the height is 85 m.

#### 7.3.4 The constant term B

It was shown from equation 5 in section 7.3.3 that the constant term B represents the potential gradient above the region of space charge and due to charges in the cloud and higher up which are considered constant over the period considered. Values of B, unlike A, are both positive and negative and vary over a large range. These values are liable to suffer from greater errors than A, especially if the mean point of the line is not close to the origin, since small changes in A may result in large changes in the intercept, B. The frequency distribution of B, shown in Fig. 7.8, is more symmetrical than for A since both positive and negative values are permissible. The class interval has been taken as  $50 \text{ Vm}^{-1}$  and the range of the distribution is from  $-350 \text{ Vm}^{-1}$  to  $+500 \text{ Vm}^{-1}$ . One value of  $-820 \text{ Vm}^{-1}$ , from record 23.2, was excluded as apparently not belonging to the population. The most frequent values are close to zero, between 0 and  $50 \text{ Vm}^{-1}$ . Within this interval the frequency of occurrence is 15 or 37 per cent of the total. Between  $-50 \text{ Vm}^{-1}$  and  $+150 \text{ Vm}^{-1}$ , the frequency is 31 i.e. 76 per cent. From Fig. 7.8 the mode and mean may be calculated. These are

$$\bar{B} = 28.5 \text{ Vm}^{-1}$$

with standard deviation,  $S_B = 113 \text{ Vm}^{-1}$

and the mode =  $25 \text{ Vm}^{-1}$

Table 7.3

Summary of values for relation between F and  $\phi$

<u>Quantity</u>	<u>Value</u>	<u>Standard deviation</u>
Slope of line of best fit ( $Vm^{-1}$ per $pC\ m^{-3}$ )		
Mean for all records, $\bar{A}_1$ :	6.32	3.84
Mean for $n(A) > 1$ , $\bar{A}_2$ :	5.01	0.83
Median:	4.9	0.83
Mode:	4.6	
Constant term ( $Vm^{-1}$ )		
Mean, $\bar{E}$ :	28.5	113
Median:	21	
Mode:	25	
COLLIN et.al.	53	
Mean height of space charge (m)		
From $\bar{A}_1$ , $\bar{h}_1$ :	56	34
From $\bar{A}_2$ , $\bar{h}_2$ :	44.4	7.3
COLLIN et.al.	85	

From Fig. 7.9, the median has a value of  $21 V_m^{-1}$ . All three values are close compared with the standard deviation of the mean, implying a near symmetrical distribution. The results of COLLIN, RAISBECK and CHALMERS gave a mean value for the constant term of  $53 V_m^{-1}$  from their 3 expressions.

The values of A and B, mean, mode and median, together with other relevant values are summarized in Table 7.3 for convenience.

CHAPTER 8

DISCUSSION OF RESULTS

8.1 The Fair-Weather Diurnal Variations

8.1.1 Summary of results

Before discussing the importance of the results set out in Chapter 6, it is convenient to give a brief summary of the diurnal variations for the whole year. For potential gradient (Fig. 6.18), the diurnal variation follows closely the equivalent variations measured over the oceans, which are assumed to reflect the variation of the potential of the electrosphere. On the other hand the diurnal variation of air-earth current density (Fig. 6.20) appears to be due mainly to variations in the columnar resistance. An estimate of the diurnal variation of columnar resistance (Fig. 6.22) has a similar shape to that measured over New Hampshire. The space charge density varies in a similar way to the air-earth current density, both of which have minimum values in the afternoon. The amplitude of the variation of both these is about 40 per cent from the mean compared with about 20 per cent for potential gradient.

The following discussion will be concerned in explaining the observed variations of  $F$ ,  $I$  and  $\rho$ . Clearly, the views generally held at present, that, in areas not free from pollution,  $I$  is more likely than  $F$  to follow  $V$ , are not necessarily correct. At Lanehead,  $F$  closely follows the variation in  $V$ , as derived from measurements at sea, whereas the variation of  $I$  is determined mostly by the

variation in R. It will be shown that these observations may be explained by considering the nature and source of the pollution at Lanehead, together with the mechanisms of convection and turbulence.

### 8.1.2 Potential gradient and air-earth current

It is helpful to begin the discussion by considering the relations between the parameters involved. Neglecting convection currents, the following equations are obtained from Chapter 1:

$$I = \lambda F \quad \dots\dots 1$$

$$I = \frac{V}{R} \quad \dots\dots 2$$

and from equations 1 and 2.

$$F = \frac{V}{\lambda R} = \frac{Vr}{R} \quad \dots\dots 3$$

From equation 2

$$\frac{1}{R} \frac{dR}{dt} = \frac{1}{V} \frac{dV}{dt} - \frac{1}{I} \frac{dI}{dt}$$

from which the percentage variation of R was calculated.

In a similar manner, equation 3 can be differentiated to give:

$$\frac{1}{F} \frac{dF}{dt} = \frac{1}{V} \frac{dV}{dt} + \frac{1}{r} \frac{dr}{dt} - \frac{1}{R} \frac{dR}{dt}$$

At Kew, WHIPPLE (1936) found that the percentage diurnal variations of R and r ran closely together for both Winter and Summer, with the exception of a short period of time in the morning, before convection was able to carry the nuclei at the ground to greater heights. If the same applies at Lanehead, this

means that:

$$\frac{1}{r} \frac{dr}{dt} = \frac{1}{R} \frac{dR}{dt} \dots\dots\dots 4$$

so that

$$\frac{1}{F} \frac{dF}{dt} = \frac{1}{V} \frac{dV}{dt} \dots\dots\dots 5$$

If, therefore, the variation of  $r$  is similar to that of  $R$ , the diurnal variation of  $F$  will be similar to that of  $V$ .

It has been shown, therefore, that in the absence of appreciable convection currents the diurnal variations of both  $F$  and  $I$  are accounted for in terms of the variations of  $r$  and  $R$ . If appreciable convection currents are present, equation 4 will no longer be true, so for equation 5 to hold, a more complex relation than equation 4 is needed. Since, in Winter, convection currents are expected to be less than in Summer, the seasonal difference (Fig. 6.2) in the variations of  $F$  can, perhaps, be accounted for. The seasonal difference for  $I$  and  $\rho$  will be explained below in terms of the effect of nuclei in the atmosphere.

## 8.2 Atmospheric Pollution Effects

### 8.2.1 Ions and nuclei

The preceding discussion involving the air-earth current and columnar resistance has shown that there is an appreciable difference in the atmospheric electric characteristics between the oceans and land stations such as Lanehead. Over the oceans there is very little variation of the columnar resistance, yet at Lanehead the estimated



variation is up to about 40 per cent of the mean, each way. On land, the conductivity at all heights within the austausch region depends on the concentration of nuclei in the air. Near the ground, the conductivity is affected appreciably by local pollution, but even where this is low, such as at Lanehead, there are still sufficient nuclei in the air to modify the columnar resistance.

Over the oceans the nucleus concentration is small so that the conductivity would be expected to be much greater than over land. However, the rate of production of ions over land is about 5 or 6 times greater than at sea due to radioactive substances in the ground. These two effects balance out so that the conductivity at sea is about the same as a reasonably unpolluted site on land. Above the austausch region the conductivity increases rapidly for several reasons: the relatively small number of nuclei, the increased cosmic ray intensity and the increased ionic mobility due to the decrease in pressure. EVERLING and WIGAND (1921) found that, at 8km, the nucleus concentration had decreased by a factor of  $10^4$  from its value at the ground. SAGALYN and FAUCHER (1954) pointed out that the austausch region contributes from 40 to 73 per cent of the total columnar resistance. The evidence suggests, therefore, that the diurnal variation of columnar resistance is mostly due to processes within the austausch region.

### 8.2.2 The diurnal variation of the columnar resistance

It has been shown that, at Lanehead, the diurnal variation of potential gradient is independent of the variations of conductivity at the ground, so long as seasonal and other effects are averaged out or otherwise eliminated. It was also shown (8.1.2) that this can be partly explained if the air-resistivity near the ground varies as the total columnar resistance. The diurnal variation of the columnar resistance can be explained by reference to the results of SAGALYN and FAUCHER (1956), who made measurements of the time variations of conductivity and charged nucleus concentration between 200m and 4,500m above the ground in New Hampshire. Fig. 6.22 shows the diurnal variation of columnar resistance, which was found to be similar to their results for the nucleus concentration. The minimum occurs at about sunrise and the maximum at 15h local time. SAGALYN and FAUCHER showed that the increase after sunrise was due primarily to turbulent transfer and convection.

The slow fall-off after 15h was attributed to coagulation and subsidence of the nuclei. In the lower parts of the austausch region the decrease was due mainly to coagulation but higher up the additional mechanism of subsidence had the effect of lowering the level of the top of the austausch region, sometimes by as much as 800m. Advection, caused by high winds, inhibited these mechanisms and so, in such conditions, no regular decrease was observed. For this reason the Winter months are more liable to irregular variations of the columnar resistance. SAGALYN and FAUCHER also

related their results to surface measurements, where the afternoon minimum of nucleus concentration was accounted for by convection and turbulence carrying nuclei to greater heights, and the minimum at night by coagulation. They pointed out that these two processes, plus the nature of the source of the nuclei, would govern the diurnal variation of large ions at the ground.

At Lanehead, the air-earth current variation (Fig. 6.20) shows a minimum in the afternoon, for Summer, coinciding with the maximum in columnar resistance. The space charge also has a minimum in the afternoon which, from the preceding discussion, is presumably due to the depletion of ions at the surface by convection. In Winter, the convection is expected to be less, so accounting for the less regular variation of both air-earth current and space charge. At night, coagulation will allow an increase in the conductivity near the ground, while in the morning nuclei from distant sources of pollution will be carried into the area by the increased winds, assuming higher windspeeds during day-time. The conductivity can then be expected to decrease during the morning and early afternoon, in a similar manner to the increase in columnar resistance. By this means the necessary conditions for the observed diurnal variation of potential gradient can be realized. Apart from WHIPPLE (1936), already mentioned, further evidence of these conditions can be found in the results of WAIT (1943), who found that during the Summer at Watheroo, Western Australia, the resistivity near the

ground did vary in the same manner as the columnar resistance.

### 8.2.3 The effects of pollution at atmospheric electric stations

Measurements of the fair-weather diurnal variations of the atmospheric electric elements have been made in a variety of locations. At sea, measurements have yielded results dependent on world-wide effects, while on land atmospheric pollution has modified the variations. OGAWA (1960) showed that the diurnal variations of air-earth current at polluted sites, such as Kew, can be explained if the equation  $I = V/R$  holds, where the variation of  $R$  is locally dependent and that of  $V$  dependent on the world thunderstorm activity. Measurements at high altitudes on mountains have yielded results similar to those found at sea. One of the most promising of these sites is at Mauna Loa, Hawaii (COBB and PHILLIPS, 1962). This site, at about 3km, is above the austausch region for much of the time, so that the nucleus concentration should be low and representative of that level (COBB, 1968). The air-earth current density at Mauna Loa has a diurnal variation close to that found from the Carnegie (TORRESON et.al., 1946), yet if the variation with local time is considered it is similar to the diurnal variation of air-earth current found at Lanehead. Here the variation is due, probably, to variations in columnar resistance, but at Mauna Loa no such variation should exist. For two diurnal variations to have similar shapes for different reasons seems unlikely, although no reason for their similarity is apparent as yet.

Lanehead seems to be in a position enjoying a relatively pollution-free atmosphere, yet still within the austausch region. Pollution from sources several tens of kilometres away provide a supply of nuclei in the atmosphere which, as has been seen, result in the observed diurnal variation of columnar resistance, by means of the mechanisms of convection and coagulation. At more polluted sites, the variation of conductivity depends on the variation of the production of pollution which will therefore affect the variation of potential gradient and space charge. However, at Lanehead, the potential gradient depends on world-wide effects while the space charge depends on the mechanisms by which the variation of columnar resistance is produced. KAWANO (1957) gives a Summer diurnal variation of space charge density, at Hongo, which also has an afternoon minimum, local time, together with a second minimum after midnight and before sunrise, presumably due to coagulation. For Lanehead, on the other hand, the space charge density is almost constant at this time. The difference between these two may be that there are higher winds at Lanehead than at Hongo during the night, so inhibiting coagulation.

#### 8.2.4. Seasonal variations

The processes of convection, turbulence and advection will be dependent on the weather and, therefore, the season. The variation of columnar resistance should then reflect this seasonal dependence.

The air-earth current variation for May, which was cold and overcast for the time of year, is less than either April or June. The weather conditions have therefore inhibited the convection of nuclei to higher levels, so the variation in columnar resistance has been reduced. The seasonal variation is manifest in the much smaller variation of air-earth current in Winter compared with Summer and Autumn. The space charge is affected in a similar way, but not to such a great extent, presumably due to the reduced convection in Winter.

The annual variations have shown a wide range of variation throughout the year. The double maxima and minima for each parameter is not usual. All three vary in the ratio of 3 or 4 to 1 between their maximum and minimum values. At Kew (SCRASE, 1934) the potential gradient variation was only 2 to 1 and showed a single maximum in the Winter and a minimum in the Summer. The air-earth current, at Kew, had a maximum in the Summer, unlike Lanehead, and a range of about 3 to 1. The Winter minima at Lanehead may be associated with the snow which was on the ground for most of December, January and February, while Spring and Autumn are susceptible to high winds which may have caused these high values. In summer, the low values may be ascribed, for air-earth current density and space charge density at any rate, to the higher columnar resistance during the afternoon.

### 8.2.5 Concluding remarks

This discussion has shown that it is not necessarily correct to assume that, except over the oceans or above the austausch region, F will be dependent on local effects, but that I is more likely to depend on V. On the contrary, as at Lanehead, F may follow V but I is, almost certainly, dependent on the variations in R, which in turn depends on the nucleus concentration in the atmosphere above the station. Seasonal changes have shown the importance of convection in modifying the variation of R and, therefore, of I. Space charge measurements have further confirmed the effects of convection in carrying nuclei to higher levels during the daytime.

## 8.3 Space Charge in Precipitation

### 8.3.1 Summary of results

The results of measurements of space charge density and potential gradient, during precipitation from nimbo-stratus clouds, have shown that the variations in potential gradient under such conditions are due almost entirely to a region of space charge reaching up some tens of metres and, in some way, apparently associated with the charging of the rain drops. The conditions were such that neither point discharge nor splashing would have occurred, so some other source of the space charge must be looked for. The correlation coefficients were mostly greater than 0.8 and many of these were higher than 0.9, so that the estimated, empirical relations between potential gradient and space charge

were thought to be free from large random errors. From 42 records the following mean relation was calculated:

$$F = 5.01 \rho + 28$$

where  $F$  is in  $\text{Vm}^{-1}$  and  $\rho$  in  $\mu\text{C m}^{-3}$ . The distribution of slopes indicated a 2 out of 3 chance of a value between 3 and 6  $\text{Vm}^{-1}$  per  $\mu\text{C m}^{-3}$  occurring. The constant term showed a wider variation of both positive and negative values, but with the more frequent values close to zero. Assuming the space charge density to be constant with height, a value of the mean height of the space charge region was estimated from the above relation as 44m.

### 8.3.2 The correlation of space charge and potential gradient

Most previous workers on precipitation electricity have assumed that the potential gradients observed at the ground under precipitating nimbo-stratus clouds are due to charges in the clouds. Measurements of space charge in rain, the few there have been, have usually shown low values, unless conditions are suitable for point discharge or splashing. However, as described in Chapter 1, some past workers have hinted at the results presented in Chapter 7, in particular COLLIN, RAISBECK and CHALMERS (1963). In accounting for the source of the space charge it is necessary to explain the fact that the space charge density values at all heights within the first few tens of metres vary in phase. If this space charge is associated directly with the precipitation, by some method of charge transfer, it is likely to



accompany the cloud as both will move with the wind. The rain-drops, on the other hand, will fall to the ground and be left behind the advancing cloud and space charge. In such circumstances the space charge would reach the recording site before the rain, so that this could account for the decrease in space charge and potential gradient before the onset of rain.

Previous measurements in steady rain have often involved deriving an empirical relation between the precipitation current and potential gradient. The inverse relation between these two quantities is accounted for if the charging of the raindrops results in an opposite charge being given to the cloud or the air below. This space charge, of opposite sign to the charge on the rain, will produce the observed potential gradient at the ground. If there is no wind and the cloud system is stationary, there should be a high negative correlation between precipitation current and potential gradient, but if the winds are high, the distribution in drop size will cause rain from different charging regions to be collected. The result may be to decrease the apparent correlation between the two, which may explain the lower correlation coefficients usually found than for space charge and potential gradient in the present work.

The positive space charge due to the charge on the rain must also be considered, since if it is of sufficient magnitude, the potential gradient at the ground may be seriously modified. If  $J$

is the precipitation current density and  $v$  the velocity of fall, the space charge on the rain is  $J/v$ . The rate of change of potential gradient with height is then:

$$\frac{dF}{dh} = - \frac{J}{\epsilon_0 v}$$

For  $J = 10 \text{ pA m}^{-2}$  and  $v = 4 \text{ ms}^{-1}$ , this becomes:

$$\frac{dF}{dh} = 0.28 \text{ Vm}^{-1} \text{ per metre.}$$

For a height of 50m, the resultant potential gradient difference between ground level and this height is  $14 \text{ Vm}^{-1}$ . This is small compared with the values of potential gradient observed, but may affect the value of the constant term in the derived relation between potential gradient and space charge density. This value is an over-estimate if the rain acquires its charge within 50 m of the ground. If, however, the rain acquires the charge in the cloud, the effect of its space charge is greater. For a cloud base height of 500m, the above value becomes  $140 \text{ V m}^{-1}$ , which is about the same order of magnitude as the observed values of potential gradient.

#### 8.4 The Electrification of Precipitation

##### 8.4.1 Distribution of charge

Nimbo-stratus clouds can be assumed of sufficient horizontal extent for the conduction currents through them to be everywhere vertical, except close to the edges of the cloud. For a non-precipitating cloud, the reduced conductivity inside it will give rise to space charges at its boundaries, positive at the top

and negative at its base. A precipitating cloud will contain a net negative charge if the charge separation process occurs within the cloud, since the positive charge will be removed by the rain. CHALMERS (1959) discusses the electrical properties of both snow and rain clouds. He considers that in both types the precipitation commences in the solid state and, in the case of rain, melts at some later stage. Measurements by him (CHALMERS, 1956) show that for snow clouds the average total current is negative while for rain it is positive. Average values of potential gradient were found to be negative in both cases. Taking his measured average values of total current density and potential gradient for each case, CHALMERS (1959) estimated the variations of potential with height for different conditions of space charge concentration resulting from charge separation at different heights. He concluded that, for both the snow cloud and rain cloud, the charging mechanism is much more likely to take place within the cloud. The rain will, therefore, commence as snow with a negative charge and in the process of melting will acquire a positive charge.

If, in the present investigation, the rain acquired its charge solely in the cloud, the question arises as to how the negative space charge near the ground occurs. It is inconceivable for space charge at the ground and in the cloud, several hundred metres higher, to vary in phase unless due to the same cause. In this case the space charge must reach up from the ground to

the cloud. If the cloud base is, say, 500m above the ground the space charge density would decrease with height to be compatible with the present results. For an exponential decrease with height, the space charge density at the cloud would then be about  $5 \times 10^{-6}$  of the value at the ground.

The estimated relation between potential gradient and space charge gives an average value, for the potential gradient at the top of the space charge region, of  $28 \text{ Vm}^{-1}$ . Assuming a value of  $-200 \text{ Vm}^{-1}$  at the ground and 50m for the height of the space charge region, it is possible to estimate the variation of potential with height, if it can be assumed that the density of space charge remains constant within the region. At 50m, the top of the space charge region, the potential is  $-4,500 \text{ V}$ . If the cloud base is at 500m, and assuming no appreciable space charge between 50m and 500m, the base of the cloud is at about  $7,000 \text{ V}$ . CHALMERS (1959) showed that if the cloud extends to a height of 10m, the potential at its top is about  $3.6 \times 10^5 \text{ V}$ , if the potential of the electrosphere is  $4 \times 10^5 \text{ V}$ . This requires an average potential gradient inside the cloud of about  $3 \times 10^3 \text{ Vm}^{-1}$ . If in the cloud there are no charges due to charge separation, as assumed here, the current through the cloud will be the conduction current alone. Assuming this to be close to the fair-weather value, of about  $3 \text{ pA m}^{-2}$ , the conductivity in the cloud must, on average, be about  $10^{-15} \Omega^{-1} \text{ m}^{-1}$ . Measurements at Lanehead of the positive

conductivity at the ground indicate values of between about  $0.5 \times 10^{15} \Omega^{-1} \text{ m}^{-1}$  and  $2 \times 10^{15} \Omega^{-1} \text{ m}^{-1}$  during the heavier parts of the rain. If the values of both conductivities are similar to these values within the cloud, it is possible for the above conditions to be satisfied.

Some further points must be added to this simplified picture. A limited number of measurements of negative conductivity indicate an increase at the onset of rain. These results are by no means conclusive, but indicate that the positive conductivity may be decreased by recombination with the excess of negative ions as well as by attachment to large ions and nuclei. ADKINS (1959b) found, from laboratory experiments as well as measurements during rain, that the result of splashing is to give minute water droplets to the air. He found that these droplets had mobilities similar to those of small ions. Although splashing is probably not the origin of the space charge, it is still possible that it may comprise these minute charged droplets. The mobility of these 'ions', if similar to small ions, will be about  $10^{-4} \text{ m s}^{-1}$  per  $\text{V m}^{-1}$ . For a potential gradient of  $-500 \text{ V m}^{-1}$ , their velocity will be  $5 \times 10^{-2} \text{ m s}^{-1}$  downwards. Those starting at a height of 50m would take  $10^3 \text{ s}$  to reach the ground. CHALMERS (1967a) gives the average lifetime of a small ion as about 50s. In rain, when attachment is more likely, this time will be less, so that the 'ions' will not remain as such for long, compared with the time taken to traverse 50m.

In the cloud, it is still not certain whether or not a value of  $10^{-15} \Omega^{-1} \text{ m}^{-1}$  for the conductivity is likely. For a non-raining cloud, values will almost certainly be greater than this. The above explanation is undoubtedly an over-simplification, but no further comment can be made without more detailed information of conditions inside the cloud itself.

#### 8.4.2 Origin of charge separation

It is convenient here to assume that a charge separation occurs below the cloud, giving positive charge to the rain and negative to the air. The ion-capture mechanism, first considered by WILSON (1929), requires high potential gradients to be present before the charge separation can occur. The extension of this theory by SIMPSON (1949) involves the capture of point-discharge ions giving a precipitation current of the same sign as that of the space charge from point discharge. Also, simultaneous measurements of natural point discharge at Lanehead by Mr. I.M. Stromberg have shown that potential gradients of around  $5,000 \text{ Vm}^{-1}$  are necessary before point discharge occurs from the tallest conifers (20 to 25 m). A metal point, 4m high, began to discharge at about  $1,600 \text{ Vm}^{-1}$ , which is still appreciably higher than the potential gradients observed. Splashing at the ground, as shown by ADKINS (1959b), results in a space charge of sign opposite to that of the potential gradient.

GUNN (1955) considered the role of ionic diffusion in

charging droplets of rain. Considering mist and light rain he derived an expression for the charge gained by a drop falling through an ionized medium. The sign of the charge was found to depend on the ratio of the polar conductivities, an excess positive conductivity giving a positive charge. This process is not dependent on the existence of a potential gradient but could not result in a negative excess of small ions since the mechanism would cease when the two conductivities became equal.

The effects of melting is a further possible mechanism. DINGER and GUNN (1946) found that snow, on melting, acquires a positive charge while the previously entrapped air escapes with a negative charge. OWOLABI and CHALMERS (1965), during one period of precipitation of both snow and sleet, found that the precipitation current lagged behind the potential gradient by 40s. This implied that a process of charge separation was occurring at a height from which the precipitation took 40s to fall. At the time, the freezing level was probably at about 250 m, and if the charge separation was that of melting it would have occurred from this level downwards. They found these values to be consistent with the charging being connected with melting. Such a process, however, implies a difference between the results for Winter and Summer which was not noticed.

### 8.4.3 Further discussion

From the preceding discussion there appears a contradiction between the present results and past theories of the electric structure of nimbo-stratus clouds. The likelihood of some charge separation process being confined within the first 50 m or so from the ground seems at first remote, so it is necessary to look for any peculiarities in the site or the methods of measurement. Firstly, the site is not completely open so that there may be electrical effects associated with the nearby trees and building, although splashing and point discharge have both been ruled out. The altitude (440m) of the site means that for some of the time the cloud bases are not far above the ground. However, if this had affected the results, the conditions in Summer and Winter would have differed.

The nature of the surrounding ground may have been such as to produce the negative space charge near the ground upwind of the station, so that by the time it had reached the station the space charge would have diffused upwards sufficiently. Although there was insufficient data for any reliable conclusions to be drawn, the measurements of negative conductivity imply that the space charge is being produced at or close to the site, so that if it was produced very close to the ground it would not have time to be carried upwards.

A further remark concerns the methods of measurement. The



high correlation excludes any possibility of instrumental errors, such as insulation breakdown in the space charge collector. The field mill, being inverted, may respond more to space charges near the ground than to the same concentration of space charge about it. The remarks in Chapter 3 indicate that the effect of this will not be serious. At any rate, the instrumental errors cannot be very great, so that it is certain that the space charge must reach up several tens of metres. Finally, it may be mentioned that the presence of such a region of space charge was implied by KELVIN (1860) and CHAUVEAU(1900), as mentioned in Chapter 1, and recently by COLLIN, RAISBECK and CHALMERS (1963).

## CHAPTER 9

### CONCLUSION AND SUGGESTIONS FOR FURTHER WORK

#### 9.1 General Conclusions

##### 9.1.1 The fair-weather electric climate

The diurnal variations previously presented are the results of a statistical analysis, to cancel out the disturbances which have caused the comparatively large departures on individual days from the mean for the full year. However, in order to understand the processes which produce these disturbances, it would be necessary to adopt synoptical methods, as proposed by ISRAËL (1955). Such methods would require simultaneous meteorological measurements on a scale not possible in the present investigation. Statistical methods have proved successful, and the fair-weather diurnal variations for the full year have made it possible to establish an electric climate for Lanehead. The measurements of wind and rainfall were found to be less useful than initially anticipated, although if a synoptical approach had been used they would have been necessary.

##### 9.1.2 The Lanehead Investigation

The results of this investigation have been divided into 2 separate sets, fair-weather and disturbed. The data for both sets, however, were obtained from different parts of the same

records. The apparatus at Lanehead has continuously monitored the atmospheric elements within the range of conditions considered. This first part of the initial aim, to make continuous measurements, has been realized. Secondly, an atmospheric electric recording station has been established. With the necessary facilities and with the more important instruments permanently installed, the station offers scope for further work for some time to come. Many problems have already been overcome, as described in Chapter 4, but various improvements and additions are necessary before the station is fully equipped and operating reliably and efficiently without requiring the full time attention of any one person. Several suggestions for improvements and additional work are outlined below.

## 9.2 Improvements

### 9.2.1 The apparatus

Much of the apparatus could be improved by the replacement of worn parts. For example the field mill rubber mounts, which perish easily, need replacing by a more durable type. The fan unit has already been mentioned in Chapter 4, but the provision of a more robust fan would help to cut down maintenance. In addition, a new filter unit for the space charge collector would prolong the life of the fan by requiring less pressure. Some device for preventing insulation breakdown, due to spiders and snow, would

help to prevent loss of air-earth current records. A wider gap between collector and guard ring may provide part of the solution.

Measurements of both polar conductivities could be made on the one instrument by reversing the polarity at intervals. Normally the instrument takes about 10 min to settle down after the bias voltage has been reversed, but if only hourly means are required a change-over every half-hour would suffice. For shorter periods the time constant would have to be reduced and the V.R.E. input resistor shorted during the change-over.

For a complete coverage of the atmospheric electric elements it would be necessary to have a second, or even a third, set of apparatus. Duplicate equipment would also help to solve the problem of instrumental break-down, especially if both sets of apparatus are working permanently. This is particularly true for V.R.E's, which take up to 24 hours to settle down after being switched on.

#### 9.2.2 The recording system

The pen recorders used in this investigation made it difficult to synchronize records on different charts. A multi-channel potentiometric recorder, although not giving a continuous record, would allow all parameters to be recorded on one chart. An improvement over the potentiometric recorder would be a **digital** system which recorded on punched paper tape, for direct analysis by computer. Such a system could be arranged to record the hourly

means during fair weather, while for disturbed weather a faster recording speed could be used. At present, such a system is being incorporated by Mr. W.P. Aspinall and, at the time of writing, will soon be in operation.

### 9.3 Suggestions for Further Work

#### 9.3.1 Space charge and conductivity

The present investigation has presented several problems still to be solved. Fig. 6.25 implies a correlation between the diurnal variations of space charge and the difference between positive and negative conductivities. That is, the variation in space charge may be due to the variation in the relative concentrations of positive and negative small ions. If this is so the space charge must arise locally, possibly by the electrode effect, since small ions have a limited life. The evidence of Fig. 6.25 is by no means conclusive, but may be worth pursuing. A second Gerdien chamber could be used, as an Ebert ion counter, to measure the concentrations of small ions of either sign, and the results compared with those of the space charge collector.

Measurements of both signs of conductivity may be useful in determining the departure of the total air-earth current density from the product  $\lambda F$ . The convection current component could then be estimated. Measurements of the diurnal variation of conductivity could be compared with the estimated variation

of columnar resistance. This and further space charge measurements might provide a complete explanation for the diurnal variation of potential gradient. If possible, these measurements should be carried out for a year, so that, as with the present results, the seasonal variations can be cancelled out.

Alternatively, a synoptical approach could be used by measuring all parameters simultaneously under carefully specified weather conditions i.e. of cloud cover, wind, temperature etc. Such a method would require manual observations of the weather at the time of recording, but should yield results in a shorter period of time.

Further work in rain should help to explain the presence of the negative space charge. Possibly, measurements of the precipitation charges, on individual drops, together with space charge density and potential gradient are required. The height of the base of the cloud is also needed, and measurements of small ion densities would confirm the presence of small negative ions comprising the space charge.

### 9.3.2 A mountain top site

The top of the mountain (630 m) is 2km to the N of Lanehead. The site is comparatively flat and very exposed, so ideal for making atmospheric electric measurements. Simultaneous observations there and at Lanehead might be useful for making measurements during precipitation, especially if the cloud base was

between the two sites. At present an instrumented Land-Rover is intended to be used in conjunction with measurements at Lanehead. However, a permanent site at this altitude, recording continuously and simultaneously with those at Lanehead, may be capable of providing useful information of a different type from the above mentioned measurements.

The practical problems of establishing such a station would be considerable with the difficulties of access, power supplies and maintenance. Using modern semiconductors it should be possible, however, to construct electrometer amplifiers to measure the low currents involved. Telemetry, radio or line, could be used to relay observations direct to Lanehead. The instrumental problems involved are probably too great to be solved at present, but an attempt could be made to set up a temporary station for use in the warmer months.

FIG. 3.7 Field Mill Amplifier (Final design)

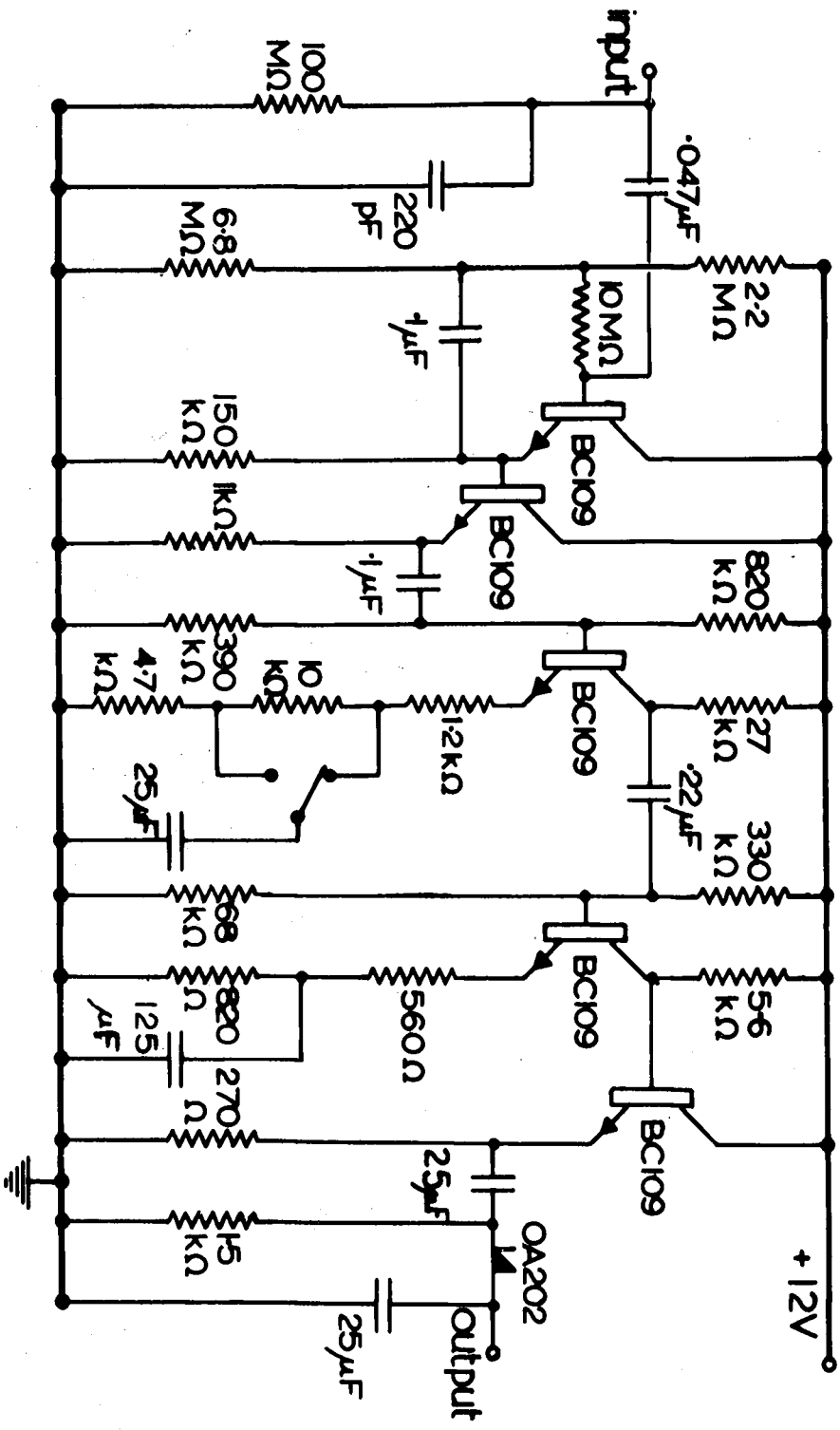




**FIG.620** Diurnal variations of Air-earth current & Space charge  
July 1967 to June 1968

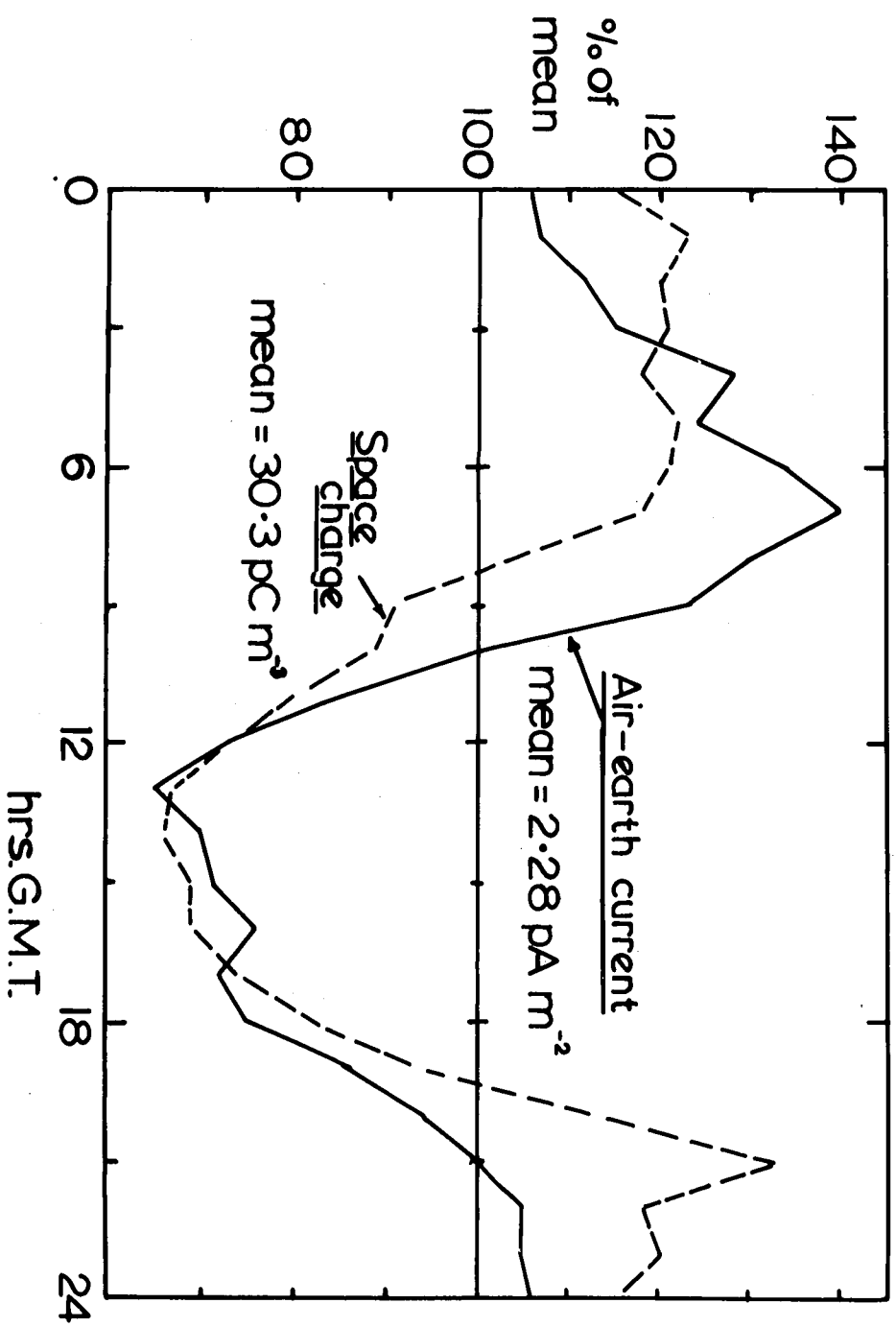


FIG.7.4. Scatter diagram record 9.1a

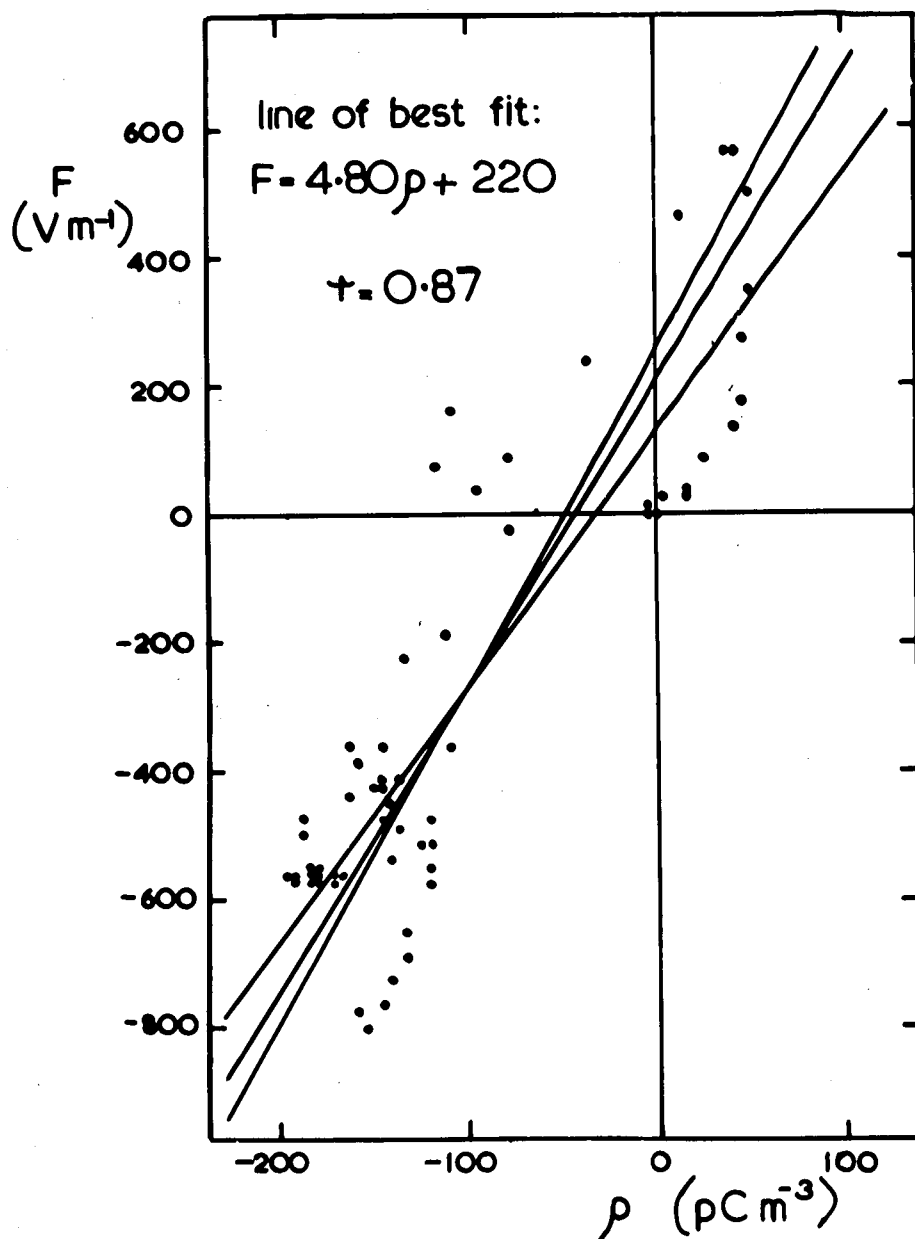


FIG.7.5. Scatter diagram — record 19.1

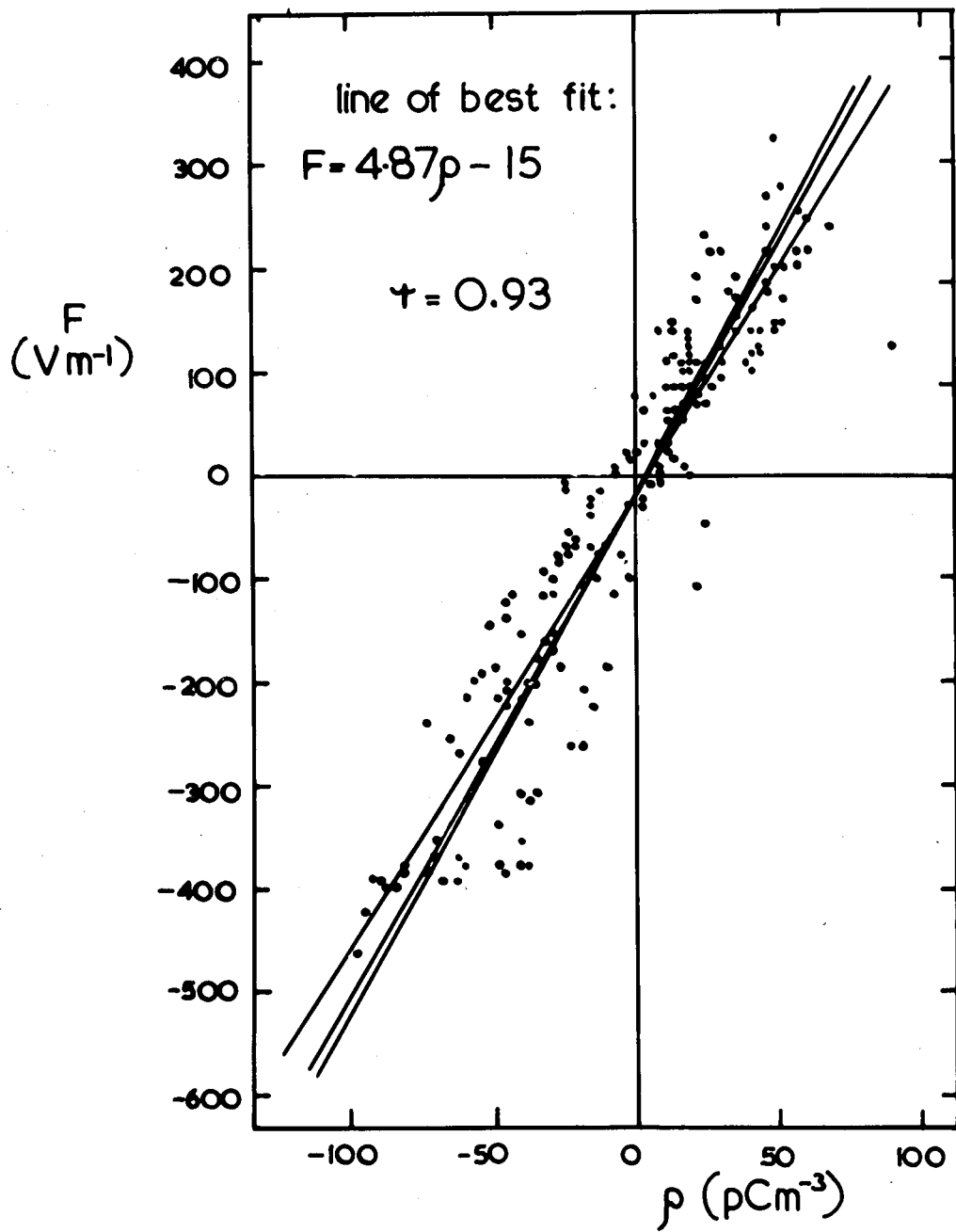


FIG.6.16. Diurnal variations — JUNE 1968

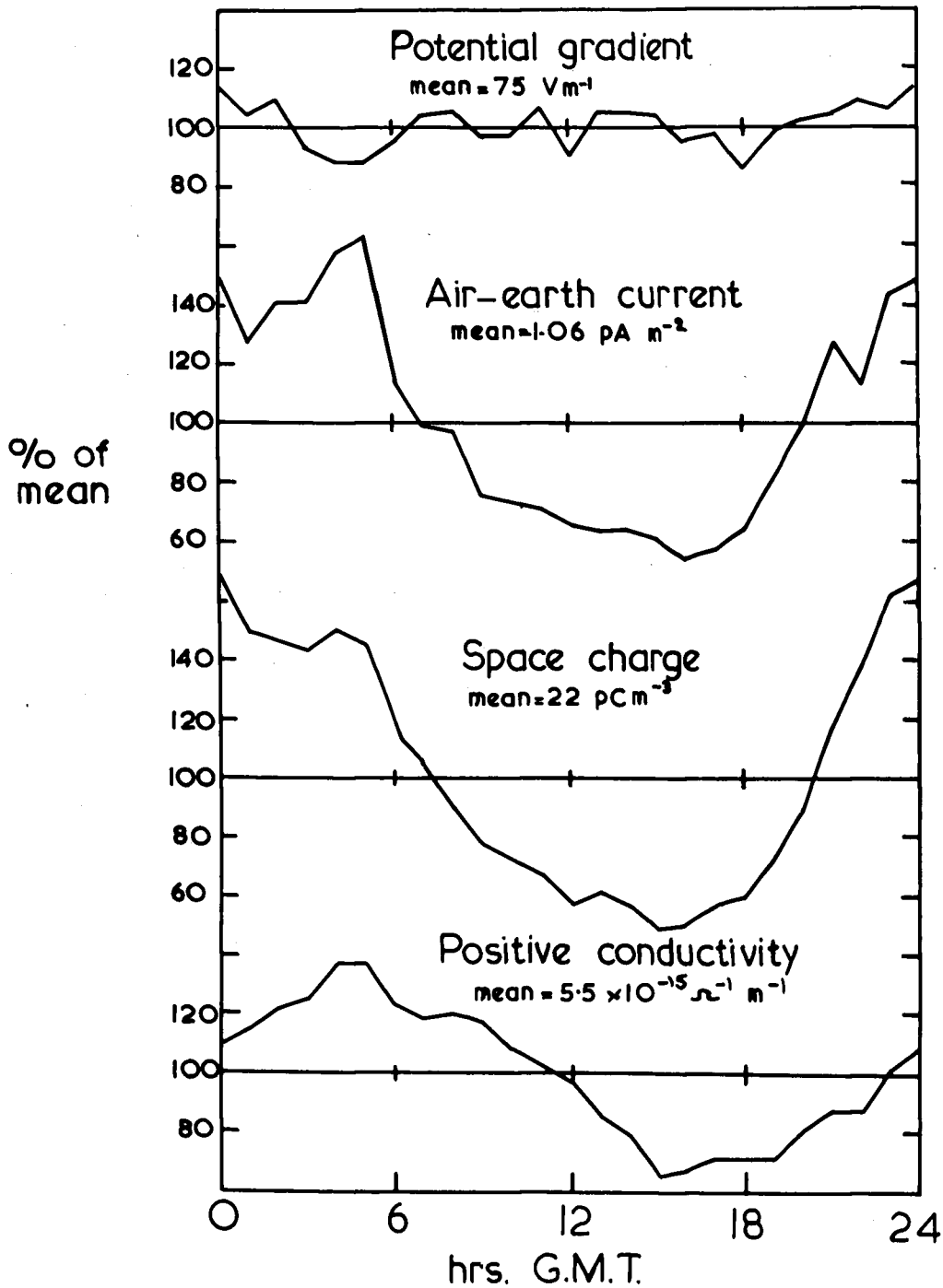


FIG.6.15. Diurnal variations - MAY 1968.

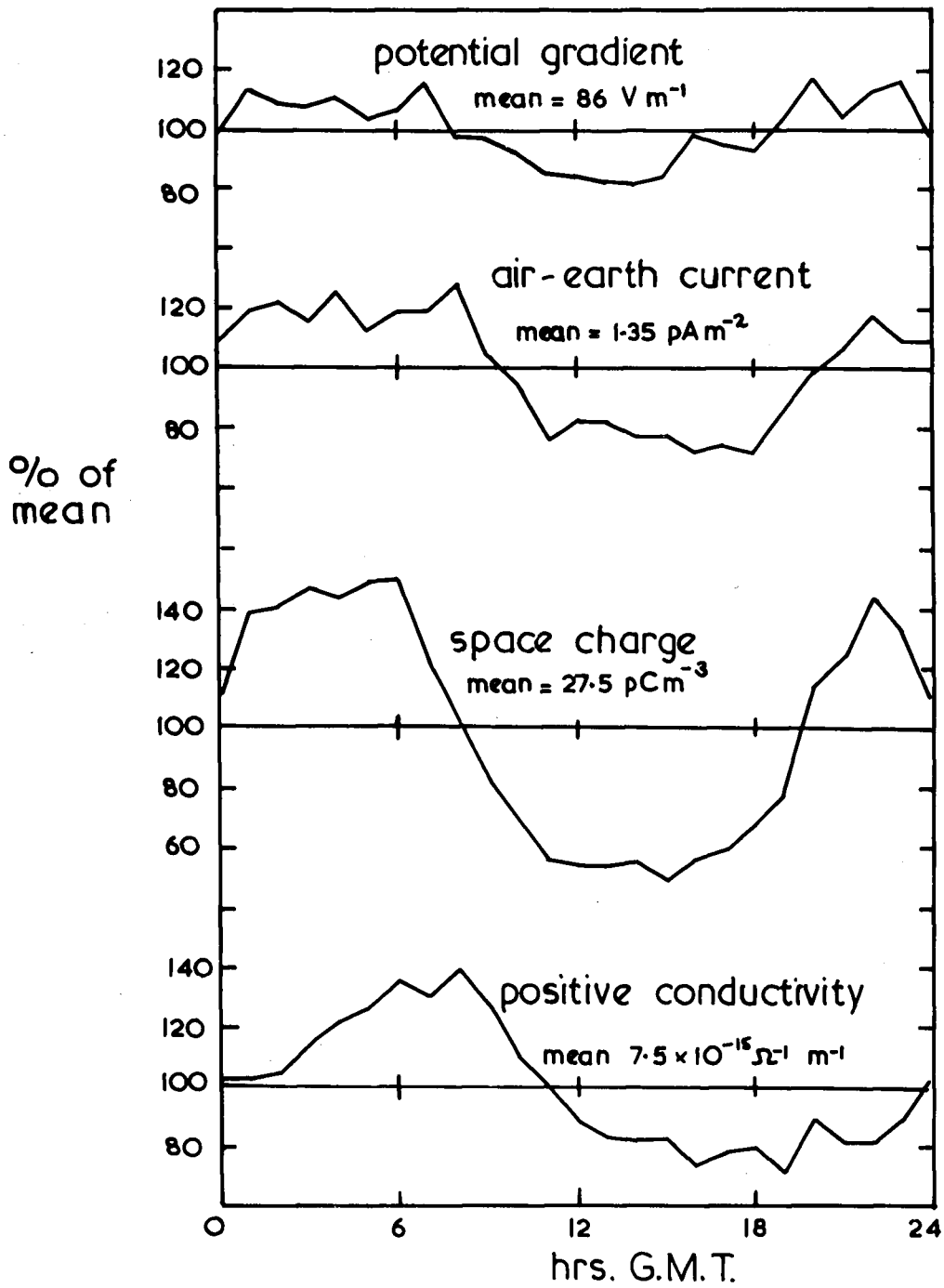


FIG.6.14. Diurnal variations — April 1968

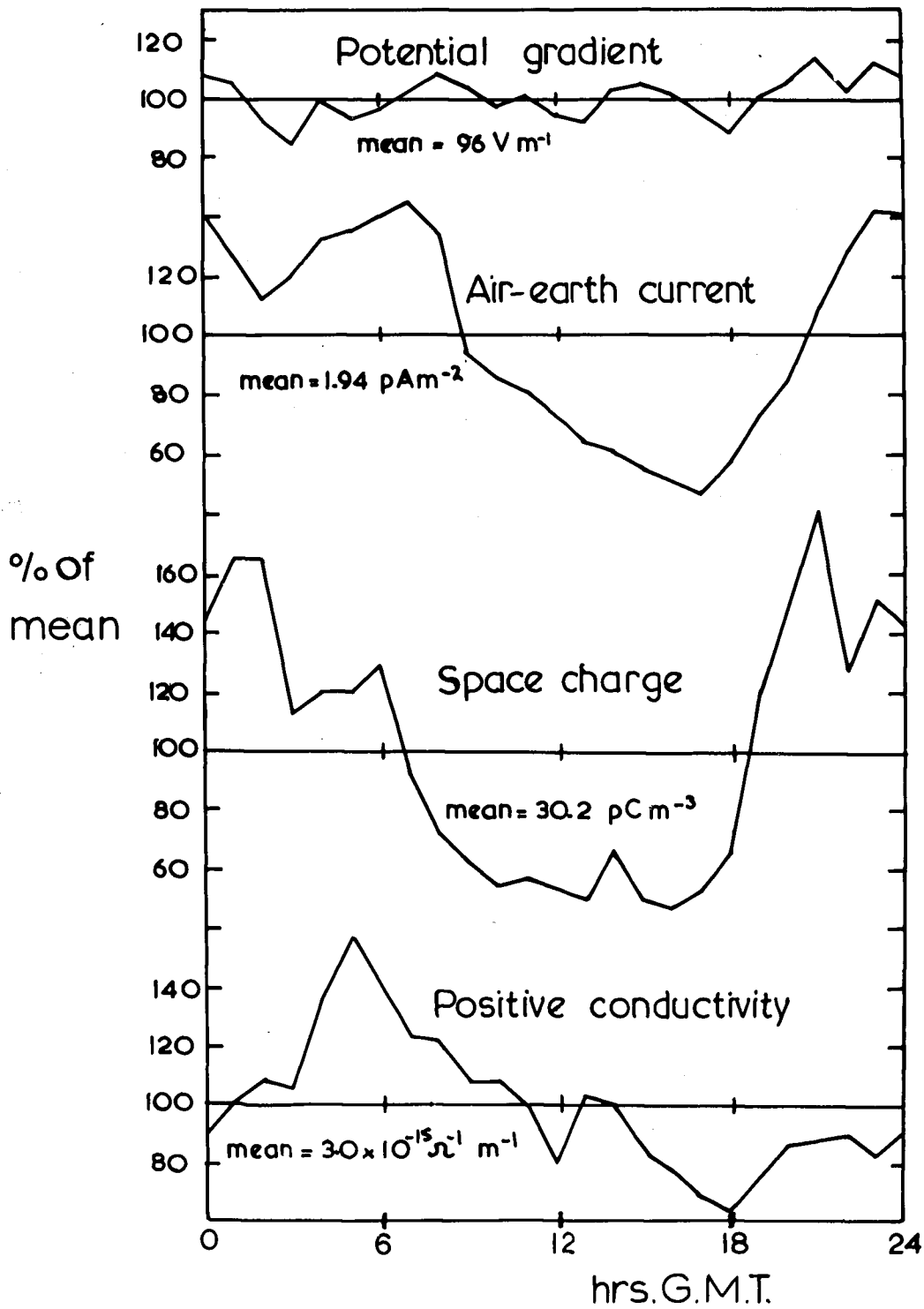


FIG.6.13. Diurnal variations— March 1968

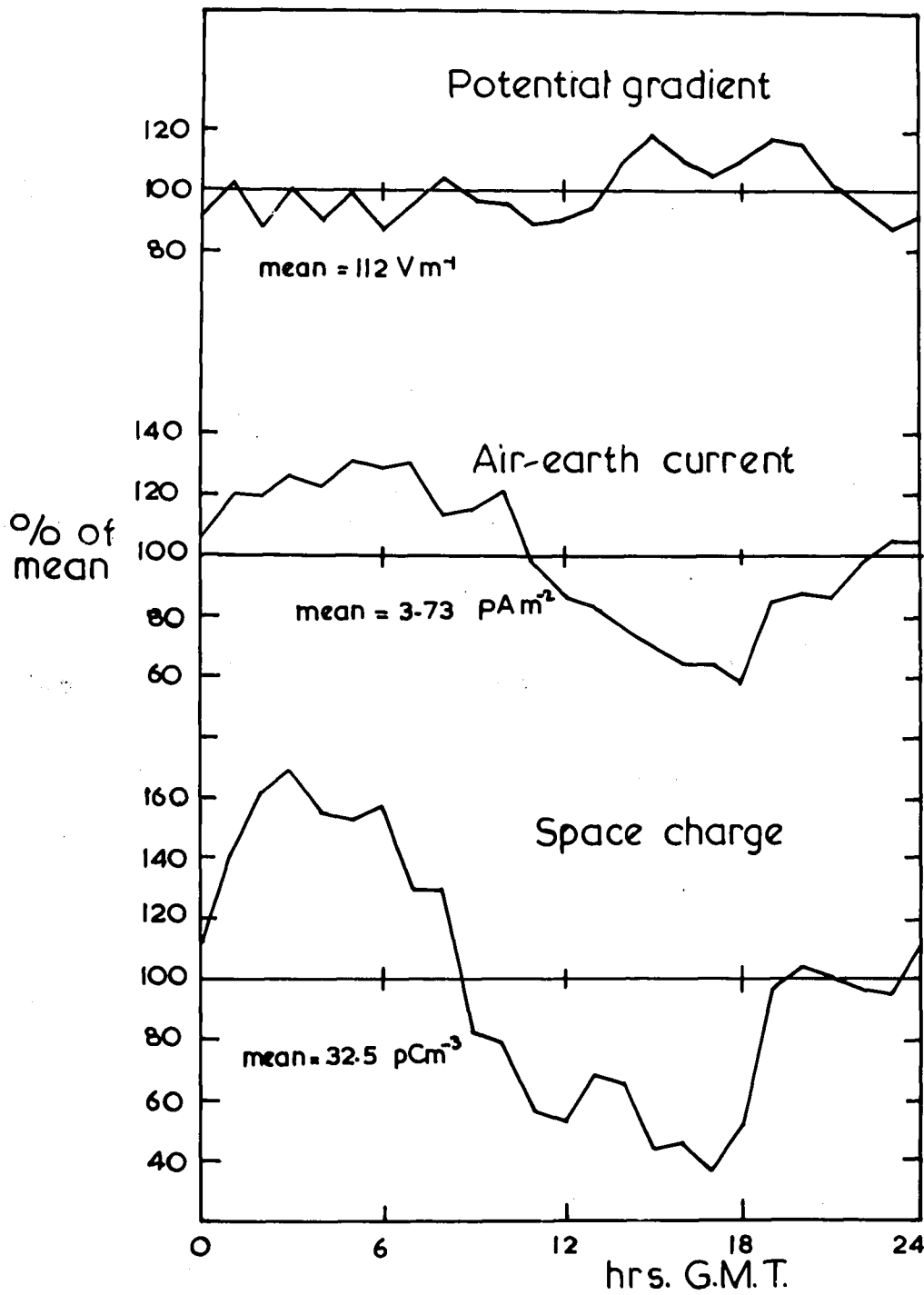


FIG.6.12. Diurnal variations

February 1968

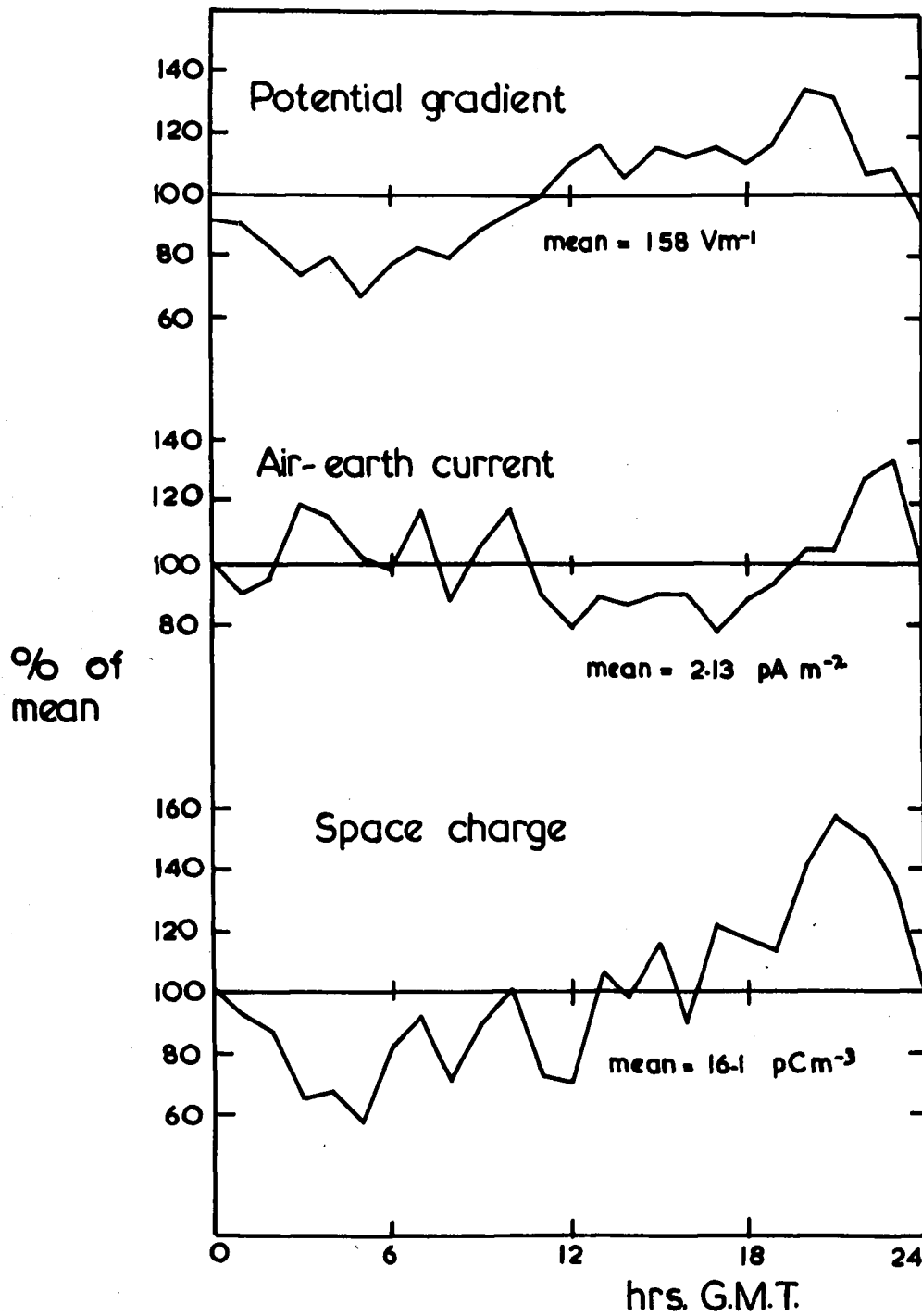




FIG6.II. Diurnal variations-JANUARY, 1968.

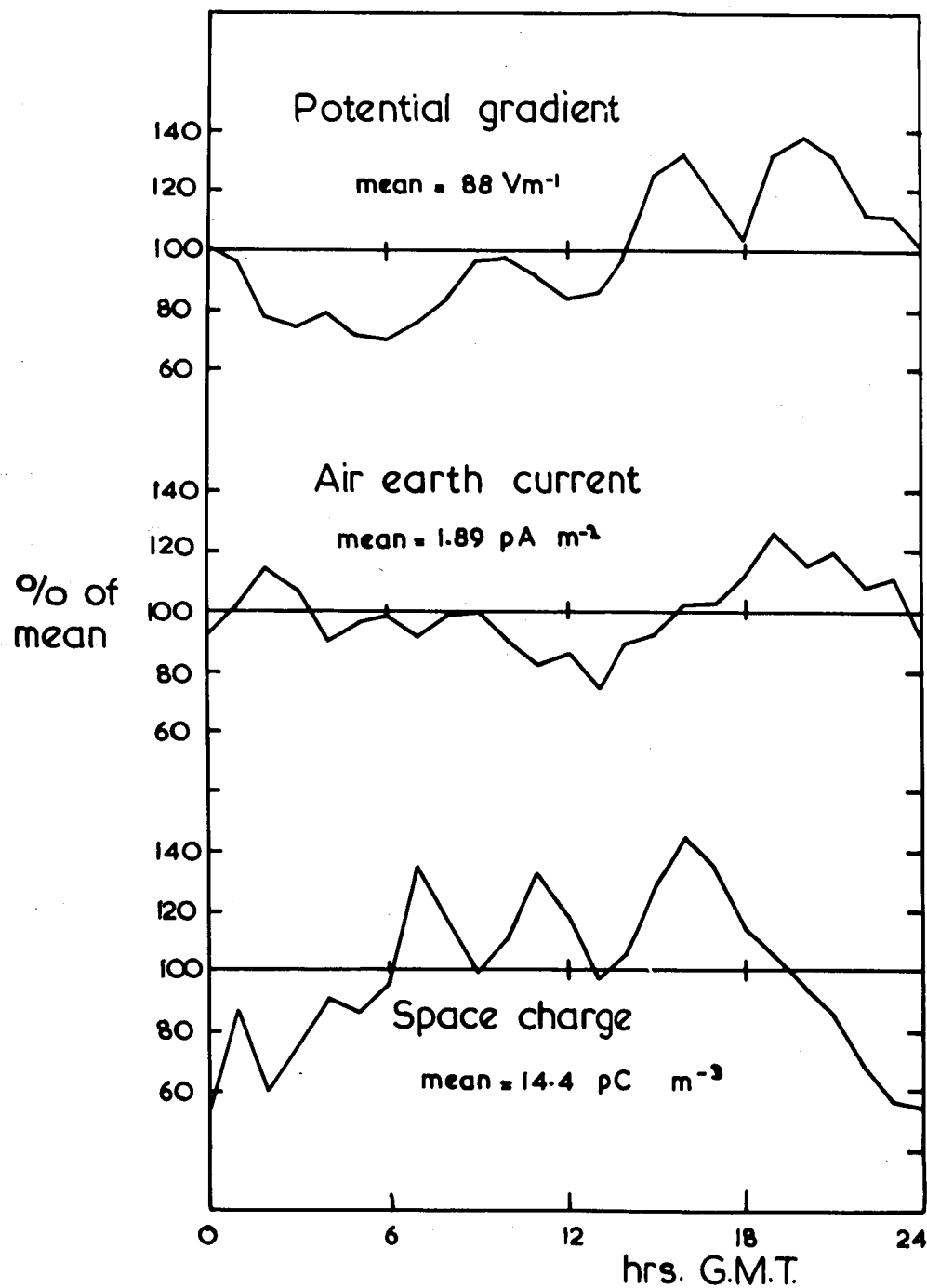


FIG.6.10 Diurnal variations — December 1967

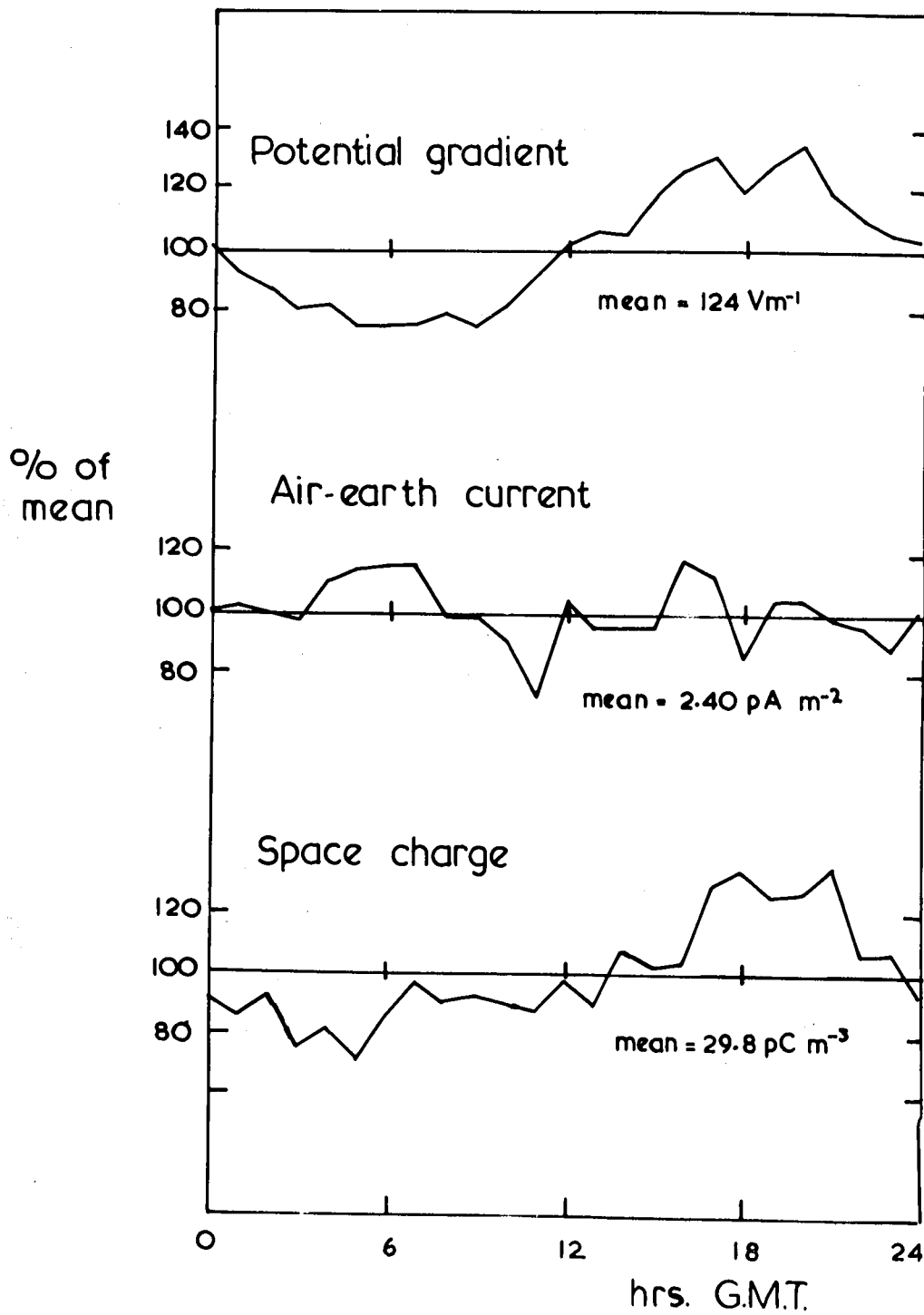


FIG.6.9. Diurnal variations — November 1967

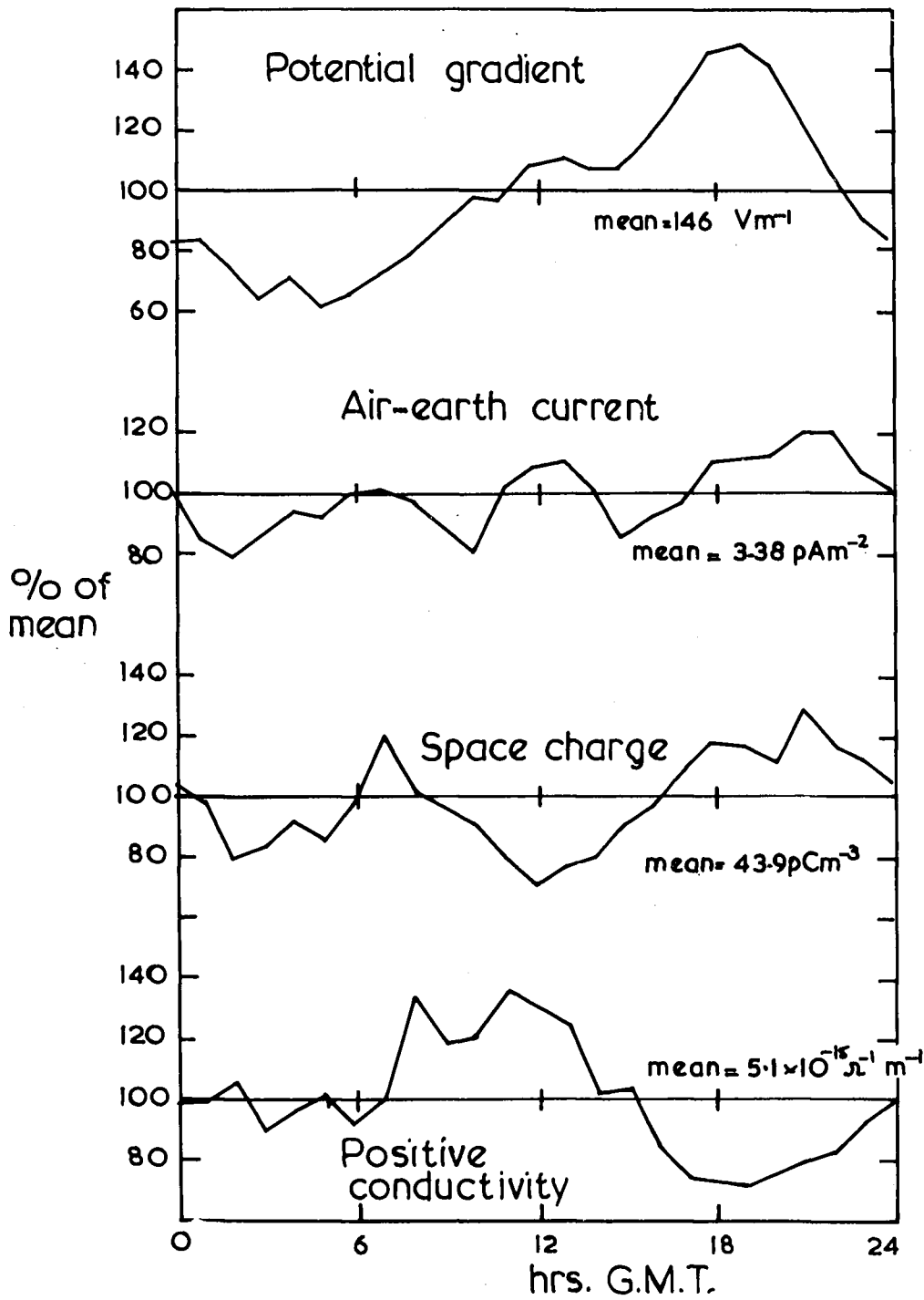


FIG6.8. Diurnal variations — October 1967

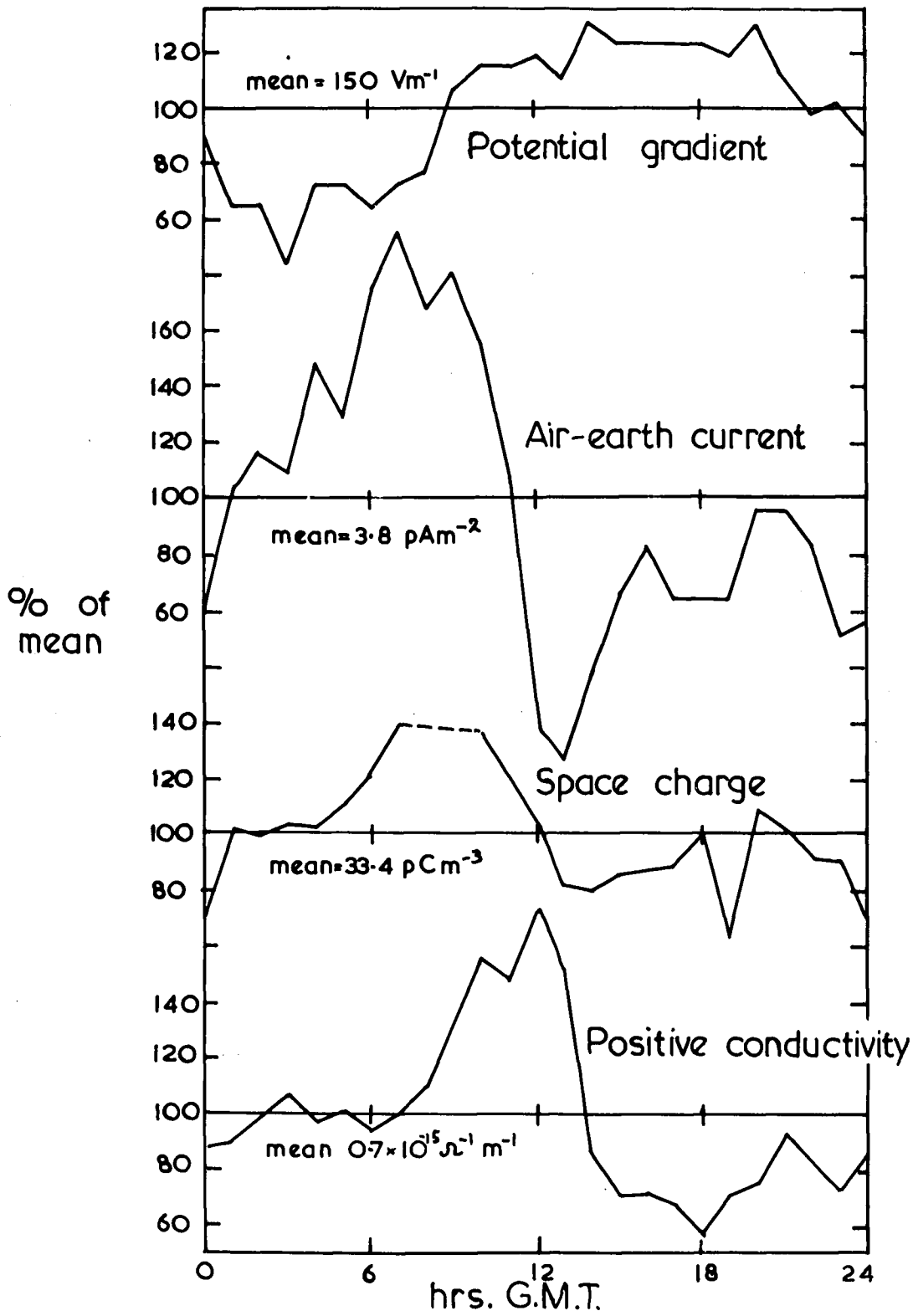


FIG. 6.7. Diurnal variations — September 1967

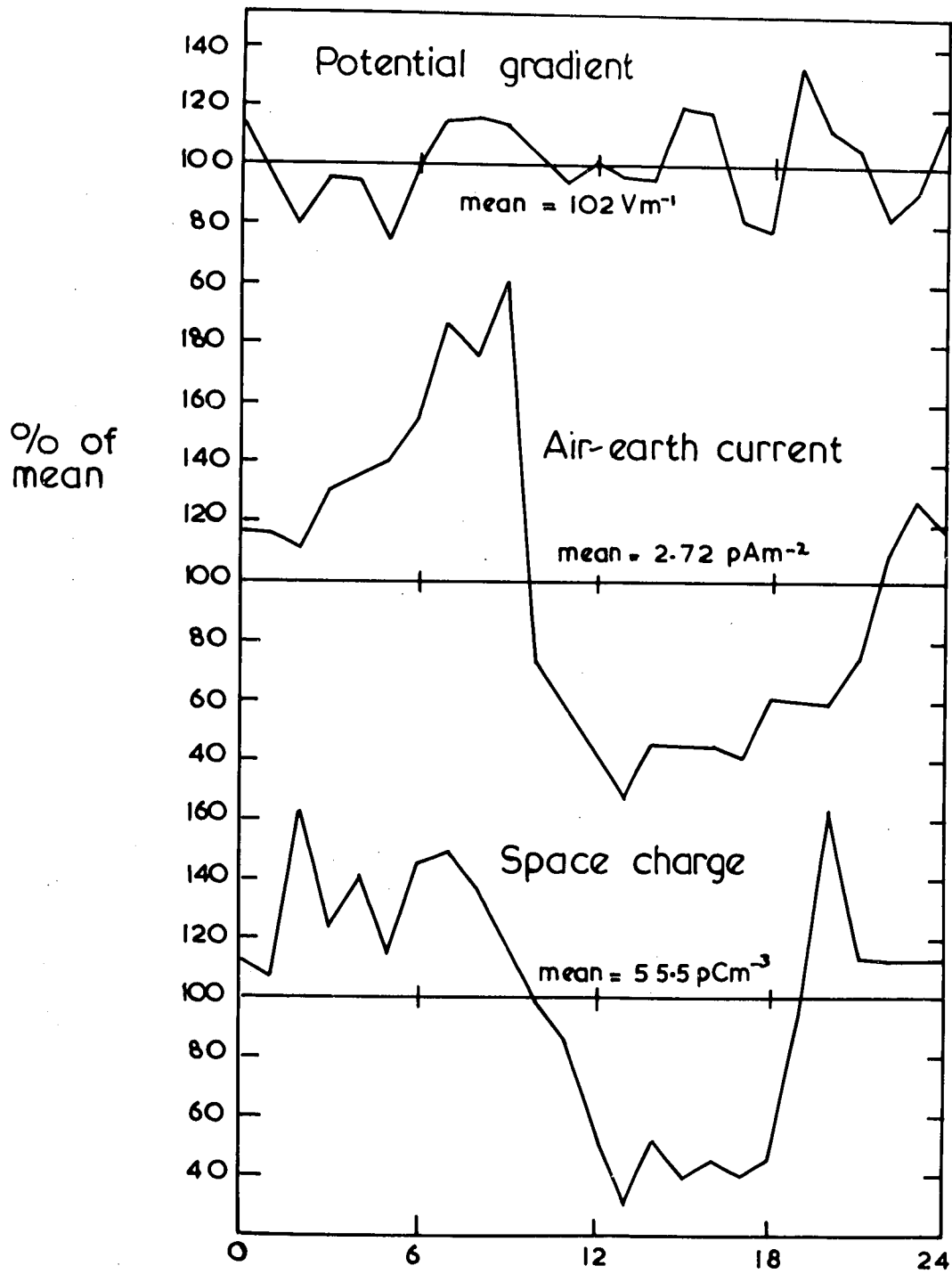


FIG.6.6. Diurnal variations – August 1967

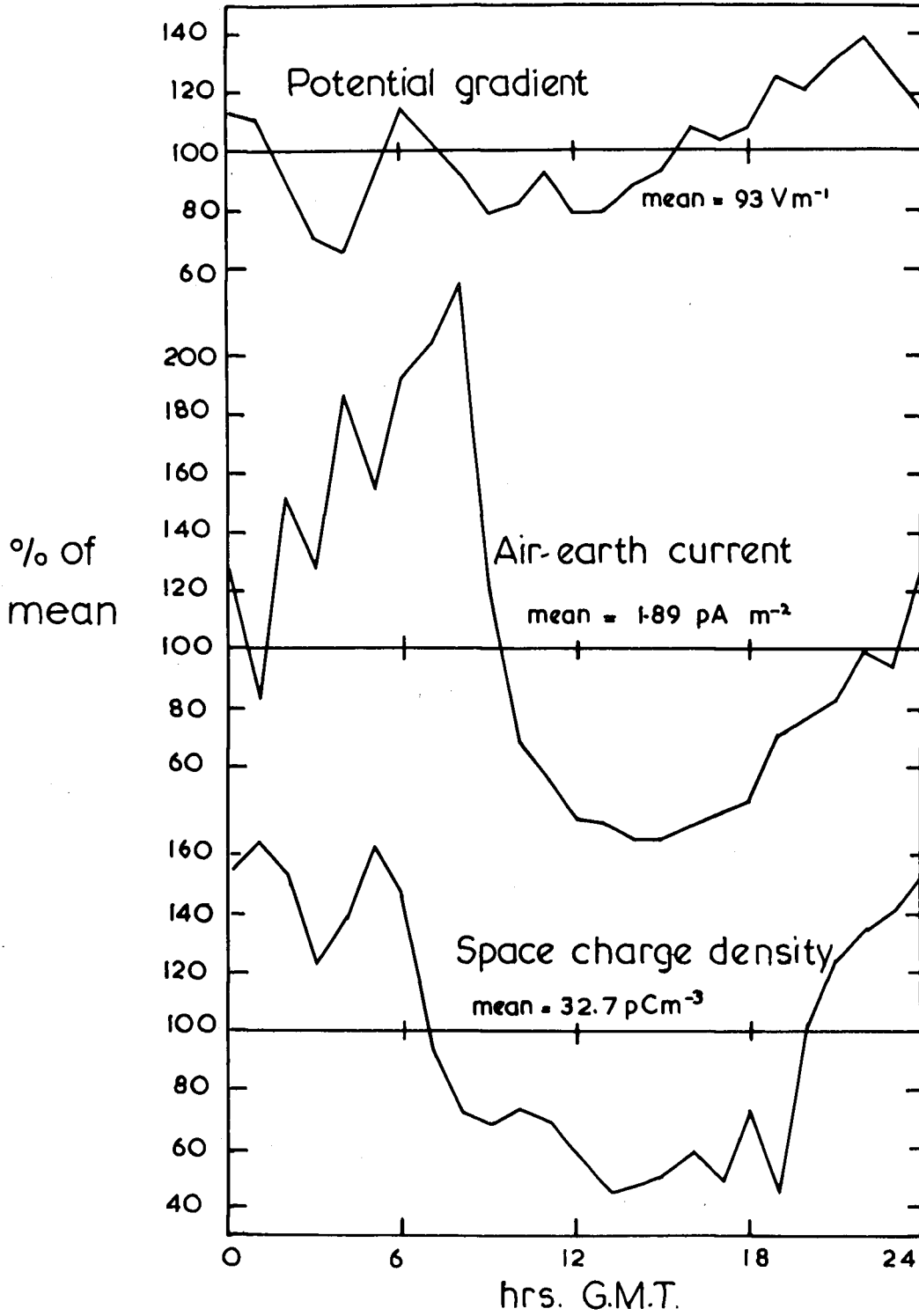
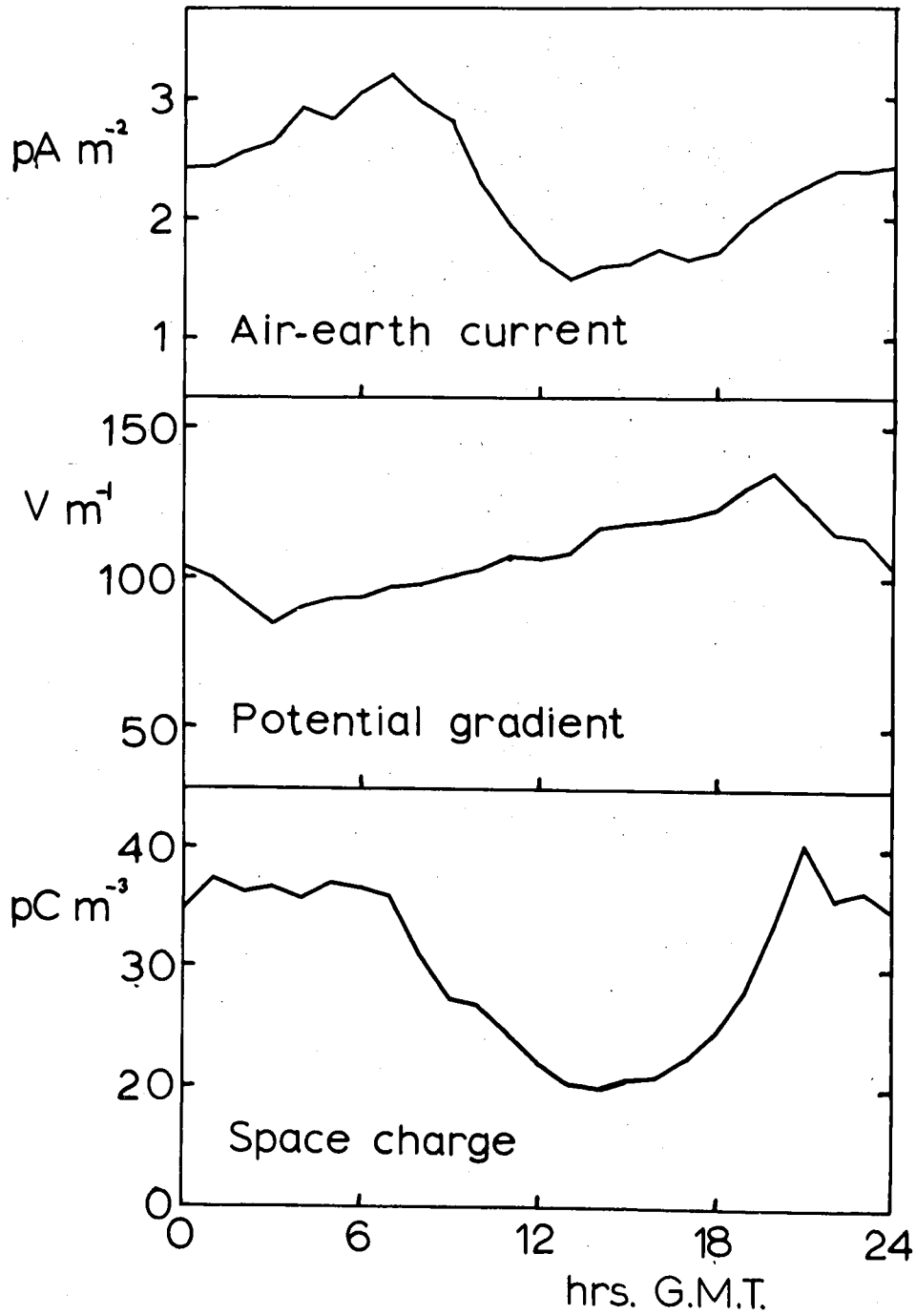
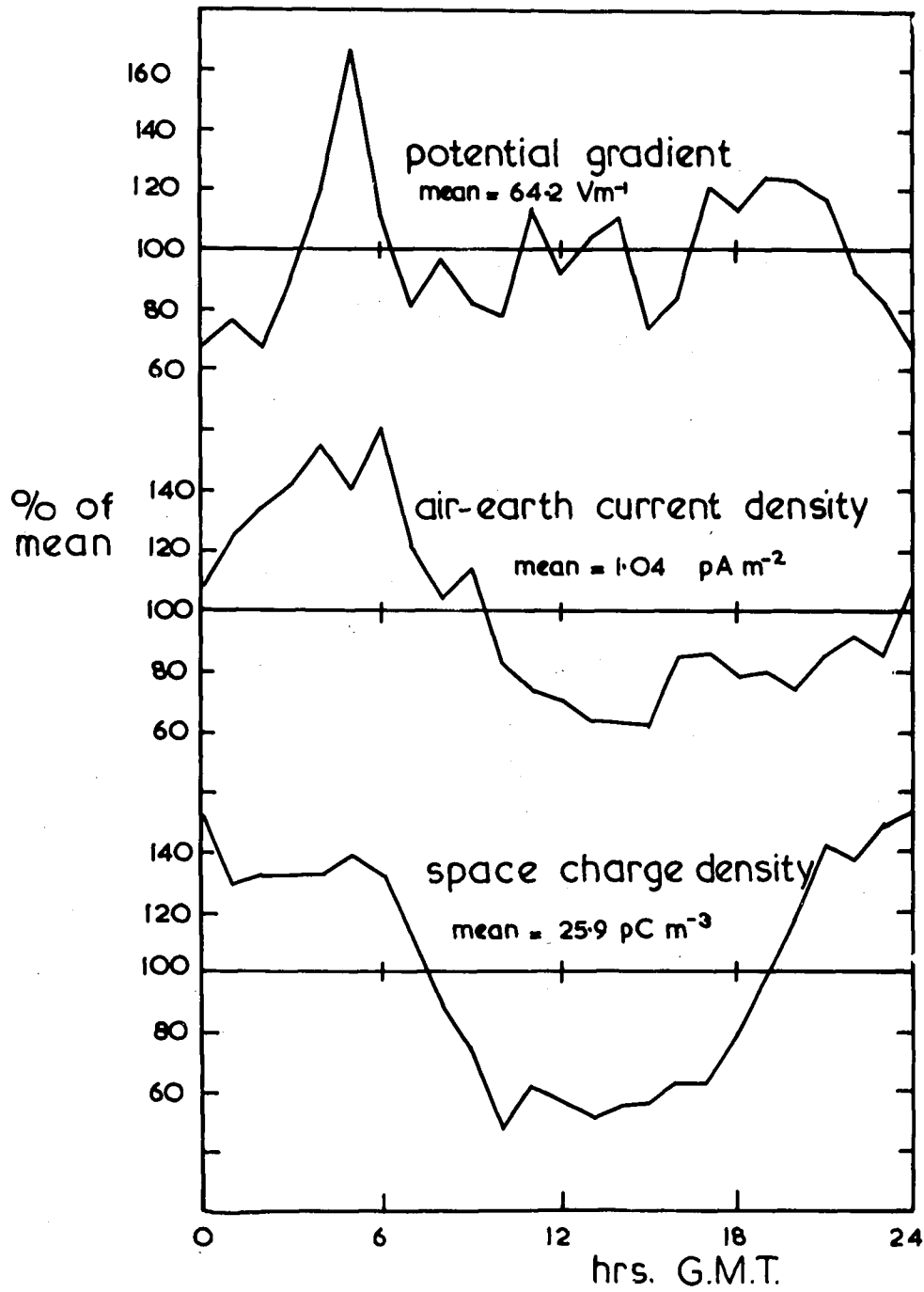


FIG.6.1 Diurnal variations, JUL.1967-JUN.1968



23

FIG. 6.5. Diurnal variations - JULY, 1967





REFERENCES

- ADKINS, C.J. (1959a) Measurements of the atmospheric potential gradient on a Canadian glacier.  
Quart. J.R.Met.Soc. 85, 60-4
- ADKINS, C.J. (1959b) The small ion concentration and space charge near the ground.  
Quart.J.R.Met.Soc. 85, 237-52
- APPLETON, E.V. (1925) Discussion on ionization in the atmosphere.  
Proc.Phys. Soc., Lond. 37, 48D-50D
- BENT, R.B. (1964) The testing of apparatus for ground fair-weather space charge measurements.  
J.Atmosph.Terr.Phys. 26, 313-8
- BENT, R.B. and HUTCHINSON, W.C.A. (1966) Electric space charge measurements and the electrode effect within the height of a 21m mast.  
J.Atmosph.Terr.Phys. 28, 53-73
- BROOKS and CARRUTHERS (1953) "Handbook of Statistical Methods in Meteorology".  
Met. Office, pub. H.M. Stationery Office
- BROWN, J.C. (1930) The relation of space charge and potential gradient to the diurnal system of convection in the lower atmosphere.  
Terr. Magn. Atmos. Elect. 35, 1-15.
- CHALMERS, J.A. (1952) Negative electric fields in mist and fog.  
J. Atmosph.Terr. Phys. 2, 155-9

- CHALMERS, J.A. (1956) The vertical electric current during continuous rain and snow.  
J. Atmosph. Terr. Phys. 2, 311-21
- CHALMERS, J.A. (1959) The electricity of nimbo-stratus clouds  
Recent Advances in Atmospheric Electricity - Pergamon Press
- CHALMERS, J.A. (1966) The theory of the electrode effect  
Parts I-IV.  
J. Atmosph. Terr. Phys. 28, 565-72, 695-97, 1029-33.  
29, 217-9.
- CHALMERS, J.A. (1967a) 'Atmospheric Electricity'  
2nd edition, Pergamon Press
- CHALMERS, J.A. (1967b) Positive charges from the Earth and the maintenance of the Earth's fine-weather potential gradient  
J. Atmosph. Terr. Phys. 29, 307-10
- CHAUVEAU, B. (1900) Études de la variation de l'électricité atmosphérique  
Annales de B.C.M. 5, 1
- COBB, W.E. (1968) The atmospheric electric climate at Mauna Loa Observatory, Hawaii  
J. Atmos. Sci. 25, 470-80
- COBB, W.E. and PHILLIPS, B.B. (1962) Atmospheric electric measurement results at Mauna Loa Observatory.  
Tech. Paper No. 46, Weather Bureau, U.S. Department of Commerce.
- COLLIN, H.L., RAISBECK, I.A. and CHALMERS, J.A. (1963) Measurements of atmospheric electricity at the top and foot of a 25m mast.  
J. Atmosph. Terr. Phys. 25, 631-6

- CROZIER, W.D. (1963) Electrode effect during night-time low-wind conditions.  
J. Geophys. Res. 68, 3451-8
- DINGER, J.E. and GUNN, R. (1946) Electrical effects associated with a change of state of water.  
Terr. Magn. Atmos. Elect. 51  
477-94
- DOLEZALEK, H. (1958) Problems in atmospheric electric synoptic investigations.  
Rec. Adv. 195-212.
- EVERLING, E. and WIGAND, A. (1921) Spannungsgefälle und vertikaler-Leitungsstrom in der freien Atmosphäre nach Messungen bei Hochfahrten im Freiballon.  
Ann. Phys. 66, 261-82
- GERDIEN, H. (1905) Demonstration eines Apparates zur Absoluten Messung der Elektrischen Leitfähigkeit der Luft.  
Phys. Z. 6 800-1
- GROOM, K.N. (1966) Ph.D. Thesis, Durham
- GUNN, R. (1955) The systematic electrification of mist and light rain in the lower atmosphere.  
J. Geophys. Res. 60, 23-7.
- HATAKEYAMA, H. and KAWANO, M. (1953) On the diurnal variation of atmospheric potential gradient in the Japan Archipelago.  
Pap. Met. Geophys. 4, 55.
- HIGAZI, K.A. and CHALMERS, J.A. (1966) Measurements of atmospheric electrical conductivity near the ground.  
J. Atmosph. Terr. Phys. 28,  
327-30
- HOGG, A.R. (1950) Air-earth current observations in various localities.  
Arch. Met. Wien. A, 3, 40-55.

- ISRAËL, H. (1955) Synoptical researches on atmospheric electricity  
Wentworth Conf. pp.11-19
- ISRAËL, H. (1957) Atmospheric electric and meteorological investigations in high mountain ranges.  
Contract AF 61(514) - 640  
Final Report
- ISRAËL, H. and De BRUIJN, P. (1967) The present status of atmospheric electric research.  
Arch. Met. Geoph. Bickl. A, Bd. 16, H.4, pp.281-99
- ISRAËL, H. and LAHMEYER, G. (1948) Das Auswahlprinzip der luft elektrisch "ungestörten Tage".  
Terr. Magn. Atmos. Elect. 53, 373-86
- KAHLER, K. (1927) Die elektrische Raumladung der Atmosphäre in Potsdam.  
Met. Z 44, 1-5
- KASEMIR, H.W. (1955) Measurement of the air-earth current density.  
Wentworth Conf., pp.91-5
- KAWANO, M. (1957) The general expression of the diurnal variation of the atmospheric electric field considering the influence of eddy diffusion near the ground.  
J. Geomag. Geoelect. 9, 123-132.
- KELVIN, LORD (1860) Atmospheric electricity.  
Roy. Instn. Lect., Pap. on Elec. and Mag., 316-20
- LAW, J. (1963) The ionisation of the atmosphere near the ground in fair weather.  
Quart. J.R. Met. Soc. 89, 107-21

- MAPLESON, W.W. and  
WHITLOCK, W.S. (1955) Apparatus for accurate and continuous measurements of the earth's electric field.  
J. Atmosph. Terr. Phys. 7,  
61-72.
- MAUCHLY, S.J. (1923) Diurnal variation of the potential gradient of atmospheric electricity.  
Terr. Magn. Atmos. Elect. 28  
61-81
- MORGAN, W.A. (1960) Determination of the straight line of best fit to observational data of two related variates when both sets of values are subject to error.  
Quart. J.R. Met. Soc. 86, 107-13
- NOLAN, J.J. and  
De SACHY, G.P. (1927) Atmospheric ionisation  
Proc. R. Irish Acad. A, 37,  
71-94.
- OBOLENSKY, W.N. (1925) Über elektrische Ladungen in der Atmosphäre  
Ann. Phys. Lpz. 77, 644-66.
- OGAWA, T. (1960) Types of diurnal variation of air-earth current.  
J. Geomagn. Geoelect. 11,  
165-73.
- PARKINSON, W.D. and  
TORRESON, O.W. (1931) The diurnal variation of the electric-potential of the atmosphere over the oceans.  
Bul.8, Internat. Assn. Terr. Mag. and Elect., IUGG, C-R.  
Stockholm Assembly, 340-5, Paris
- REITER, R. (1955) Ergebnisse luftelektrischer Messungen auf dem Zugspitzplatt im 2500m Seehöhe.  
Geofis. Pur. Appl. 30, 155-9.

- REITER, R. (1965) Precipitation and cloud electricity  
Quart. J.R. Met. Soc. 91, 60-72.
- SAGALYN, R.C. and  
FAUCHER, G.F. (1954) Aircraft investigation of the large  
ion content and conductivity of the  
atmosphere and their relation to  
meteorological factors.  
J. Atmosph. Terr. Phys. 5,  
253-72.
- SAGALYN, R.C. and  
FAUCHER, G.F. (1956) Space and time variations of  
charged nuclei and electrical  
conductivity of the atmosphere.  
Quart. J.R. Met. Soc. 82, 428-43
- SCRASE, F.J. (1933) The air-earth current at Kew  
Observatory.  
Geophys. Mem., Lond. 58
- SCRASE, F.J. (1933) Observations of atmospheric  
electricity at Kew. A survey  
of results obtained from 1843 to  
1931.  
Geophys. Mem. Lond. 60
- SCRASE, F.J. (1938) Electricity on rain  
Geophys. Mem. Lond. 75
- SIMPSON, G.C. (1915) The electricity of atmospheric  
precipitation  
Phil. Mag. 30, 1-12.
- SIMPSON, G.C. (1942) The electricity of cloud and rain.  
Quart. J.P. Met. Soc. 68, 1-34
- SIMPSON G.C. (1949) Atmospheric electricity during  
disturbed weather.  
Geophys. Mem. Lond. 84, 1-51
- SMIDDY, M. and  
CHALMERS, J.A. (1958) The double field mill  
J. Atmosph. Terr. Phys. 12, 206-  
10

- SMIDDY, M. and  
CHALMERS, J.A. (1960) Measurements of space charge in  
the lower atmosphere.  
Quart. J.R. Met. Soc. 86, 79-84
- SMITH, L.G. (1955) The electric charge of raindrops  
Quart. J.R. Met. Soc. 81, 23-47
- TORRESON, O.W.,  
GISH, O.H.,  
PARKINSON, W.C. and  
WAIT, G.R. (1946) "Scientific Results of Cruise VII  
of the Carnegie during 1928-9"  
Pub. Carnegie Instn, Washington  
D.C. No. 568
- WAIT, G.R. (1943) Cause for the radical change with  
season in the type of potential  
gradient diurnal variation curves  
at Watheroo.  
Trans. Amer. Geophys. Union.  
1943, 219-220.
- WHIPPLE, F.J.W. (1936) The influence of urban conditions  
on the circulation of electricity  
through the atmosphere.  
Trans. Faraday. Soc. 32,  
1203-9
- WHIPPLE, F.J.W. and  
SCRASE, F.J. (1936) Point discharge in the electric  
field of the earth.  
Geophys. Mem. Lond. 68, 1-20
- WILSON, G.T.R. (1920) Investigation on lightning  
discharges on the electric field  
of thunderstorms.  
Phil. Trans. A., 221, 73-115.
- WILSON, C.T.R. (1929) Some thundercloud problems  
J. Franklin Inst. 208, 1-12

